

**PROTEOMIC ANALYSES OF *Elaeis guineensis* Jacq.  
(AFRICAN OIL PALM) BASAL STEM ROT DISEASE  
RELATED TO *Ganoderma boninense***

**LEONA DANIELA JEFFERY DAIM**

**FACULTY OF SCIENCE  
UNIVERSITY OF MALAYA  
KUALA LUMPUR**

**2017**

PROTEOMIC ANALYSES OF *Elaeis guineensis* Jacq.  
(AFRICAN OIL PALM) BASAL STEM ROT DISEASE  
RELATED TO *Ganoderma boninense*

LEONA DANIELA JEFFERY DAIM

THESIS SUBMITTED IN FULFILMENT OF THE  
REQUIREMENTS FOR THE DEGREE OF  
DOCTOR OF PHILOSOPHY

INSTITUTE OF BIOLOGICAL SCIENCES  
FACULTY OF SCIENCE  
UNIVERSITY OF MALAYA  
KUALA LUMPUR

2017

## ABSTRACT

*Ganoderma boninense* is a basidiomycete fungal pathogen. It mainly attacks the roots of oil palms which will lead to the basal stem rot (BSR) disease. The oil palm industry suffers yearly crop losses that are attributed to the spread of this disease. To obtain a clearer picture of expression profiles of the ever changing global protein network in ganoderma infected plants, a gel-based proteomics approach was conducted using leaf tissues sampled from young palms. Leaf tissues were used for experimental analysis mainly because they were easier to sample than root tissues. Even though the mechanism of infection of this disease is through the root systems, early detection of the disease by source of leaves is an added advantage. This is because tissues could be sampled without wounding the roots, thus rendering them exposed to possible disease infection. Differential analysis of the leaf proteome revealed 116 protein spots that changed in abundance. Identification of these spots revealed proteins that changed in carbohydrate metabolism, cellular component, energy production, fatty acid biosynthesis, immunity and defence, nitrogen metabolism, protein metabolism, stress response, transport, and photosynthesis. Some of these changes were then validated using Western blots. In-depth literature reviews showed that proteins involved in immunity and defence, specifically peroxiredoxin, detoxify reactive oxygen species that are harmful to the plants: Protein-protein interaction studies showed that peroxiredoxins interacted with a disease resistance protein. These results suggest the possibility of further investigation into disease resistance proteins in host-pathogen interactions. The results obtained from the proteomic analyses of leaf tissues from inoculated oil palms could be used as a tool in early detection of the BSR disease. Additional validation and further investigations into these proteins could improve our biological understanding towards this disease.

## ABSTRAK

Kulat patogen *Ganoderma boninense* termasuk dalam kategori basidiomycete. Ia menyebabkan penyakit reput pangkal batang yang tidak boleh diubati pada kelapa sawit. Penyakit ini menyebabkan kerugian tanaman tahunan yang besar kepada industri kelapa sawit. Untuk mendapatkan gambaran terhadap perubahan global profil pengekspresan protein pada tumbuhan yang dijangkiti penyakit, satu pendekatan proteomik berasaskan gel telah dijalankan dengan menggunakan tisu dedaun yang diperolehi daripada kelapa sawit muda. Tisu-tisu dedaun digunakan untuk kajian analisis diutamakan kerana ia mudah diperolehi berbanding tisu-tisu akar. Walaupun mod jangkitan penyakit reput pangkal batang mensasarkan sistem akar, pengesanan awal penyakit melalui dedaun tanpa mencederakan akar-akar seterusnya mendedahkan sistem akar terhadap penyakit tersebut merupakan satu kelebihan. Analisis perbezaan proteome dedaun mendedahkan 116 titik protein yang berubah dari segi perbezaan ekspresi protein. Pengenalpastian titik protein menunjukkan perubahan dari segi metabolisme karbohidrat, komponen sel, pengeluaran tenaga, biosintesis asid lemak, imuniti dan pertahanan dari segi penyakit, metabolisme nitrogen, metabolisme protein, tindak balas stres, pengangkutan dan fotosintesis. Sebahagian daripada perubahan ini disahkan dengan menggunakan pemblotan Western. Kajian lepas terhadap protein yang berfungsi dari segi imuniti dan pertahanan penyakit, terutamanya, peroxiredoxin, menunjukkan bahawa ia berupaya menyahtoksik spesies reaktif oksigen yang berbahaya terhadap pokok kelapa sawit. Kajian interaksi protein menunjukkan bahawa peroxiredoxin berinteraksi dengan satu protein rintangan penyakit. Hasil keputusan ini mencadangkan kemungkinan siasatan lanjut terhadap protein rintangan penyakit dalam interaksi perumah-patogen. Hasil-hasil yang diperolehi daripada analisis proteomik pokok kelapa sawit yang telah diinokulasi ini berpotensi dijadikan sebagai satu alat pengesanan awal bagi penyakit reput pangkal batang.

Pengesahan dan kajian lanjut terhadap protein-protein ini boleh menambahkan pemahaman dari segi biologi terhadap penyakit ini.

University of Malaya

## ACKNOWLEDGEMENT

I duly acknowledge Sime Darby Technology Centre Sdn Bhd for fully funding my PhD research program. I would like to express my sincere gratitude and appreciation to both my supervisor and co-supervisor namely Associate Prof. Dr Saiful Anuar Karsani and Dr Nazia Abdul Majid for their inspiration, guidance, support and technical assistance during the course of my study. Their valuable comments, opinions and advice in my thesis has nurtured me into what I am today.

Special thanks to Dr Tony Ooi Eng Keong and Nalisha Ithnin for their constructive criticisms and scientific guidance in all our brainstorming sessions. I sincerely thank Pn Normahnani Md Noh, Dr Nazir Basiran and Dr Sanusi Jangi for their passion, support and friendship. I would like to thank Dr Hirzun Mohd Yusof and Dr Harikrishna Kulaveerasingam for their continuous encouragement and mental support throughout my post-graduate study.

To my loving family, no words will be able to describe my heartfelt gratitude and appreciation to both my parents who have been the biggest supporters in encouraging me throughout my PhD period. My journey in accomplishing this PhD would not have been possible without my understanding husband (Dr Tan Joon Sheong) for his support and unconditional love and by taking good care of both of our children (Regina Tan Siew Lam and Russell Tan Kah Seng).

## TABLE OF CONTENTS

<b>ORIGINAL LITERARY WORK DECLARATION</b>	ii
<b>ABSTRACT</b>	iii
<b>ABSTRAK</b>	iv
<b>ACKNOWLEDGEMENT</b>	vi
<b>TABLE OF CONTENTS</b>	vii
<b>LIST OF FIGURES</b>	xii
<b>LIST OF TABLES</b>	xv
<b>LIST OF SYMBOLS AND ABBREVIATIONS</b>	xvi
<b>LIST OF APPENDICES</b>	xix
<b>CHAPTER 1: INTRODUCTION</b>	1
<b>CHAPTER 2: LITERATURE REVIEW</b>	3
2.1 <i>Ganoderma</i> in relation to basal stem rot	4
2.1.1 The symptoms of <i>Ganoderma</i> disease	5
2.1.2 Possible sources of <i>Ganoderma</i> infection	5
2.1.3 Previous studies on BSR caused by <i>Ganoderma sp.</i> in oil palm	6
2.1.4 Interaction between plants and pathogens	7
2.2 Mechanisms of defence to pathogens: biochemistry and physiology	8
2.2.1 Cell wall apposition	9
2.2.2 Callose deposition	9
2.2.3 Lignification	10
2.2.4 Roles of phytoalexins in the defence response	10
2.2.5 Hypersensitive response	11

2.3	Disease control and management strategies	12
2.3.1	Current agronomic practices	12
2.3.2	Surgery and soil mounding	13
2.3.3	Fungicides	14
2.3.4	Replanting techniques	14
2.4	Current approaches to detect BSR	16
2.4.1	Non-molecular techniques	16
2.4.2	Molecular techniques	18
2.5	Development of resistant varieties	19
2.6	Proteomics – Technologies and applications	21
2.6.1	Two-dimensional electrophoresis (2-DE)	22
2.6.2	Mass spectrometry (MS)	24
2.6.3	Bottom-up and top-down proteomics	26

### **CHAPTER 3: METHODOLOGY** 28

3.1	Plant material	28
3.2	Sources of <i>Ganoderma</i> culture	28
3.3	Preparation of fungal culture, rubber wood block (RWB) inoculums and nursery trial	28
3.4	Total protein extraction protocols	29
3.4.1	Phenol-guanidine isothiocyanate method (M1)	30
3.4.2	TCA-acetone precipitation method (M2)	30
3.4.3	Sucrose method (M3)	31
3.4.4	TCA-acetone-phenol method (M4)	31
3.5	Protein extraction of leaf tissues for 2-DE	32

3.6	Protein quantification	33
3.7	SDS-PAGE	33
3.8	2-DE analyses	33
3.8.1	Optimization of 2-DE protocol	33
3.8.2	Analytical gels	34
3.8.3	Protein visualization, image acquisition and data analysis	35
3.8.4	Tyrpsin digest and LC-QToF analysis	36
3.9	Protein blotting	37
3.9.1	Immunoprobng with antibodies	38
3.9.2	Visualization with chromogenic substrates	39
3.9.3	Quantification of western blots	39
3.10	Characterization of 2-cys peroxiredoxin	40
3.10.1	Bioinformatic analysis	40
3.10.2	RNA extraction	40
3.10.3	Reverse-transcription polymerase chain reaction (RT-PCR)	41
3.10.4	Amplification of cDNA encoding 2-cys peroxiredoxin gene	42
3.10.5	Cloning and transformation	43
3.10.6	Preparation of vector and insert	44
3.10.7	Expression of recombinant 2-cys peroxiredoxin protein	46
3.10.8	Soluble cytoplasmic fraction	46
3.10.9	Purification of recombinant 2-cys peroxiredoxin protein	47
3.10.10	Protein-protein interaction analysis using pull-down assay	48
	<b>CHAPTER 4: RESULTS</b>	<b>50</b>
4.1	<i>Ganoderma boninense</i> culture and inoculum	50
4.2	Nursery trial set-up	51

4.3	Destructive sampling of oil palm seedlings	52
4.4	Evaluation of protein extraction protocols	56
4.5	2-DE analyses	60
4.6	Leaf proteins that changed in abundance during <i>G. boninense</i> infection	76
4.7	Validation of protein abundance by Western blotting	80
4.8	Bioinformatic analysis of 2-cys peroxiredoxin	83
4.9	RNA extraction and cloning of cDNA encoding 2-cys peroxiredoxin	84
4.10	Protein expression	86
<b>CHAPTER 5: DISCUSSION</b>		91
5.1	Protein extraction and analysis	92
5.1.1	Phenol-guanidine isothiocyanate method	93
5.1.2	TCA-acetone precipitation method	93
5.1.3	Sucrose method	94
5.1.4	TCA-acetone-phenol method	95
5.2	Leaf protein candidates that changed in abundance in relation to BSR	96
5.2.1	Photosynthesis	96
5.2.2	Carbohydrate metabolism	99
5.2.3	Protein metabolism	100
5.2.4	Immunity and defence	102
5.2.5	Energy production	103
5.2.6	Stress response	104
5.2.7	Transport	105
5.2.8	Cellular component	106
5.2.9	Fatty acid biosynthesis	107
5.2.10	Nitrogen metabolism	107

5.2.11	Main proteins of importance to changes in leaf proteome	107
5.3	Protein validation, expression and characterization	108
5.4	Functions of known protein homologs in relation to disease infection	110
5.5	Future prospects	114
5.5.1	Resistant planting materials	115
<b>CHAPTER 6: CONCLUSION</b>		117
<b>REFERENCES</b>		118
<b>LIST OF PUBLICATIONS AND PAPERS PRESENTED</b>		142
<b>APPENDIX</b>		164

## LIST OF FIGURES

<b>Figure 2.1:</b>	Strategies for protein identification and characterization using mass spectrometry.	27
<b>Figure 4.1:</b>	<i>Ganoderma boninense</i> cultures were maintained on PDA plates.	50
<b>Figure 4.2:</b>	RWBs were inoculated with mature <i>G. boninense</i> and incubated in the dark for three months until the blocks were fully colonized by the fungus.	50
<b>Figure 4.3:</b>	Nursery set-up for <i>Ganoderma boninense</i> trial.	51
<b>Figure 4.4:</b>	The overall vegetative growth of both non-inoculated and inoculated oil palm seedlings (2mpi to 5mpi).	53
<b>Figure 4.5:</b>	The overall vegetative growth of both non-inoculated and inoculated oil palm seedlings (6mpi to 7mpi).	54
<b>Figure 4.6:</b>	Basidiocarp can be seen emerging from the boles of 6-mpi seedlings.	55
<b>Figure 4.7:</b>	The overall physical appearances of 6-mpi oil palm seedlings were compared.	55
<b>Figure 4.8:</b>	The cross section of the stems of 6-mpi oil palm seedlings.	56
<b>Figure 4.9:</b>	SDS-PAGE profiles of oil palm leaf tissues from young (YL) and mature (ML) oil palms.	58
<b>Figure 4.10A:</b>	2-DE protein profiles of leaf tissues extracted from young oil palms.	59
<b>Figure 4.10 B:</b>	2-DE protein profiles of leaf tissues extracted from mature oil palms.	59

<b>Figure 4.11:</b>	A diagrammatic representation of the proteomics workflow to detect differences in the proteome of leaf tissues of inoculated and non-inoculated oil palm seedlings.	62
<b>Figure 4.12a:</b>	Representative 2D-PAGE gel images of 2 month-old oil palm leaf tissues from non-inoculated (A) and inoculated seedlings (B).	63
<b>Figure 4.12b:</b>	Representative 2D-PAGE gel images of 3 month-old oil palm leaf tissues from non-inoculated (C) and inoculated seedlings (D).	64
<b>Figure 4.12c:</b>	Representative 2D-PAGE gel images of 4 month-old oil palm leaf tissues from non-inoculated (E) and inoculated seedlings (F).	65
<b>Figure 4.12d:</b>	Representative 2D-PAGE gel images of 5 month-old oil palm leaf tissues from non-inoculated (G) and inoculated seedlings (H).	66
<b>Figure 4.12e:</b>	Representative 2D-PAGE gel images of 6 month-old oil palm leaf tissues from non-inoculated (I) and inoculated seedlings (J).	67
<b>Figure 4.12f:</b>	Representative 2D-PAGE gel images of 7 month-old oil palm leaf tissues from non-inoculated (K) and inoculated seedlings (L).	68
<b>Figure 4.13:</b>	Western blotting detection of leaf proteins in non-inoculated and inoculated oil palm seedlings.	83
<b>Figure 4.14:</b>	Total RNA extracted from leaves of oil palm seedlings and PCR products of cyclophilin and 2-cys peroxiredoxin genes were run on agarose gels.	84
<b>Figure 4.15:</b>	The 822 bp ORF sequence for 2-cys peroxiredoxin has 274 amino acids.	85

<b>Figure 4.16:</b>	Agarose gel images of the pET-49b expression vector and gene insert prior to protein expression.	87
<b>Figure 4.17:</b>	Aligned sequence consensus of the 2-cys peroxiredoxin gene with restriction enzymes cutting sites.	88
<b>Figure 4.18:</b>	Expression of the target gene in the soluble cytoplasmic fraction before and after induction was accessed on SDS-PAGE.	89
<b>Figure 4.19:</b>	The recombinant 2-cys peroxiredoxin protein was purified using a polyhistidine-tagged nickel column.	90
<b>Figure 4.20:</b>	Prey proteins were detected in the first elution in the leaf tissues (L560 and L351) of <i>Ganoderma</i> -inoculated oil palm seedlings but not in the stem (S560).	90
<b>Figure 5.1:</b>	A zigzag model illustrating the quantitative output of the plant immune system (Jones & Dangl, 2006).	112

## LIST OF TABLES

<b>Table 3.1:</b>	The list of commercially available plant antibodies that were used for Western validation of four candidate proteins.	39
<b>Table 4.1:</b>	Four different extraction methods were used to extract proteins from oil palm leaf tissues.	58
<b>Table 4.2:</b>	The total number of detectable spots varied among different extraction methods.	58
<b>Table 4.3:</b>	Image and statistical analyses were performed to determine the number of protein spots that changed in abundance between inoculated and non-inoculated tissues.	61
<b>Table 4.4:</b>	The numbers of unique proteins that are expressed in leaf tissues of inoculated oil palm seedlings (based on time points) were obtained by removing proteins with the same UniProt entries and identities.	69
<b>Table 4.5:</b>	List of proteins with different abundance, according to time points, in leaf tissues of inoculated oil palm seedlings.	77
<b>Table 4.6:</b>	Five plant antibodies were used to detect the presence of candidate proteins in leaf tissues and RbcL was used as a loading control.	82
<b>Table 4.7:</b>	The abundance ratio obtained from Western blots were compared to the ratios obtained from 2-DE.	82
<b>Table 4.8:</b>	The recombinant 2-cys peroxiredoxin protein was identified using mass spectrometry and was searched against the oil palm database (Sime Darby Technology Centre).	89

## LIST OF SYMBOLS AND ABBREVIATIONS

$\beta$ -ME	beta-mercaptoethanol
$^{\circ}\text{C}$	degree centigrade
$\mu\text{A}$	microampere
$\mu\text{g}$	microgram
$\mu\text{L}$	microliter
x g	gravitational acceleration
2D	two-dimensional
2-DE	two-dimensional electrophoresis
2D-PAGE	two dimensional-polyacrylamide gel electrophoresis
ACN	acetonitrile
ATP	adenosine triphosphate
Avr-R	avirulence protein
BCIP	5-bromo-4-chloro-3'-indolyphosphate
bp	base pair
BSA	bovine serum albumin
BSR	basal stem rot
$\text{CH}_3\text{COOH}$	acetic acid
CHAPS	3-[(3-Cholamidopropyl)dimethylammonio]-1-propanesulfonate hydrate
DTT	dithiothreitol
ETI	effector triggered immunity
ETS	effector triggered susceptibility
<i>G. boninense</i>	<i>Ganoderma boninense</i>
$\text{H}_3\text{PO}_4$	phosphoric acid

hr	hour
HR	hypersensitive response
IAA	iodoacetamide
IEF	isoelectric focusing
IPG	immobilized pH gradient
IPTG	isopropyl-thio- $\beta$ -D-galactoside
kDa	kilo Dalton
L	litre
LB	Luria-Bertani
LC-MS	liquid chromatography mass spectrometry
LC-QTOF MS	liquid chromatography-quadrupole time of flight mass spectrometry
M	molar
m/z	mass-to-charge ratio
mA	milliampere
MeOH	methanol
min	minute
mL	milliliter
mm	millimetre
mM	millimolar
mpi	months-post-inoculation
MPOB	Malaysian Palm Oil Board
Na <sub>2</sub> CO <sub>3</sub>	sodium carbonate
Na <sub>2</sub> S <sub>2</sub> O <sub>3</sub>	sodium thiosulfate
NADP	nicotinamide adenine dinucleotide phosphate
NBS-LRR	nucleotide binding site-leucine rich repeat

NBT	nitro-blue tetrazolium
NCBI	National Center for Biotechnology Information
ng	nanogram
$\text{NH}_4\text{HCO}_3$	ammonium bicarbonate
$(\text{NH}_4)_2\text{SO}_4$	ammonium sulfate
NL	non-linear
PAMP	pathogen associated molecular patterns
PBS	phosphate-buffered saline
PBS-T	phosphate-buffered saline with Tween 20
PCD	programmed cell death
pI	isoelectric point
PRR	pattern recognition receptor
PTI	PAMPs triggered immunity
PVPP	polyvinylpyrrolidone
RWB	rubber wood block
s	second
SDS	sodium dodecylsulfate
SDS-PAGE	SDS-polyacrylamide gel electrophoresis
SOC	Super optimal broth with catabolite repression
TBS	tris buffered saline
Tris-HCl	tris-hydrochloride
V	volt
Vh	volt-hour

## LIST OF APPENDICES

<b>Appendix A:</b>	List of proteins with different abundance between healthy and diseased leaf tissues of oil palm seedlings.	164
<b>Appendix B:</b>	Protein yields that were obtained from young and mature leaf tissues of oil palms using four different protein extraction methods.	173
<b>Appendix C:</b>	Number of protein spots that were detected after gel image analysis from young and mature leaf tissues of oil palms using four different protein extraction methods.	174
<b>Appendix D:</b>	Gel replicates of 2-DE profiles of leaf tissues extracted from young and mature oil palms using different extraction methods.	175
<b>Appendix E:</b>	Gel replicates of 2-month-old oil palm leaf tissues extracted from non-inoculated and inoculated seedlings.	179
<b>Appendix F:</b>	Gel replicates of 3-month-old oil palm leaf tissues extracted from non-inoculated and inoculated seedlings.	183
<b>Appendix G:</b>	Gel replicates of 4-month-old oil palm leaf tissues extracted from non-inoculated and inoculated seedlings.	187
<b>Appendix H:</b>	Gel replicates of 5-month-old oil palm leaf tissues extracted from non-inoculated and inoculated seedlings.	191
<b>Appendix I:</b>	Gel replicates of 6-month-old oil palm leaf tissue extracted from non-inoculated and inoculated seedlings.	195
<b>Appendix J:</b>	Gel replicates of 7-month-old oil palm leaf tissues extracted from non-inoculated and inoculated seedlings.	199

## CHAPTER 1: INTRODUCTION

The African oil palm *Elaeis guineensis* Jacq., is mainly planted in developing countries in Southeast Asia, particularly Malaysia, Indonesia and Thailand. This crop is the main economic backbone of these countries which depend very heavily on the production and exportation of palm oil. The palm oil industry has gradually developed and progressed to mature into one of the most sought after perennial plantation crop (Price *et al.*, 2007). However, a considerable threat to the development of this agricultural crop is the emerging presence of diseases. Oil palm crop loss particularly due to the basal stem rot (BSR) disease is increasingly becoming more apparent. The *Ganoderma boninense* fungus is found to be the causal agent of BSR but no effective method has been found to cure the disease. An effective method to detect the disease at its early stage is also unavailable. The fungus first attacks and decays the roots of the oil palm. The disease slowly progresses towards the trunk, thereby causing the crown of the palm to wilt and the palm eventually collapses (Rees *et al.*, 2009).

Many experiments in attempting to detect the presence of BSR disease using diagnostic procedures involving roots have largely been unsuccessful (Utomo and Niepold, 2000; Mohd As'wad *et al.*, 2011). Moreover, invasive methods such as sampling of root tissues are most often not feasible. This is because it is not an easy task to correctly sample diseased root tissues from infected oil palms in mature fields. This is due to the complex architecture of the root system belowground that consists of a mixture of networks of roots that may include those from neighbouring palms. However, it is relatively easy to sample leaf tissues as the sampling process could be done without potentially wounding the roots of mature oil palm.

Limited information is available on the exact method of infection that occur during BSR. The global protein expression of leaves of infected plants were also not known. However, it is well known that defence responses are activated when plant roots are exposed to underground pathogens. This is done by sending a series of signalling molecules to the aboveground foliar. This hypothesis has been clearly shown in roots of plants where the defence responses were triggered and transported to aboveground. The plants are therefore better prepared for defence strategies (Bezemer & van Dam, 2005; Kumar & Bais, 2012; van Geem *et al.*, 2013). The expression of defence related genes were found to be detected in both leaves and roots of *Ganoderma*-infected oil palm seedlings (Alizadeth *et al.*, 2011; Tan *et al.*, 2013).

Therefore, this work has utilized a comparative proteomics approach to identify changes in plant proteins that may be associated with *Ganoderma* infection. The proteome profiles of plants inoculated with *Ganoderma* were compared with non-inoculated plants. The analysis was performed on leaf tissues during the early stages of infection (up to seven months post-infection).

The ultimate long term goal of this study is to develop potential biomarkers to identify oil palms that are infected by *G. boninense*. In order to achieve this goal, the following objectives have been identified:

1. To compare the leaf proteome profiles of oil palms inoculated and non-inoculated with *Ganoderma boninense*,
2. To identify leaf proteins that change in abundance with fungal infection,
3. To predict, by bioinformatics means, the function(s) of proteins that change with fungal infection.

## CHAPTER 2: LITERATURE REVIEW

The African oil palm, *Elaeis guineensis*, is a woody monocotyledon and monoecious (Corley and Tinker, 2016). Oil palm can be considered as the most productive cash crop, giving far higher yields when compared to soybean, rapeseed and sunflower (Murphy, 2007). The world palm oil production in 2014 increased to 59.3 million tonnes in comparison to the 56.3 million tonnes achieved in 2013 (MPOB, 2015). The rise of 3.0 million tonnes was due to further growth in matured oil palm areas especially in Indonesia. Current varieties of oil palm cultivated in plantations have economic life-spans between 25–30 years and produce fruits around the year (Barcelos *et al.*, 2015).

Although oil palm is the basis of a lucrative commodity business, it is likely to get infected with diseases and attacked by insects. An important disease, yet still without a cure, that is affecting the present oil palm industry is basal stem rot (BSR). In 1915, the presence of the disease was first detected in the Republic of Congo, West Africa (Wakefield, 1920). In Malaysia, Thompson (1931) detected the disease that was infecting palms over 25 years of age that were due for replanting. The causal agent for BSR disease is the fungal species, *Ganoderma boninense*. It is considered to be detrimental to the oil palm industry in Indonesia and Malaysia (Ariffin *et al.*, 1989; Rao, 1990). BSR progresses slowly and eventually causes the death of infected palms. The disease is capable of infecting all developmental stages of the oil palm. Palms infected early in its life usually show no symptoms until they are more than 12 years old (Paterson, 2007).

Many field studies have been carried out to monitor the disease progress and spread, followed by detection of the disease (Durand-Gasselin *et al.*, 2005; Santoso *et al.*, 2011;

Rees *et al.*, 2012). Since disease progress and spread is slow, reporting of field test results have subsequently been delayed. This has resulted in limited number of publications on the outcome of field trials being reported between 2005 and 2013. Hence, most of the cited literature reviews were obtained more than a decade ago. However, there has been marked improvements with many disease detection technologies continuously being developed for field applications (Markom *et al.*, 2009; Liaghat *et al.*, 2014; Nurnadiah *et al.*, 2014). Research findings on the molecular detection of the basal stem rot disease has also been forthcoming (Chong *et al.*, 2011; Mercière *et al.*, 2015; Ho *et al.*, 2016).

## **2.1 *Ganoderma* in relation to basal stem rot**

The *Ganoderma* fungus, a versatile basidiomycete, are capable of causing white rot diseases in hardwoods such as ash, maple, oak and sycamore. They mainly decompose cellulose, lignin and polysaccharides (Blanchette, 1984; Adaskaveg and Ogawa, 1990; Adaskaveg *et al.*, 1991, 1993). *Ganoderma boninense* Pat. is known to be the causal agent of BSR in oil palm (Ho and Nawawi, 1985; Abadi, 1987; Soepena *et al.*, 2000).

In the second and third replanting of oil palm, the symptoms can appear as early as one to two years after planting out in the field (Soepena *et al.*, 2000). A more acute *G. boninense* problem is likely to surface over the next few years as the fungus increases its geographical range and virulence (Murphy, 2007). Singh (1991a) quantified yield losses based on fresh fruit bunch production found that it was adversely affected by incidence of the disease. Losses due to BSR could be incurred through direct reduction on the numbers of standing oil palms. This could also happen with the dwindling number in fruit bunch and weight from diseased standing palms as well as those with sub-clinical infections (Turner, 1981). The disease can result in the death of the palms

with only one-fifth still left standing in a *Ganoderma* infested field. These palms could still be producing fruit bunches either at their prime (8-15 years) or are more than 15 years old. Economic losses reaching 30% have quite frequently been reported (Corley and Tinker, 2016).

### **2.1.1 The symptoms of *Ganoderma* disease**

Infected young palms usually exhibit the following symptoms: yellowing of leaves with or without the presence of spots on the lower fronds, followed by necrosis (Singh, 1991a). Other significant observations of the canopy include shorter unfolded leaves, chlorosis (pale or yellow) and necrosis (death of cells) (Arrifin *et al.*, 2000). Palms may appear pale with significant retardation in growth as the disease gradually advances.

Similar symptoms, multiple unopened spears as well as pale and drooping leaf canopies, are also observed in mature palms. Once these foliar symptoms are observed in the field, 50% of the basal stem tissue could be found to be infected by the fungus. With the first appearance of foliar symptoms, infected young palms in the field may take between six months to two years before they succumb to the disease. Mature palms may take several years to die (Paterson, 2007; Cooper *et al.*, 2011).

### **2.1.2 Possible sources of *Ganoderma* infection**

Flood *et al.* (2000) observed the presence of BSR in oil palms planted on lands that have been converted from coconut plantations. These symptoms may develop after 10 to 14 years of planting (Flood *et al.*, 2005). Utomo *et al.* (2005) also indicated that fungus starts to invade the root systems starting from the second and subsequent replanting cycles of oil palm. Spores released from the fruiting bodies (basidiomata)

were identified as the most likely sources of inocula for subsequent infection via root contact (Lim and Fong, 2005).

### **2.1.3 Previous studies on BSR caused by *Ganoderma* sp. in oil palm**

Miller *et al.* (1999) referred to BSR as a significant constraint in oil palm plantations. In the subsequent year, Flood *et al.* (2000) categorised BSR as an increasingly important disease of oil palm for the past eight decades. Severe economic losses particularly in Malaysia and northern Sumatra has been associated with the continuous presence of the disease. According to Paterson (2007), it may take several years for the symptoms to develop in mature palms, while they are frequently undetected in immature palms. The infection rate in older palms is approximately 2% (Ariffin *et al.*, 2000). Although losses of up to 80% has been reported, these occur after many planting cycles. However, economical losses below 20% is not considered to be significant. The palms are left standing in the fields without any plans for replanting (Rao *et al.*, 2003; Conte *et al.*, 2012). These data show us that a standard measuring tool needs to be clearly defined on the seriousness of the disease.

Ariffin *et al.* (2000) described how basidiomata may initially develop from an infected root and spread towards the basal stem. The approximate locations of the diseased area inside the palm may be estimated using the positions of the basidiomata. The study by Abdullah (2000) on *Ganoderma* in coconut, favoured the spread from independent secondary inocula and neither supported root to root nor airborne spore spread.

A review by Paterson (2007) suggested otherwise, where the mode of spread was thought to be primarily from roots. This idea became noticeably accepted among

scientists doing research on ganoderma. The infection was proposed to have resulted from root to root contact between healthy tissues and diseased tissues that remained in the soil.

However, the role(s) of basidiospores still could not be ascertained (Ariffin *et al.*, 2000). Sanderson *et al.* (2000) also backed the idea that for healthy roots to become diseased, they have to come in contact with infected debris. They agree that the disease is spread through this contact and without the absence of spores. Interestingly, Bridge *et al.* (2004) mentioned that different isolates of *G. boninense* varied from one another and emphasized the importance of basidiospores.

Most of the findings of these field studies were published more than a decade ago, due to the long life cycle of the oil palm and the slow mode of infection of the fungus. This also intensifies the need to increase efforts to solve the basal stem rot disease using faster advanced technologies compared to conventional methods.

#### **2.1.4 Interaction between plants and pathogens**

Plants are constantly in a battle to survive from invasions by their pathogens (Mcdowell and Simon, 2006). Pathogens often secrete virulence factors that contribute to the pathogenicity of the pathogens. These virulence factors target specific molecules within or outside plant cells (Chang *et al.*, 2004; Tameling and Takken, 2008). Different strains of the same species of pathogen may secrete different types of virulence factors (Lukasik & Takken, 2009). Therefore, a defence system capable of recognizing distinct types of pathogen-encoded molecules has slowly developed in plants. These molecules are termed pathogen-associated molecular patterns (PAMPs). Highly conserved PAMPs in distantly related pathogens are also recognized by plants (Swiderski, *et al.*, 2009).

PAMP detection is a type of non-host resistance in plants. It detects the presence of potential pathogens and sends early warnings to the plant. This type of defence system is also considered as one of the first line of defence in plants (Ingle *et al.*, 2009).

Another type of defence system that has evolved in plants is known as resistance (R) proteins. Resistance proteins detect specific pathogen virulence factors as indications of potential attack. However, the virulence factor will be redefined as avirulent when detected by the host (Martin *et al.*, 2003; Bernoux *et al.*, 2011). To prevent further pathogen spread, this R-protein-dependent recognition system triggers a hypersensitive response. This response then activates programmed cell death at the site of infection, thus stopping further proliferation of the disease.

## **2.2 Mechanisms of defence against pathogens: biochemistry and physiology**

Plant pathogens typically enter the hosts through cell walls. A lot of useful information has been documented on the roles demonstrated by the cuticle and various forms of cell wall strengthening (Vorwerk *et al.*, 2004; Ho and Tan, 2015). There is no doubt that this cell wall concept has been the subject of major consideration. Paterson (2007) has proposed the lignin cell wall as the main defence mechanism against BSR disease. He also highlighted the importance of looking into developing highly tolerant or preferably resistant cell-lignin oil palm as a way to counter *G. boninense* infection. The possibility of differences in susceptibility to the disease within oil palm of similar genetic origin was also highlighted by Durand-Gasselin *et al.* (2005). He further elaborated that these variations in susceptibility can be identified within oil palms of the African (Deli, Angola and the La Mé) origins.

### **2.2.1 Cell wall apposition**

A review paper by Garcion *et al.* (2007) acknowledged the role of cell wall appositions as the first line of defence in resistance to pathogens. Phenolic compounds are in abundance in the cell wall, where they can be found deposited at the site of infection (Tronchet *et al.*, 2010; Micali *et al.*, 2011; Underwood, 2012). Appositions are targeted within the plant cell wall at the site of attempted penetration (Collinge, 2009).

Appositions are observed in many plant species. They comprise of an outer halo surrounding the inner papilla (a fleshy projection on a plant). As demonstrated by chemical and histological analyses, the papillae consist of protein, callose, phenolic compounds, inorganic compounds and even reactive hydrogen species (Zeyen *et al.*, 2002; Underwood, 2012). Penetration is often thought to be arrested by the presence of papillae. However, it is still unclear which particular component of the papillae is responsible for the successful defence against a specific pathogen. Results of a study on the functions of papilla in wheat infected with *Blumeria graminis* suggested that lignification of the papilla stopped further penetration by the fungus (Bhuiyan *et al.*, 2009).

### **2.2.2 Callose deposition**

Callose is an amorphous  $\beta$ -(1,3)-glucan polymer and is present in the plant cell wall (Luna *et al.*, 2011). It is an effective barrier that prevents the entry of pathogen invasion at the site of infection. It also serves as a deposition platform for antimicrobial compounds. Callose deposition is typically triggered by conserved PAMPs and the specific delivery of chemical defences in the cellular level are provided at the site of attack (Ellinger *et al.*, 2013; Nedukha, 2015). Some examples of potent callose-inducing PAMPs from fungal cell walls are chitin and chitosan. Other than PAMPs, callose

depositions can be activated by the presence of endogenous elicitors from herbivore- or pathogen-damaged plant tissues. Oligogalacturonides are some examples of damage-associated patterns (Ferrari *et al.*, 2013).

### **2.2.3 Lignification**

Lignin deposition usually occurs on the onset of pathogen invasion. It is represented as a strong barrier against potential pathogen invasion (Vanholme *et al.*, 2010; Malinovsky *et al.*, 2014). Lignin accumulates either only at the infection site, or over the entire wall of the infected cell or group of cells. Deposition of lignin in the plant cell wall will cause it to become more resistant to the mechanical pressure that is applied during fungal penetration. This prevents access to cell wall degrading enzymes (Bhuiyan *et al.*, 2009; Wang *et al.*, 2013).

Lignification is important for plant growth and structural development of plant cell walls. However, depending on the developmental process of the plant, the monomeric composition of lignin can differ greatly. Therefore, lignin in vascular tissues are significantly different from defence lignin accumulated by an elicitor treatment. This suggests that genes controlling lignin biosynthesis are differentially regulated during defence (Bhuiyan *et al.*, 2009; Wang *et al.*, 2013).

### **2.2.4 Roles of phytoalexins in the defence response**

Phytoalexins are low molecular mass secondary metabolites. They possess antimicrobial activities that are often induced by stress or during plant defence. In their natural forms, phytoalexins are toxic towards nematodes, fungi, bacteria and higher animals. They are classified as weak antibacterial and antifungal agents (Ahuja *et al.*, 2012; Thakur and

Sohal, 2013). However, phytoalexins have been shown to be detected in host plants at the sites of pathogen attacks (de León and Montesano, 2013).

Phytoalexins show biological activity towards a variety of pathogens. They are thus considered as molecular markers of disease resistance (Ahuja *et al.*, 2012). Phytoalexins were introduced based on the findings on *Solanum tuberosum* tuber tissues that have been infected with an incompatible race of *Phytophthora infestans*. In response to the incompatible interaction, the tuber tissues produced substances (phytoalexins) that managed to inhibit the pathogen. These substances gave a form of protection to the tuber tissues against later infections by other compatible races of pathogens (Coleman *et al.*, 2011; Pedras *et al.*, 2011).

### **2.2.5 Hypersensitive response**

In multicellular organisms, programmed cell death (PCD) often takes place during routine physiological processes (Garcion *et al.*, 2007). This phenomenon has been observed during developmental processes. It also occurs in response to both biotic and abiotic stresses. PCD is often observed in plants. It is also known as the hypersensitive response following fungal, bacterial or viral infections. This HR is described as the accelerated failure of the plant cells to function properly, ultimately resulting in death at the site of the attempted infection. HR is often presumed to hinder the spread of a disease towards healthy neighbouring tissues by confining the pathogen. However, plants can also initiate HR without requiring induction by disease causing microbes (Zurbriggen *et al.*, 2010; Bashir *et al.*, 2013).

In the decade since then, the field of plant PCD has begun to mature. Although much of the work in this field has drawn heavily on comparative analyses using paradigms derived from animal systems, especially those of the apoptotic pathways, distinctive features and adaptive characteristics that correlate to the lifestyle of plants are also

beginning to be recognized. Several highly conserved or more distantly related components have also been revealed genetically to regulate PCD across eukaryotes (Hofius *et al.* 2009; Coll *et al.*, 2010; Chichkova *et al.*, 2010). In a few cases, it has become possible to join these components into pathways (Sundström *et al.*, 2009). Single-gene mutations in most of these PCD components are viable and their effects on cell death induction and execution are usually quantitative in nature. These observations are thus consistent with the view that plant PCD pathways involve combinatorial modules to insure their proper control under a constantly changing environment that is superimposed on internal developmental cues (Bozhkov and Lam, 2011).

### **2.3 Disease control and management strategies**

At present, there is no ultimate solution towards the spread of BSR in oil palm plantations. Efforts are therefore, more focused on short term control and developing a management system to contain the outbreak of BSR. Several mechanisms have been practiced in the oil palm industry to prevent and control BSR problems in plantations. Finding a solution to BSR problem in oil palm is possible, but it will require a thorough understanding of the biological nature of the fungus, including its life cycle and interaction with the oil palm.

#### **2.3.1 Current agronomic practices**

One of the more effective measures to control BSR is to exercise good agronomic practices. To prevent the further spread of mycelia from the invading pathogen, trenches were dug around diseased palms adjacent to healthy palms (Chung, 2011). Trenches were thought to act as natural barriers between root-to-root contacts. However, this particular practice has not been demonstrated to be successful (Turner, 1981). This is because the depth of the trenches was not deep enough to hamper the growth and

movements of the roots to neighbouring palms. Some trenches were not regularly maintained to serve the intended purpose.

Collecting basidiomata of *G. boninense* from diseased palms (Sanderson *et al.*, 2000) and painting them with carbolineum (fungicidal paste) (Turner, 1981) to prevent spore dispersal was also recommended. However, if the spores have no direct infective ability (not virulent), then this effort is rendered futile. The increased BSR incidence in oil palm has been associated with poor agronomic practices, such as poorly drained soils, occasional flooding, nutrition imbalances and deficiencies (Teh *et al.*, 2010; Chung, 2011). Currently no conclusive evidence has been used to support these factors.

### **2.3.2 Surgery and soil mounding**

Turner (1968) proposed to control BSR by means of surgery and soil mounding. Initially, this was done through excision of diseased tissues as a form of treatment, but the results were variable. Later, Turner (1981) suggested that surgery be carried out, by using harvesting chisels, by excising the infected tissues away from the outer layer of the infected trunk. Diseased tissues from above and below the soil level were also removed using mechanical surgery (Singh, 1991b). With the removal of lesions, a protectant chemical (coaltar or thiram) was subsequently used to treat the exposed surfaces to prevent further fungal invasion.

When surgical methods are to be conducted, the age of the oil palm is an important factor to be considered. Turner (1981) reported that surgical treatments on palms more than 12 years old were more successful. This is because the disease lesions occur on the surface of the woody stems of older palms (Singh, 1991b). Infections almost always reoccur after this kind of surgical treatment if lesions are not effectively removed.

Another approach to control BSR is to mound the base of the infected palms with soil. A combination of *Trichoderma* biofungicide and endophytic fungus (arbuscular mycorrhizal fungus) is often incorporated into the mounded soil. Hasan and Turner (1998) showed that by incorporating soil mounding after surgery, the yield and vigour of mature disease palms could be increased. The economic life of *G. boninense* infected oil palms could potentially be prolonged by this treatment. It is believed that this combination of fungal cocktail helps to promote the growth of roots for nutrient absorption. Without the presence of arbuscular mycorrhizal fungus, soil mounding alone could increase the life expectancy of the oil palm. Weakened boles are thus prevented from being toppled by strong wind.

### **2.3.3 Fungicides**

The introduction of fungicides coupled with proper application techniques could potentially be the answer to controlling BSR. Screening of fungicides against *G. boninense in vitro* showed that numerous fungicides were strongly inhibitory towards the growth of *G. boninense* (Jollands, 1983; Lim *et al.*, 1990). Loh (1976) and Khairudin (1990) conducted field trials to control BSR by using systemic fungicides. However, the results of these studies were inconclusive. These fungicides could be applied either through soil drenching or trunk injection) although the latter was the preferred method (Ariffin, 2005). The most effective fungicide cocktail for trunk infection was a mixture of carboxin and quintozene. It has been shown to effectively slow down disease progression, thereby extending the life cycle of *G. boninense* infected oil palms (Ariffin, 2005).

### **2.3.4 Replanting techniques**

Besides control measures for existing stands, there are also some control measures at

replanting to control the disease in new oil palms. This can be achieved by adopting the correct technique during land preparation as the oil palm replanting process is regarded as an important part of the agronomic practice for controlling BSR (Chung, 2011). These control measures were based on the hypothesis that BSR spreads through root-to-root contact by infectious mycelia. In fields previously planted with coconuts or oil palms, the primary source of infection during replanting is the leftover tissues of former stands. By performing proper sanitation procedures, it is thought that the spread of the disease can be greatly reduced. Sanitation procedures involved the disposal of old stands (Chung, 2011).

Theoretically speaking, any approaches of disposing old stand by destructing or reducing the levels of *G. boninense* inoculum in the soil should have a beneficial effect on the subsequent replanting. Turner (1968) reported that the relationship between replanting techniques adopted and disease incidence are closely related. In the case of replanting coconut with oil palm, disease incidence has been reported to be rampant especially in coastal marine clay soils (Navaratnam, 1964). *G. boninense* is a saprophyte to coconuts. It prevails in the trunks and stumps of coconut that were left in the soil. Upon replanting, the fungus then infects the oil palm.

Smallholder farmers often practice under-planting coconut with oil palm. The under-planting of coconut with oil palm followed by poisoning or not poisoning and then felling of old coconut stands has been practiced by these smallholder farmers (Chung, 2011). Basidiomata of *G. boninense* are subsequently produced when the coconut stand starts to decompose in the field. *G. boninense* can be found in coconut plantations on dead husks and basidiomata have been observed not only on dead trunks and roots but also on living coconut seedlings. Outbreaks of BSR often occur in replanting areas

where the stumps had been retained in the ground. This is especially so in areas where oil palm has been planted after coconut. *G. boninense* infection may become apparent in oil palms as early as the first few years after planting. However, this is usually so when palms are over five years old (Singh, 1991a; Ooi and Heriansyah, 2005).

## **2.4 Current approaches to detect BSR**

Scientists working on BSR disease have managed to identify *G. boninense* as the pathogenic fungus that disrupts the growth of the oil palm (Durrand-Gasselien *et al.*, 2005; Paterson, 2007). The palm will ultimately die and collapse once the disease manifests itself onto the palm. Therefore, by identifying the causal agent of the disease, it serves as the starting point to the research and development into the disease. Methods to accurately detect the presence of the disease are currently still unavailable.

### **2.4.1 Non-molecular techniques**

One of the earliest methods to detect BSR was based on foliar observation of the palms in the fields. Symptoms such as mature leaves wilting, canopy drooping downwards, unopened spears are frequently observed and diagnosed as diseased palms (Ariffin *et al.*, 2000). The other more obvious symptom is the presence of the basidiocarp at the base of the trunk.

Another diagnostic method to test the presence of the fungus was to use drills to sample diseased tissues in an infected palm. *Ganoderma* was then cultured on *Ganoderma* selective media and then maintained them on potato dextrose agar plates (Ariffin *et al.*, 2000). Identification of the fungus is based on the presence of a brown halo surrounding the fungus and determination of morphological characteristics of the fungus. However, the correct and efficient techniques to detect the fungus were questioned. Many lacked

accurate taxonomy information whereby confusion arose with the identification of some species within the same genus (Hushiarian *et al.*, 2013). A lot of time is wasted on performing these methods and they are deemed inaccurate. However, if basidiocarps are detected at the base of the palms, it could be a sure sign that the disease has already infested the trunk tissues of the palm.

More recent and advanced techniques of detecting BSR disease include the use of electronic nose (e-nose), unmanned aerial vehicles (UAV) and high resolution field spectroradiometers. The e-nose is a device capable of mimicking the human olfactory system. It has functions for detecting, recognizing and classifying volatile compounds and odours (Markom *et al.*, 2009; Baietto *et al.*, 2010; Abdullah *et al.*, 2011; Abdullah *et al.*, 2014). Many more developments of e-noses are growing due to the increasing interest in food quality control and detection of plant diseases. Most devices that are currently available are difficult to operate and expensive, except for a device specifically for odour recognition which has easy to use algorithms (Abdullah *et al.*, 2011).

The use of UAVs of drones especially in the agriculture sectors have gradually increased. UAVs are able to gather detailed spatial information in real time. Due to its relatively low cost, the use of UAVs in conservation and ecological research has also increased (Getzin *et al.*, 2012; Peña *et al.*, 2013). The spatial and temporal data that are collected by the drones are accurate and can be used to understand disease transmission and environmental factors (Fornace *et al.*, 2014). The use of UAVs could avoid the constraints with using satellite data. The collection of satellite data could be marred by cloud contaminations, long repeat times and low spatial resolution. However, the

practical use of UAVs for field research is limited to their use to specific applications and settings (Fornace *et al.*, 2014).

Another approach which is gaining popularity is by using a spectroradiometer to capture diseases in plants. The distribution of a spectral power by a source can be measured using a spectroradiometer. Radiometric, photometric and colorimetric quantities from the spectral power distribution of light can be determined using this approach. Light sources can be measured, characterized and calibrated for various applications. High resolution field spectroradiometers are increasingly being used to analyse spectral and inspect vegetative diseases (Shafri *et al.*, 2009; Lelong *et al.*, 2010). One of the main challenges in using a spectroradiometer for automated detection of vegetative disease is the fine-tuning of its spectral parameters. This is required to enhance and subsequently fine-tune the potential of hyperspectral data to be used for early detection of diseases (Shafri *et al.*, 2009; Lelong *et al.*, 2010; Tawfik *et al.*, 2013). Using a spectroradiometer, different stages of BSR disease infection was investigated by Liaghat *et al.* (2014). They examined the efficiency of reflectance spectroscopy to detect BSR disease in the early stages of infection and subsequently managed to differentiate the spectra between *Ganoderma*-infected and healthy oil palm leaves.

#### **2.4.2 Molecular techniques**

The earliest molecular attempts to detect the presence of *Ganoderma* were based on immunoassays. To detect the presence of *G. boninense* using ELISA (enzyme-linked immunosorbent assay), polyclonal antibodies specific to the crude mycelial proteins of the fungus were used (Karthikeyan *et al.*, 2008; Kandan *et al.*, 2010). Other than the crude mycelial protein, the polyclonal antisera against basidiocarp protein and monospecific protein (62 kDa) were also used in the detection using ELISA.

Another molecular technique to detect and identify *Ganoderma* was the use of ribosomal DNA (rDNA) sequences that codes for ribosomal RNA (rRNA). The non-coding rDNA regions contain internal transcribed spacer regions (ITS). This ITS regions have also been extensively used in biodiversity screening, evolutionary studies and phylogenetic analyses of fungi. The ITS regions are generally more variable than the rRNA genes and they have been used to explore the genetic variations of the fungus (Zheng *et al.*, 2009; Chong *et al.*, 2011; Yuskianti *et al.*, 2014).

In other studies, high-performance liquid chromatograph was used to study ergosterols. Ergosterol is a membrane sterol which is present in almost all fungi. It has been detected in other *Ganoderma* species (*G. lucidum*, *G. applanatum*, *G. lipsiense*) (Mohd As'wad *et al.*, 2011). The concentration of ergosterol varies between the same fungal species depending on the physiological state of the fungus. Quantification of this component has also been done using nuclear magnetic resonance and gas chromatography coupled with mass spectrometry. These analyses could be used as a detailed diagnostic method for the early detection of BSR disease (Mohd As'wad *et al.*, 2011; Toh Choon *et al.*, 2012; Muniroh *et al.*, 2014). Ergosterol has also been used to detect fungal contamination in sugar beet and wheat (Rossard *et al.*, 2010; Wiwart *et al.*, 2011).

## **2.5 Development of resistant varieties**

To complement the effort taken in the detection of BSR, scientists are now looking into an alternation solution to control the disease. Oil palms that are resistant to *G. boninense* are being screened and developed as a long term solution to BSR disease (Durrand-Gasselin *et al.*, 2005; Breton *et al.*, 2006). However, we need to clearly understand the complexity of the disease to be able to contain it effectively. Screenings of resistant materials from existing fields have proven to produce results but it is very time

consuming (Durand-Gasselin *et al.*, 2005). Crossings of palms from different backgrounds, followed by progeny testings have to be established prior to determining the resistance or susceptibility of each material. The differences in susceptibility of the Deli material within the *E. guineensis* germplasm were detected by de Franqueville *et al.* (2001). These Deli materials were planted in Indonesia in areas with high BSR incidence. The ability to artificially inoculate oil palm seedlings with *G. boninense* opens up the possibility of screening for resistance to BSR in the nursery. Using a root inoculation technique, significant differences in susceptibility among 43 palms with different genetic backgrounds including *Dura* × *Dura* ( $D \times D$ ), *Dura* × *Pisifera* ( $D \times P$ ), *Tenera* × *Pisifera* ( $T \times P$ ), and *Tenera* × *Tenera* ( $T \times T$ ) have been identified. Of the 43 palms, the most susceptible was ( $D \times D$ ; Elmina × Elmina) while the most resistant was ( $D \times P$ ; Zaire × Cameroon) (Idris *et al.*, 2004). This tolerant palm was determined based on low severity of foliar symptoms and slow disease progression in the root and stem tissues.

Although extensive field trials have been conducted with the hope of identifying truly “resistant” planting material against BSR, little success has been found. Durand-Gasselin *et al.* (2005) stated that there is no *Ganoderma*-free variety, and it is advisable to remove all highly susceptible materials in the subsequent planting cycles once they have been tested.

In the 1980s, the prospect of improving crops for enhanced resistance to plant diseases through genetic manipulation was gaining tract with the onset of plant transformation. Different varieties of crops with agronomically important traits have moved towards genetically modifying the plants to be resistant to pathogens. In maize and cottonseed, a preharvest host plant resistance strategy against *Aspergillus flavus* has been developed

to control aflatoxin contamination (Cary *et al.*, 2011). This strategy utilizes genetic engineering to enhance resistance against potential pathogens. The production of crops with agronomically useful levels of resistance has been achieved with the increased knowledge of plant-fungal interactions and the advancement of cloning disease resistance genes. Production of transgenic oil palm carrying fungal resistance genes with the potential for protecting oil palms from *G. boninense* infection is being investigated (Ariffin, 2005).

## **2.6 Proteomics – Technologies and applications**

Proteomics is an area of study that examines the protein complement of the genome. It is a combination of techniques for protein separation (e.g. two-dimensional electrophoresis) with analysis and characterization of separated proteins (mass spectrometry). One of the direct approaches of building knowledge that will address many fundamental biological questions is by studying the machinery responsible for carrying out most biological functions (proteins). Furthermore, a direct approach to analyze proteins may reveal more accurate information than that inferred from mRNA measurements (Maier *et al.*, 2009; Laurent *et al.*, 2010). This is because more evidence is suggesting the disparity between mRNA levels and protein abundance. The disparities include regulatory processes that occur after mRNA is transcribed (Vogel and Marcotte, 2012). These include post-translational modifications, translational degradation and protein degradation.

Technological advancement and continuous improvements in the proteomics workflow have brought about many scientific researches to be published. Many branches of proteomic studies have emerged and these include protein separation, identification, quantification and sequence analysis. Other studies include structural, interaction,

modifications and cellular proteomics. However, the key techniques used are two-dimensional electrophoresis (2-DE) coupled with mass spectrometry (MS).

Proteomics has been extensively used to investigate and study infectious diseases, clinical applications and cancer research in humans (Pitteri *et al.*, 2009; Legrain *et al.*, 2011; Geyer *et al.*, 2016). A review by Hamrita *et al.* (2010) stated that proteomics profiling had been performed by many research groups on the human breast tumours, tumour cells and tumour fluids to look for biomarkers and to understand the molecular mechanisms associated with breast carcinoma. The same objectives have been applied to plant research. Proteomics analyses have been applied to study the growth course in rice (Nozu *et al.*, 2006), disease infections in rice (Chi *et al.*, 2010), host-pathogen interactions (Schmidt and Völker, 2011) and development of elite soybean cultivars (Qin *et al.*, 2013).

### **2.6.1 Two-dimensional electrophoresis (2-DE)**

Two-dimensional polyacrylamide gel electrophoresis (2D-PAGE) is capable of separating and resolving thousands of proteins in a single sample. The identities of the resolved proteins are determined by mass spectrometry. Furthermore, 2D-PAGE is also used to compare abundance of proteins between control and treated samples. It allows the classes of proteins to be determined due to these responses. Proteins that participate in similar or related process may show correlated differences in expression. This information can then be used to define the function(s) of proteins (Senkler and Braun, 2012)

2D-PAGE involves the extraction of proteins, followed by the isoelectric focusing of the extracted proteins based on their pIs (isoelectric points) (Oliveira *et al.*, 2014).

These proteins are then separated on polyacrylamide gels based on their molecular weight. The profiles of the separated proteins can then be visualized after the gels were stained.

For comprehensive proteome analysis, every protein would ideally be resolved as one detectable spot. However, low abundant proteins may not be detectable by 2D-PAGE and they may be omitted from subsequent analyses (Baracat-Pereira *et al.*, 2012; Fröhlich *et al.*, 2012).

This could be overcome by targeting these proteins (eg membrane proteins, low molecular weight proteins etc) using mass spectrometry. Furthermore, approximately 2000-3000 spots can be observed using standard visualization methods on a typical gel. In this case, several proteins will co-migrate to the same spot position, hence masking their accurate quantitation and identification using mass spectrometry (Baracat-Pereira *et al.*, 2012; Fröhlich *et al.*, 2012). Therefore, preparations of protein samples are crucial. Proteins could also be run through a pre-fractionation process, or focused on a narrow ranged immobilized pH gradient (IPG strips). The largest IPG strips (24 cm) that offers greater resolution could also be used to explore the proteome of lower-abundance proteins.

2D-PAGE is not without technical difficulties. Scientists have encountered problems with image resolution and reproducibility, proteins with extreme pIs, visualization methods and image analysis. Difficulties with the compatibility of mass spectrometric techniques are generally faced in the identification of proteins. However, many publications have managed to solve most of these problems and it has become a

relatively easy task to run 2D-PAGE (Karp *et al.*, 2007; Vincent *et al.*, 2009; Koroleva and Bindschedler, 2011).

### 2.6.2 Mass spectrometry (MS)

Analysis of complex protein samples have been made easy by mass spectrometry with the gene and genome sequence databases made accessible to the public. MS is the current choice for proteomic studies with the innovative breakthrough in protein ionization methods (Han *et al.*, 2008). Quantitative analysis of cellular and organellar proteomes have been made successful with high resolution MS methods (Walther and Mann, 2010). Traditionally, MS has been widely used for the quantitative measurement of specific small molecules, drug metabolites and hormones, with excellent precision and high specificity and high throughput (Nakamura and Oda, 2007). Nowadays, it has been widely used in differential analyses in disease research, particularly human cancers and crop diseases (Sadiq and Agranoff, 2008; Prieto *et al.*, 2014).

The mass-to-charge ratio ( $m/z$ ) of gas-phase ions is measured in an MS analysis. A basic mass spectrometer consists of an ion source, a mass analyzer and a detector. Analytes that enter through the ion source are converted into gas-phase ions. These ionized analytes are then separated by the mass analyser based on their  $m/z$  ratio. The number of ions at each  $m/z$  value is finally recorded by the detector. The mass spectrometers rely importantly on the separation of ions, hence the ionization source should be tailored depending on the application (Han *et al.*, 2008; Zhang *et al.*, 2013).

The matrix-assisted laser desorption/ionization (MALDI) and electrospray ionization (ESI) are two most frequently used ionization methods. They are categorized as soft ionization techniques. They are termed 'soft ionization' techniques since the ions

undergo little fragmentation as they were created with low internal energy (Whitelegge, 2013).

In MALDI, protein samples are mixed with an organic matrix and co-crystallized on a metal target. The matrix is then excited using a pulsed laser. Thermal energy rapidly heats up the molecules and subsequently desorbs the ions into the gas phase. On the other hand, ESI ionizes molecules directly from solution and then sprayed into the mass spectrometer at atmospheric pressure so it can be easily interfaced with a liquid chromatography equipment (Han *et al.*, 2008; Walther and Mann, 2010).

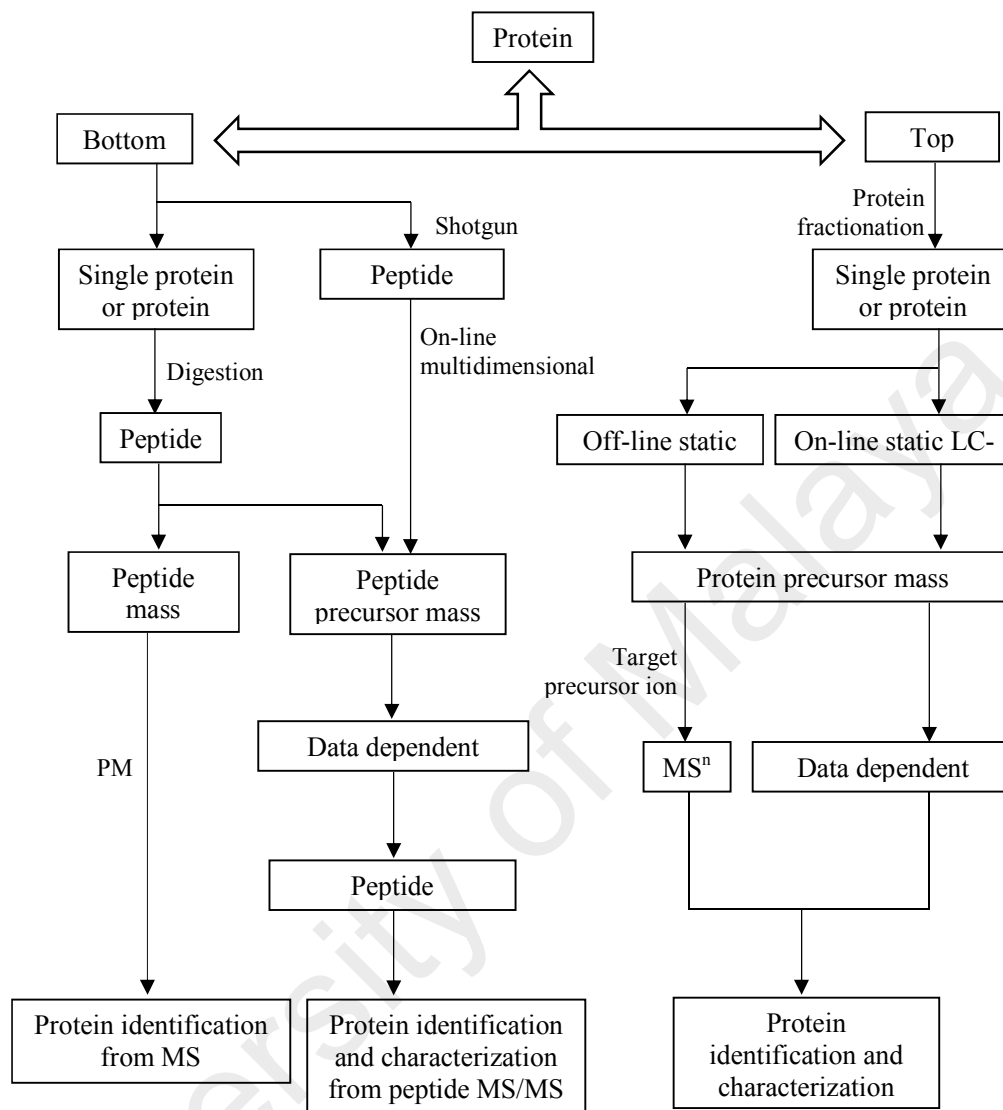
There are three types of commonly used mass analyzers for proteomics research: ion trap, quadrupole (Q) and time-of-flight (TOF). For ion traps, the mass analyzer first traps the ions for a certain time interval prior to scanning in the detector (Yates, 2004). Ion traps are able to determine the mass of a given peptide as well as its sequence. As the name suggests, quadrupoles consist of four parallel cylindrical rods. Ions are separated based on the stability of their trajectories in the oscillating electric fields when electric fields are applied to the rods (Whitelegge, 2013). In the TOF analyzer, an electrical field accelerates ions to the same kinetic energy as the velocity of the ions depending on the  $m/z$  ratio (Nakamura and Oda, 2007). Therefore, TOF measures velocity of the ions, from which the  $m/z$  ratio is determined.

A hybrid mass spectrometer is a device for tandem mass spectrometry (MS/MS). It consists of a combination of two or more different mass analyzers (Han *et al.*, 2008). MS/MS quantitates peptides more precisely and is widely used for analysis of complex mixtures (Dzieciatkowska *et al.*, 2014). Some of the hybrid instruments include triple quadrupole, quadrupole TOF, TOF/TOF.

### 2.6.3 Bottom-up and top-down proteomics

Proteomic experiments often involve concurrent analyses of many proteins from complex biological samples. The crucial feature in proteomic analysis is therefore the separation of peptides and proteins. Many MS-based proteomic strategies have been developed and improved to fulfil the various analytical and biological requirements (Fig 2.1). For these reasons, two principle proteomics approaches are employed to deliver simplified molecules from complex mixtures to the ionization source.

In top-down proteomics, intact or whole-proteins are analyzed typically using ESI. This method identifies the protein by comparing the precursor and product ion masses with those from protein databases. The main aim of top-down proteomics is to increase throughput for whole proteome analysis while preserving the inherent value of an intact protein mass measurement (Whitelegge, 2013). In bottom-up proteomics, proteins are digested into smaller peptide mixtures using trypsin. Prior to tandem mass spectrometry, these peptide mixtures are fractionated by multidimensional chromatography. When complex protein mixtures are used in the bottom-up approach, it is called shot-gun proteomics (Han *et al.*, 2008). In short, the bottom-up method measures proteolytic peptides while the top-down approach analyzes intact proteins (Zhang *et al.*, 2013).



Adapted from Han *et al.* (2008). *Current Opinion in Chemical Biology*, 12: 483-490

**Figure 2.1:** Strategies for protein identification and characterization using mass spectrometry. Proteins extracted from biological samples can be analysed by bottom-up or top-down approaches. In the bottom-up approach, proteins in complex mixtures can be separated before enzymatic or chemical digestion. This is followed by direct peptide mass fingerprinting-based acquisition, or further peptide separation coupled to tandem mass spectrometry. Alternatively, the protein mixture can be directly digested into peptides using the shotgun approach. In the top-down approach, proteins in complex mixtures are fractionated and separated into less complex mixtures. This is followed by intact protein mass measurement and intact protein fragmentation.

## CHAPTER 3: METHODOLOGY

### 3.1 Plant material

For optimisation of protein extraction protocols, oil palm leaves were obtained from both young (less than one year old) and mature (five years old) palms. Both young and mature leaves were sampled from commercial *Dura* x *Pisifera* (*DxP*) palms. Germinated *DxP* seedlings obtained from Sime Darby Seeds and Agricultural Services Sdn Bhd were used for artificial inoculation of *Ganoderma boninense*. All materials were sampled from Carey Island, Banting. Leaves from inoculated (treated) and non-inoculated seedlings obtained from nursery challenged seedlings were used for differential protein expression studies. Seedlings were destructed at 9am. In both cases, leaves were thoroughly cleaned with tap water and surface sterilized with 70% ethanol. They were then cut into shorter segments, immediately frozen in liquid nitrogen and stored at -80°C prior to protein extraction. Approximately 2.5 g of ground leaf tissue was used in each extraction.

### 3.2 Sources of *Ganoderma* culture

Cultures of *G. boninense* PER71 were obtained from *Ganoderma* & Diseases Research of Oil Palm Unit Laboratory, MPOB. The cultures were maintained on potato dextrose agar (PDA) at Crop Protection Unit, Sime Darby Research Sdn Bhd, Banting, Selangor.

### 3.3 Preparation of fungal culture, rubber wood block (RWB) inoculums and nursery trial

*Ganoderma boninense* isolate PER71 was subcultured onto PDA in the dark for 10 days. RWBs of 6 cm x 6 cm x 6 cm were used as a source of inoculum for fungal colonization. Briefly, the RWB were washed and soaked overnight in water after which they were autoclaved at 121°C for 45 min. The mature *G. boninense* plate cultures that

have been cut into smaller pieces were inoculated into the RWBs and incubated in the dark for three months until the blocks were fully colonized. All preparations of the nursery trial were carried out according to the Oil Palm Nursery Technique Good Agricultural Practices (Sime Darby Plantation). The oil palm seedlings were housed in a randomized block design. The seedlings were watered twice a day and fertilized once every month. Fungicides were not incorporated in this single stage nursery as they are lethal to the fungus. The nursery was covered with nettings which allowed 50% sunlight penetration. A total of 240 germinated seedlings were used in this study: 120 seedlings were treated with *G. boninense* inoculated RWBs while the remaining 120 seedlings were not treated with *G. boninense* inoculated RWBs. This time-course study was terminated after six months. For treatments, the inoculated RWBs were positioned in polybags half filled with soil after which they were filled up with more soil. The germinated seedlings were then sowed approximately 2 cm below the surface of the soil. The plants were left to grow in the nursery for two months before sampling activities commenced. In this time course study, destructive sampling commenced when the plants were two-months old (two-months post infection, 2-mpi) until they were seven-months old (7-mpi). Leaves were collected from these seedlings for 2-DE analysis. The physical appearances of the plants were recorded to compare the phenotypes between control and treated plants.

### **3.4 Total protein extraction protocols**

Four protein extraction methods were evaluated. All centrifugation steps were performed at 4°C unless otherwise stated. All resulting pellets were re-solubilised in Reagent 3 (ReadyPrep Sequential Extraction Kit, Bio-Rad) and centrifuged at 12,000 ×g for 10 min to remove debris. Extracted proteins were first run on SDS-PAGE, followed by three 2D-PAGE gel replicates for each extraction method that was tested.

### **3.4.1 Phenol-guanidine isothiocyanate method (M1)**

Total protein was extracted using a modified phenol-guanidine isothiocyanate method (Wong and Sazaly, 2005). Briefly, 5 mL of TRI Reagent (Molecular Research Centre, Inc) was added to homogenized tissue. This was followed by vigorous vortexing to mix the samples, and incubated at room temperature for 15 min. The mixture was then centrifuged at 12,000  $\times$ g for 10 min to remove insoluble material. The clear phenol extract (protein) was transferred into a new tube where 200  $\mu$ L of chloroform was then added into the transferred extract. The content of the tube was then vortexed vigorously for 15 s and then incubated for 10 min at room temperature. It was then centrifuged at 12,000  $\times$ g for 10 min to remove insoluble material. The RNA-containing aqueous phase was carefully discarded and 300  $\mu$ L of cold absolute ethanol was added to precipitate the nucleic acids. The tube was inverted to mix the contents and it was then incubated for 5 min. The mixture was centrifuged at 2,000  $\times$ g for 5 min, after which the phenol-ethanol supernatant (protein extract) was transferred into a new tube. The protein extract was then precipitated with 1.5 mL cold isopropanol. After incubation for 30 min at room temperature, the mixture was centrifuged at 12,000  $\times$ g for 10 min. The resulting protein pellet was then washed three times in 1.5 mL cold 0.3 M guanidine hydrochloride in 95% ethanol. During each washing step, the protein pellet was stored in the wash solution for 20 min and then centrifuged at 7,500 g for 5 min. After the final wash, the protein pellet was vortexed in 1.5 mL absolute ethanol. After incubation for 20 min, the pellet was centrifuged at 7,500  $\times$ g for 5 min and then vacuum dried.

### **3.4.2 TCA-acetone precipitation method (M2)**

Total protein was extracted using a modified TCA-acetone method (Carpentier *et al.*, 2005). Briefly, ground tissue was precipitated in 5 mL cold acetone/20% TCA/0.2% DTT at -20°C. After an overnight incubation, the mixture was centrifuged at 10,000  $\times$ g

or 30 min. Pellet was rinsed twice in cold acetone/0.2% DTT after the supernatant has been discarded. At each rinsing step, the mixture was incubated for 1 hr at -20°C after which the mixture was centrifuged at 10,000 ×g for 10 min. The resulting pellet was then air-dried.

### **3.4.3 Sucrose method (M3)**

Total protein was extracted using a modified sucrose method (He *et al.*, 2005). Briefly, 5 mL of sucrose extraction buffer (5% sucrose, 4% CHAPS, 5% β-ME and 0.05 g PVPP) was added to ground tissue. The mixture was incubated at room temperature for 10 min with gentle swirls. This was followed by centrifugation at 10 000 ×g for 5 min. The resulting supernatant was heated at 95°C for 3 min and subsequently cooled to room temperature. Proteins were precipitated by adding 5 volumes of cold acetone/0.07% DTT to the cooled supernatant. The mixture was incubated at -20°C for at least 1 hr. Following incubation, it was centrifuged at 10,000 ×g for 10 min. The pellet was resuspended in 5 mL of extraction buffer (without PVPP) and then centrifuged at 10,000 ×g for 5 min. The supernatant was then transferred to a new tube where cold acetone/0.07% DTT was added. The mixture was vortexed thoroughly and incubated at -20°C for 1 hr. It was then centrifuged at 10,000 ×g for 5 min after which the supernatant was discarded. A total of 4 volumes of cold 80% acetone/0.07% DTT was again added to the pellet, vortexed and then incubated at -20°C for 1 hr. The final resulting pellet was left to air-dry.

### **3.4.4 TCA-acetone-phenol method (M4)**

Total protein was extracted using a modified TCA-acetone-phenol method (Barraclough *et al.*, 2004, Wang *et al.*, 2003). Briefly, 10 mL of 10% TCA in acetone was added to ground leaf tissue and incubated overnight at -20°C. The mixture was then centrifuged

at 10,000 ×g for 15 min and the supernatant was discarded. The pellet was washed three times in cold acetone/0.07% DTT. During the first and second washes, the pellet was resuspended in acetone/0.07% DTT, incubated at -20°C for an hour and then centrifuged at 10,000 ×g for 15 min. For the final wash, the pellet was resuspended in acetone/0.07% DTT, vortexed and then centrifuged. After the pellet has been air-dried, it was suspended in 5 mL lysis buffer (7 M urea, 2 M thiourea, 2% CHAPS, 40 mM Tris and 75 mM DTT) and then sonicated in a water bath for 15 min. The temperature of the water bath was monitored to prevent it from rising beyond 30°C. After centrifugation at 15,000 ×g for 3 min at room temperature, the supernatant was transferred to a new tube. One volume of cold dense SDS buffer (0.1 M Tris-HCl, pH 8; 30% sucrose, 2% SDS and 5% β-ME) was added to the supernatant and vortexed. A further 1 volume of phenol (pH 8.0) was then added to the solution and vortexed. The phenolic phase was transferred to a new tube after centrifugation at 15 000 ×g for 3 min after which 1 volume of dense SDS buffer was added again. After another centrifugation, the resulting phenolic phase was collected and then 5 volumes of cold 0.1 M ammonium acetate in methanol were added. The mixture was incubated for 1 hr at -20°C and then centrifuged at 15,000 ×g for 5 min. The pellet was washed once in cold methanol and then twice in cold acetone/0.07% DTT. The final resulting pellet was allowed to air-dry.

### **3.5 Protein extraction of leaf tissues for 2-DE**

Oil palm fronds were sampled from ten non-inoculated and ten inoculated seedlings every month starting from 2-mpi to 7-mpi in this time course study. All the leaflets from each oil palm seedling were collected, with the petioles removed, cleaned under tap water, surface sterilized, cut into smaller pieces and immediately immersed in liquid nitrogen. The leaf tissues of each seedling were then ground into fine powder. The ground leaf tissues of ten individual seedlings were finally pooled together for protein

extraction. Leaf proteins were extracted using the TCA-acetone-phenol (M4) method and quantitated using Bradford assay. Proteins from each pooled sample were then run on 2D-PAGE.

### **3.6 Protein quantification**

The concentrations of solubilised protein pellets were estimated using Bio-Rad Protein Assay (Bio-Rad) according to the manufacturer's instructions with BSA (Fraction V, Sigma) as standard.

### **3.7 SDS-PAGE**

The profiles of protein extracts were evaluated for purity and quality by SDS-PAGE. For each extract, 5 µg of protein was suspended in 2.5 µL loading buffer (0.25 M Tris, 1.92 M glycine, 1% SDS, 20 mM DTT) with distilled water to a total volume of 10 µL. The solution was heated at 95°C for 10 min and immediately put on ice before it was separated through 5% stacking gels followed by 12.5% resolving gels. Electrophoresis was performed at 100 V for 1.5 h using a Mini-PROTEAN 3 Cell (Bio-Rad) with 0.75 mm thick combs to separate proteins based on their mass. The gels were stained using a modified silver staining procedure (Blum *et al.*, 1987).

### **3.8 2-DE analyses**

#### **3.8.1 Optimization of 2-DE protocol**

Protein extracts obtained from the four extraction methods were resolved by isoelectric focusing in the first dimension, followed by SDS-PAGE in the second dimension. IEF was performed using 7 cm pH3-10NL ReadyStrip IPG Strips (Bio-Rad) where the first dimension was run on the Ettan IPGphor 3 IEF system (GE Healthcare) at 20°C. Second dimension SDS-PAGE was run on Mini-PROTEAN 3 Cell (Bio-Rad). Briefly, 5 µg of

protein extracts was mixed with thiourea rehydration solution (GE Healthcare) to a total volume of 125  $\mu$ L. The strips were subsequently rehydrated for at least 16 hours before they were electro-focused on the ceramic manifold for a total of 10,525 Vh with the following programme: 100 V for 100 Vh, 300 V for 600 Vh, 1,000 V for 325 Vh at gradient mode, 5,000 V for 4,500 Vh at gradient mode and finally 5,000 V for 5,000 Vh. IEF was performed at 50  $\mu$ A for the entire focusing step. The focused strips were then equilibrated in reducing buffer [6 M urea, 75 mM Tris-HCl (pH8.8), 29.3% glycerol, 2% SDS, 0.002% bromophenol blue, 1% DTT] for 15 min followed by an alkylation buffer [6 M urea, 75 mM Tris-HCl (pH8.8), 29.3% glycerol, 2% SDS, 0.002% bromophenol blue, 2.5% IAA] for another 15 min. Equilibrated strips were then electrophoresed on 1 mm thick 12.5% polyacrylamide gels overlaid with agarose sealing solution (25 mM Tris base, 192 mM glycine, 0.1% SDS, 0.5% agarose, 0.002% bromophenol blue) at 100 V for 1.5 h.

### **3.8.2 Analytical gels**

At total of 30  $\mu$ g of proteins were mixed with thiourea rehydration solution (GE Healthcare) to a total volume of 250  $\mu$ L. Since ten biological samples were pooled, four technical replicates were run for each sample to reduce any technical variations. Protein samples were applied onto 13 cm, pH4-7 IPG strips by passive rehydration for at least 16 hours before they were electro-focused on the ceramic manifold to a total of 36,700 Vh with the following programme: 100 V for 200 Vh, 500 V for 500 Vh, 1,000 V for 750 Vh at gradient mode, 8,000 V for 11,250 Vh at gradient mode and finally 8,000 V for 24,000 Vh. IEF was performed at 50  $\mu$ A for the entire focusing step. Focused strips were electrophoresed on 1-mm-thick 12.5% polyacrylamide gels using the SE600 Ruby system (GE Healthcare) at 10 mA/gel for 15 min, followed by 50 mA/gel for 4 hrs. Preparative gels containing 90  $\mu$ g of proteins were prepared for spot picking.

### 3.8.3 Protein visualization, image acquisition and data analysis

Protein spots were visualized using a modified silver staining protocol (Blum *et al.*, 1987). Briefly, gels were soaked in fixing solution (40% MeOH, 10% CH<sub>3</sub>COOH) overnight, washed with 30% MeOH and then with milli-Q water, with each washing lasted for 20 min. This was followed by sensitization with 0.02% Na<sub>2</sub>S<sub>2</sub>O<sub>3</sub> for 20 min. Gels were then washed with milli-Q water thrice for 20 s and stained using 0.2% silver nitrate (Sigma). After washing, the gels were developed (6% Na<sub>2</sub>CO<sub>3</sub>, 0.004% Na<sub>2</sub>S<sub>2</sub>O<sub>3</sub>, 0.05% formaldehyde) until they were saturated with spots. The reaction was stopped by using 0.5% glycine. Gel images were scanned using ImageScanner III (GE Healthcare).

For preparative gels, a sensitive colloidal staining protocol with G250 (Westermeier, 2006) was used to stain the gels for spot picking. Briefly, gels were fixed in 50% ethanol/ 3% H<sub>3</sub>PO<sub>4</sub> for at least 3 hrs. They were then washed in milli-Q water, thrice, for 20 min. After that, the gels were pre-incubated for 1 hr in 34% (v/v) MeOH/ 3% (w/v) H<sub>3</sub>PO<sub>4</sub>/ 17% (w/v) (NH<sub>4</sub>)<sub>2</sub>SO<sub>4</sub> solution. Finally, 0.53 g/1.5 L of Coomassie Brilliant Blue G-250 powder was added to the solution and stained for 4-5 days on a rotary shaker. The gels were then washed in several changes of milli-Q water to remove background stain.

Gel images were analyzed using ImageMaster 2D Platinum version 7 (GE Healthcare).

The spots were quantified based on their relative volume where the spot volume is divided by the total volume of the whole set of gel spots. In this exercise, four technical replicates were performed for each sample. After spot detection, volumetric quantification and spot matching, differences in the protein amounts between the treatment and control conditions were analyzed by Student's *t*-test and the Benjamini-Hochberg procedure which were then calculated as fold-ratios. A criterion of  $p \leq 0.05$ ,

$q \leq 0.05$  and a fold-change  $\geq 2.0$  were used to define statistically significant changes in protein spot abundance between non-inoculated and inoculated samples.

#### **3.8.4 Trypsin digest and LC-QToF analysis**

Spots that changed in abundance were manually excised, destained, reduced with 100 mM DTT in 100 mM  $\text{NH}_4\text{HCO}_3$  at 60°C, alkylated with 55 mM IAA in 100 mM  $\text{NH}_4\text{HCO}_3$  in the dark and dehydrated with ACN. Digestions were subsequently carried out overnight at 37°C with 6 ng/ $\mu\text{L}$  trypsin (Trypsin Gold, Promega) in 50 mM  $\text{NH}_4\text{HCO}_3$ . The resulting peptides were extracted with ACN before they were injected into an LC-QToF (Waters Corporation) for analysis. Peptide separation was performed on a 180  $\mu\text{m}$   $\times$  20 mm Symmetry (5  $\mu\text{m}$ ) C18 precolumn (Waters Corporation) coupled to a 200 mm  $\times$  75  $\mu\text{m}$  BEH130 (1.7  $\mu\text{m}$ ) C18 column (Waters Corporation), with a gradient of 1-40% ACN over 90 min. The MS was operated in positive ion mode with a source temperature of 80°C, a cone gas flow of 40 l/h, and a capillary voltage of approximately 3 kV. Mass spectra were acquired in continuum V-mode and spectra integrated over 0.5 s intervals using MassLynx 4.1 software (Waters Corporation). The instrument was calibrated using selected fragment ions of the CID (collision-induced dissociation) of Glu-Fibrinopeptide B (Waters Corporation).  $\text{MS}^E$  was employed for MS/MS analysis. The MS spectra were collected from  $m/z$  50 to  $m/z$  1,990 and product ion MS/MS spectra were collected from  $m/z$  50 to  $m/z$  1,990. Lock mass correction of the precursor and product ions was conducted with 500 fmol/ $\mu\text{l}$  Glu-Fibrinopeptide B in 0.1% formic acid in MeOH/water (50:50, v/v) respectively, and introduced via the reference sprayer of the NanoLockSpray interface. ProteinLynx Global-SERVER v2.3 (PLGS, Waters Corporation) software was used as a platform for data processing of the spectra and database search. A 10 ppm peptide, 0.1 Da fragment tolerance, one missed cleavage, peptide charge 1+, monoisotopic experimental mass values, and variable

oxidation (M) and carbamidomethylation (C) were used as search parameters. The resulting mass spectra were searched against the protein index of the Swiss-Prot protein database for protein identification applying the algorithm implemented in the PLGS software. The false discovery rate was set to 4% of proteins included in the database. All samples were run as technical triplicates. Protein identifications consistent in two out of three LC-MS runs were considered as present in that sample.

### **3.9 Protein blotting**

Leaf tissues from three individual oil palms each were sampled from 3-mpi non-inoculated and inoculated seedlings. Total proteins from these leaf tissues were extracted using the TCA-acetone-phenol method. The concentrations of the proteins were determined using Bio-Rad Protein Assay as discussed previously. Following this, 10 µg of protein was loaded into a 7 cm SDS-PAGE and run at 100V until the dye front reaches the end of the resolving gel. After electrophoresis is completed, the gel was equilibrated in the transfer buffer (25 mM Tris, 192 mM glycine, 20% MeOH) for 30 min.

A 0.45µm PVDF membrane was cut according to the size of gel, soaked in methanol and then equilibrated in the transfer buffer. Three sheets of filter papers saturated with transfer buffer were placed on the anode. The equilibrated PVDF membrane was placed on top of the filter paper stack. Bubbles between the membrane and filter papers were removed by rolling a test tube over the surface of the membrane. The gel was placed on top of the membrane. A test tube was gently rolled over the surface of the gel to insure intimate contact between gel and membrane and also to remove any interfering bubbles. Finally, the transfer stack is completed by placing another three pieces of filter papers on top of the gel and the bubbles were removed as described above.

To complete the circuit, the top electrode was placed onto the transfer stack. The high-voltage leads were carefully connected to the power supply and a constant current of 150 mA for 45 min was applied to initiate protein transfer. The membrane was removed from the transfer stack and the orientation of the stack was marked using a pencil. The membrane was left to air-dry before immunoprobing.

### **3.9.1 Immunoprobing with antibodies**

Five rabbit polyclonal plant antibodies, namely 14-3-3 GRF (14-3-3-like protein GF14 psi, Agrisera), CSD2 (Cu/Zn superoxide dismutase, Agrisera), MnSOD (manganese superoxide dismutase, Agrisera), cAPX (ascorbate peroxidase, Agrisera) and RbcL (Rubisco large subunit, Agrisera) were used to detect the specific proteins that are present in both control and inoculated (treated) leaf tissues. RbcL was used as a loading control.

The PVDF membrane was first activated by rinsing it in methanol. It was then washed three times in cold 0.05% PBS-T (0.05% Tween 20 in 1X-PBS) for 10 min each. The membrane was incubated in a blocking buffer (0.05% Tween 20 in 1X PBS) containing 5% BSA for 1 hr. This is followed by incubating the membrane overnight at 4°C with agitation, in a blocking buffer containing 1% BSA. The primary antibodies of choice were diluted accordingly (Table 3.1). The membrane was then washed in cold 0.05% PBS-T for 10 min, thrice. The alkaline phosphatase-based polyclonal secondary antibody of choice (GeneTex) was first diluted in a blocking buffer containing 5% BSA before the membrane was incubated for 2 hr at room temperature. The secondary antibody used was a goat anti-rabbit in which the primary antibody was raised. The membrane was then washed in cold 0.05% PBS-T for 10 min, thrice before proceeding with detection.

**Table 3.1:** The list of commercially available plant antibodies that were used for Western validation of four candidate proteins. RuBisCO large subunit-binding protein as the loading control.

Primary antibody		Dilution
14-3-3 GRF (14-3-3 like protein)	Rabbit polyclonal	1: 2,000
MnSOD (manganese superoxide dismutase)	Rabbit polyclonal	1: 2,000
CSD2 (Cu/Zn superoxide dismutase)	Rabbit polyclonal	1: 5,000
cAPX (ascorbate peroxidase)	Rabbit polyclonal	1: 10,000
RbcL (control)	Rabbit monoclonal	1: 10,000

### 3.9.2 Visualization with chromogenic substrates

The NBT/BCIP colour development substrate (Promega) was used to detect the alkaline phosphatase conjugated secondary antibody. For every 5 mL of alkaline phosphatase buffer [100 mM Tris-HCl (pH 9.0), 150 mM NaCl, 1 mM MgCl<sub>2</sub>], 33 µL of NBT and 16.5 µL BCIP was added. The NBT was added first and mixed well. This was then followed by the BCIP and mixed again. The solution was used within 1 hr. Any unused solutions were discarded.

### 3.9.3 Quantification of western blots

Protein bands from western blots were quantified to reflect the relative amounts of protein bands as a ratio that is present in the sample in relation to the loading controls. The blots were scanned using Typhoon FLA 9000 (GE Healthcare) and analysed using ImageQuantTL (GE Healthcare). In this analysis, lanes and the area of interest which corresponds to the position of detectable bands were specified. This is followed by background subtraction where the background intensity is compensated in the image, so that the measured band volumes are a closer representation of the amount of material in the bands. The rolling ball method was used a background subtraction. Once

background has been subtracted, bands were detected to define the bands in the image lanes. After that, the positions of the bands were calibrated with reference to a protein ladder. This was also used to calculate the properties of bands in other samples. The amount of material in all bands in the image was calculated from the band volume (total sum of pixel intensities), calibrated from values entered for bands with known amounts. Finally, normalization was calculated based on band volumes relative to a defined value for one or more reference bands.

### **3.10 Characterization of 2-cys peroxiredoxin**

#### **3.10.1 Bioinformatic analysis**

The amino acid sequence of 2-cys peroxiredoxin, a protein candidate identified in Section 3.8 above, was compared against the nucleic acid sequence of the oil palm transcriptome (Sime Darby Technology Centre Sdn Bhd) for the presence of possible transcripts. The transcriptome consists of pooled oil palm root tissues of both non-inoculated and those that have been artificially inoculated with *G. boninense*. The predicted amino acid sequence was searched using InterProScan for protein sequence analysis and classification.

#### **3.10.2 RNA extraction**

RNA was extracted from leaf tissues of oil palm seedlings according to Asemota and Shah (2004). A total of 5 g of ground oil palm leaf tissue was used for this purpose. Fifteen mL of extraction buffer [0.1 M Tris-HCl (pH 7.6), 0.1 M NaCl, 6% p-aminosalicylic acid, 1% SDS, 0.35%  $\beta$ -mercaptoethanol and 5% phenol] and 2% (w/v) PVPP were added into the sample and vortexed to mix. A ratio of phenol: chloroform: isoamyl alcohol (25:24:1) was then added into the mixture and thoroughly vortexed. It was then centrifuged at 4°C at 10,000 rpm for 15 min. The supernatant was transferred

to a new tube and an equal volume of chloroform: isoamyl alcohol (1:1) was added. The solution was then mixed, centrifuged and the resulting supernatant was collected. This step was repeated by adding an equal volume of chloroform: isoamyl alcohol (1:1). The supernatant obtained after this step was added with one third volume of 8 M LiCl. It was then incubated overnight at -20°C. After centrifugation at 4°C, 10,000 rpm for 30 min, the resulting pellet was resuspended in DEPC-treated water. The dissolved pellet was transferred to 1.5 mL microcentrifuge tubes where one third volume of 8 M LiCl was added. The solution was incubated at 4°C for 4 hr. After centrifugation at 4°C, 10,000 rpm for 30 min, the pellet was finally resuspended in DEPC-treated water. The NanoDrop spectrophotometer was used to quantify and assess the purity of the extracted RNA. It was run on 1% agarose gels at 110 V for 40 min to determine the integrity of the RNA.

### **3.10.3 Reverse-transcription polymerase chain reaction (RT-PCR)**

One  $\mu\text{g}$  RNA was reverse-transcribed into cDNA using the SuperScript III Reverse Transcriptase (Invitrogen) according to the manufacturer's instructions. Cyclophilin was used as a control for reverse transcription. The RNA was treated with RQ1 RNase-free DNase (Promega) prior to RT-PCR to degrade both double-stranded and single-stranded DNA. One unit of RQ1 RNase-free DNase, 1  $\mu\text{L}$  RQ1 RNase-free DNase 10X Reaction Buffer and 1  $\mu\text{L}$  RNA were used to prepare the reaction. Nuclease-free water was added to a final volume of 10  $\mu\text{L}$ . The mixture was incubated at 37°C for 30 min in a heating block. One  $\mu\text{L}$  of RQ1 DNase Stop Solution was added into the tube to terminate the reaction. The following components were added to the DNase treated RNA: 1  $\mu\text{L}$  of 50 mM oligo(dT)<sub>20</sub>, and  $\mu\text{L}$  10 mM dNTP mix (Invitrogen). The mixture was heated in a heating block at 65°C for 5 min and was immediately incubated on ice for at least 1

min. The tube was briefly centrifuged to collect the contents of the tube. The following components were added into the tube: 4  $\mu\text{L}$  of 5X First-Strand Buffer, 1  $\mu\text{L}$  0.1 M DTT, 1  $\mu\text{L}$  RNaseOUT™ Recombinant RNase Inhibitor and 1  $\mu\text{L}$  of SuperScript III RT. The contents of the tube were mixed by gently pipetting up and down before incubation at 60°C for 1 hr. The reaction was finally inactivated by heating the tube at 70°C for 15 min.

#### **3.10.4 Amplification of cDNA encoding 2-cys peroxiredoxin gene**

A list of transcripts was generated from the search against the oil palm root transcriptome. The priority of transcripts for cloning work was chosen based on those with the highest score (bits) and E value. Primer pairs for amplification of the transcripts were designed using Primer Premier version 3 (Premier Biosoft International). Isotig\_46827 was amplified using a forward primer (5' AGTGAACGAGCGAAGGGTA 3') and a reverse primer (5' AACCCACAAACTGAAACCCTTATT 3'). The following components were mixed prior to PCR amplification: 200 ng cDNA, 25  $\mu\text{L}$  MyTaq HotStart Red Mix (Bioline), 1  $\mu\text{L}$  of 20  $\mu\text{M}$  forward primer, 1  $\mu\text{L}$  of 20  $\mu\text{M}$  reverse primer and sterile distilled water was added to a total volume of 50  $\mu\text{L}$ . PCR amplification was carried out with the following cycling conditions: initial denaturation at 95°C for 1 min, denaturation at 95°C for 15 s, annealing at 50°C for 15 s and extension at 72°C for 10 s for 35 cycles. The PCR products were run on 1% agarose gels at 110 V for 40 min to determine the size of amplicons.

Amplicons with the correct size were first gel purified using Wizard SV Gel and PCR Clean-up System (Promega). Bands were excised from the gel, cut into smaller pieces and transferred into a microcentrifuge tube. Ten  $\mu\text{L}$  of Membrane Binding Solution was

added to 10 mg of gel slice. The tube was vortexed vigorously and incubated at 60°C until the gel slices were fully dissolved. The dissolved gel mixture was transferred into an SV Minicolumn which has been inserted into a collection tube. The column was centrifuged at 16,000 ×g for 1 min, after which the flow-through was discarded. A total of 700 µL of Membrane Wash Solution (containing ethanol) was added to the column, centrifuged at 16,000 ×g for 1 min and the flow-through was discarded. Another 500 µL of Membrane Wash Solution (containing ethanol) was added, centrifuged at 16,000 ×g for 5 min and the flow-through was discarded. The column was centrifuged for another 1 min to remove any residual alcohol. The column was then transferred to a clean microcentrifuge tube where 30 µL of nuclease-free water was added. The reaction was incubated at room temperature for 1 min, centrifuged at 16,000 ×g for 1 min to collect the eluant.

### **3.10.5 Cloning and transformation**

The purified gel product was cloned into Zero Blunt TOPO<sup>®</sup> cloning vectors (Invitrogen) and transformed into competent TOP10 chemically competent *E. coli* cells for plasmid extraction using PureYield<sup>™</sup> Plasmid MiniPrep (Promega). The extracted plasmids were sent for DNA sequencing to determine the precise order of nucleotides of the amplicons. The following components were mixed together to set up the cloning reaction: 2 µL of purified gel product, 1 µL of Salt Solution, 1 µL pCR<sup>™</sup>II-Blunt-TOPO and 2 µL of sterile distilled water to a total volume of 6 µL. The cloning reaction was gently mixed, incubated at room temperature for 5 min and on ice for 10 min.

For transformation, 2 µL of the cloning reaction was added to a vial of OneShot<sup>®</sup> TOP10 chemically competent *E. coli* cells and mixed gently. The cells were heat shocked for 30 s at 42°C. The tube was then immediately transferred on ice where 200

$\mu\text{L}$  of room temperature SOC medium was added to the reaction. The tube was then incubated at  $37^{\circ}\text{C}$  at 200 rpm for 1 hr. Fifty  $\mu\text{L}$  of the transformants were spread onto LB plates containing 50  $\mu\text{g}/\text{mL}$  kanamycin and then plates were incubated at  $37^{\circ}\text{C}$  overnight.

White, positive transformants were analysed by culturing one single colony into LB medium containing 50  $\mu\text{g}/\text{mL}$  kanamycin at  $37^{\circ}\text{C}$  overnight. A total of 100  $\mu\text{L}$  of Cell Lysis Buffer was added to a 600  $\mu\text{L}$  overnight culture. The tube was inverted six times after which 350  $\mu\text{L}$  of cold Neutralization Solution was added. The contents of the tube were thoroughly mixed and centrifuged at  $16,000 \times g$  for 3 min. The supernatant was transferred to a PureYield™ Minicolumn which is attached to a collecting tube. This was followed by centrifugation at  $16,000 \times g$  for 15 s, after which the flow-through was discarded. A total of 200  $\mu\text{L}$  of Wash Buffer was added to the minicolumn and centrifuged at  $16,000 \times g$  for 15 s. A total of 400  $\mu\text{L}$  of Column Wash Solution (containing ethanol) was added to the minicolumn and centrifuged at  $16,000 \times g$  for 30 s. After that, the minicolumn was transferred to a clean microcentrifuge tube where 20  $\mu\text{L}$  of Elution Buffer was added. The column was left to stand for 1 min at room temperature. Plasmid DNA was eluted from the column by centrifugation at  $16,000 \times g$  for 1 min and sent for DNA sequencing to confirm the sequence of the 2-cys peroxiredoxin gene construct.

### **3.10.6 Preparation of vector and insert**

After verification of the sequences, primer pairs were designed to include restriction cutting sites for cloning the 2-cys peroxiredoxin gene into an expression vector, pET-49(b) (Novagen). The sequences of the primers are as follows: forward primer 5' GAATTCAATGGCTTGCTCCGTTCTCT 3' and reverse primer 5'

TGCGGCCGCCTATATAGCTGCGAAGTA 3'. The PCR products were run on 1% agarose gel to determine their sizes. Amplicons with the correct size were then gel purified, cloned and transformed into competent TOP10 chemically competent *E. coli* cells for plasmid extraction (Section 3.10.3). The extracted plasmids were sent for DNA sequencing to determine the sequences of the amplicons.

Once the correct sequences have been verified, the expression vector was digested and gel-purified to release the insert. Once the insert has been prepared, it was cloned into the pET vector. A standard reaction containing 2  $\mu$ L 10X ligase buffer (with 10 mM ATP and DTT), 1  $\mu$ L linearized pET-49b(+) vector, 3  $\mu$ L 2-cys peroxiredoxin insert, 2  $\mu$ L T4 ligase and 3  $\mu$ L nuclease-free water to a total of 10  $\mu$ L. The solution was mixed gently and incubated at 16°C overnight. One  $\mu$ L of ligation reaction was used for transformation into TOP10 chemically competent *E. coli* cells (Section 3.10.6). Plasmids from the positive transformants were subsequently sequenced to confirm the orientation of the insert and the correct reading frame of the 2-cys peroxiredoxin gene construct in the expression vector.

Once the orientation and reading frames have been confirmed, the expression vector carrying the correct insert was transformed into BL21(DE3) competent *E. coli* cells. A total of 5  $\mu$ L containing 10  $\mu$ g of the plasmid was added to the competent cells. The contents of the tube was mixed by carefully flicking the tube, heat shocked at 42°C for 30 s and immediately cooled on ice. A total of 200  $\mu$ L of SOC medium was added to the tube and incubated at 200 rpm for 1 hr at 37°C. A total of 50  $\mu$ L of transformants were evenly spread onto LB agar containing 50  $\mu$ g/mL kanamycin and 2% glucose. The plates were incubated at 37°C overnight. A negative control containing only the pET49b(+) vector and a positive control containing  $\beta$ -galactosidase were also

transformed into the competent cells.

### **3.10.7 Expression of recombinant 2-cys peroxiredoxin protein**

White, positive transformants were picked for protein expression. A single colony from each transformation was cultured in 5 mL LB medium containing 50 µg/mL kanamycin and 2% glucose at 200 rpm, overnight at 37°C. A total of 500 µL of overnight broth culture was transferred into fresh 10 mL LB medium containing 50 µg/mL kanamycin and 2% glucose. The fresh cultures were incubated at 200 rpm at 37°C to an OD<sub>600</sub> of approximately 0.5. Prior to induction, the culture was split into 2 x 2 mL cultures. Two mL of fresh LB broth and IPTG were added to a final concentration of 0.5 mM IPTG, while the other was treated as an uninduced control. The induced culture was then incubated at 200 rpm for 3 hr at 37°C for the expression of recombinant protein. After induction, 1 mL of the induced culture was transferred to a fresh tube for the extraction of recombinant proteins.

### **3.10.8 Soluble cytoplasmic fraction**

The soluble cytoplasmic fraction was extracted using the BugBuster Protein Extraction Reagent (Novagen). The cells were harvested from the liquid culture by centrifugation at 10,000 ×g for 10 min. The supernatant was decanted and the pellet was allowed to drain, to remove any excess liquid. For every 1 g of pellet, 5 mL of BugBuster reagent was used to completely resuspend the pellet. Five µL of Benzonase per mL of BugBuster reagent was used for the suspension. The cell suspension was then incubated on a rotating mixer for 20 min at room temperature, after which they were collected by centrifugation at 16,000 ×g for 20 min at 4°C. The pellet was resuspended in 5 mL of BugBuster reagent and mixed by vortexing. Lysozyme was added to a final concentration of 200 µg/mL. The cell suspension was mixed by vortexing and incubated

for 5 min at room temperature. Six volumes of 1:10 diluted BugBuster reagent was added to the suspension and vortexed for 1 min. The suspension was then centrifuged at 16,000  $\times$ g for 15 min at 4°C to remove the supernatant. The resulting pellet was resuspended in 1X PBS (Thermo Scientific). The extracted proteins were run on SDS-PAGE (Section 3.7) and stained using silver nitrate (Section 3.8.3). The band containing the expressed protein was excised from the polyacrylamide gel, destained, trypsin digested and identified using LC-QToF mass spectrometer (Section 3.8.4).

### **3.10.9 Purification of recombinant 2-cys peroxiredoxin protein**

The recombinant protein was purified using HisPur™ Ni-NTA Purification Kit (Thermo Scientific) from the soluble protein extract. The spin column, containing 1 mL resin bed, was first equilibrated to room temperature. At the same time, the soluble protein extract was mixed with 1 mL of Equilibration Buffer containing 10 mM imidazole. The storage buffer from the spin column was removed by centrifugation at 700  $\times$ g for 2 min. The column was then equilibrated with 2 mL of Equilibration Buffer containing 10 mM imidazole where it was allowed to enter the resin bed. The column was centrifuged at 700  $\times$ g to remove the buffer. This is followed by the addition of the protein extract to the column where it was also allowed to enter the resin bed. For maximal binding, the sample was incubated for 30 min at room temperature on a rotating platform. The column was centrifuged at 700  $\times$ g for 2 min to collect the flow-through. The resin was washed with 2 mL of Wash Buffer containing 25 mM imidazole, centrifuged at 700  $\times$ g for 2 min where the fraction was collected. One mL of Elution Buffer containing 250 mM imidazole was added into the resin, centrifuged at 700  $\times$ g for 2 min and the fraction was collected. The imidazole from the purified His-tagged recombinant protein was removed by passing it through a 0.5 mL centrifugal filter unit with a 10K Nominal Molecular Weight Limit (NMWL, Merck). A total of 1 mL of 1X TBS (Thermo

Scientific) was added to the centrifugal unit, centrifuged at 14,000 ×g for 30 min. This process was repeated thrice before the purified His-tagged recombinant protein was recovered.

#### **3.10.10 Protein-protein interaction analysis using pull-down assay**

This pull-down polyhistidine assay was carried out using Pierce™ Pull-Down PolyHis Protein:Protein Interaction Kit (Thermo Scientific). The HisPur Cobalt Resin was first equilibrated with 1:1 wash solution of TBS: Pierce Lysis Buffer and 4M Imidazole Stock Solution to a final concentration of 10 mM imidazole. The resin was thoroughly resuspended by using a vortex mixer. A total of 50 µL of the slurry and 400 µL of the wash solution were added into the spin column. Both ends of the column were capped and inverted several times to equilibrate the immobilized cobalt-chelate resin. Both caps were removed and the spin column was placed inside a collection tube. The column was centrifuged at 1,250 ×g for 1 min to remove the wash solution. The wash volume was then discarded. This washing step was repeated for a total of five washes.

A total of 100 µg of purified His-tagged recombinant protein (bait) was added to the equilibrated spin column, incubated for 30 min at 4°C on a rotating mixer and centrifuged at 1,250 ×g for 1 min to collect the bait flow-through. A total of 400 µL of wash solution was added to the spin column, inverted several times to mix thoroughly and centrifuged at 1,250 ×g for 1 min. The wash volume was then discarded. This washing step was repeated for a total of five washes.

Total protein extracted from leaf and stem tissues of *Ganoderma*-inoculated oil palm seedlings were used as prey proteins. A total of 100 µg of prey protein was dissolved in 1X TBS with 4 M Imidazole Stock Solution to a final concentration of 10 mM

imidazole. The prey protein was added to the spin column containing the immobilised polyhistidine-tagged bait protein, incubated at 4°C for 1 hr and centrifuged at 1,250 ×g for 1 min to collect the prey flow-through. A total of 400 μL of wash solution was added to the spin column, inverted several times to mix thoroughly and centrifuged at 1,250 ×g for 1 min. The wash volume was then discarded. This washing step was repeated for a total of five washes.

A total of 250 μL of Elution Buffer was added to the spin column, incubated for 5 min with gentle rocking and centrifuged at 1,250 ×g for 1 min to obtain the eluted prey protein. This elution was repeated for one more time. The eluted prey protein was analysed using SDS-PAGE (Section 3.7) and stained using silver nitrate (Section 3.8.3). The band containing the eluted protein was excised from the polyacrylamide gel, destained, trypsin digested and identified using LC-QToF mass spectrometer (Section 3.8.4).

## CHAPTER 4: RESULTS

### 4.1 *Ganoderma boninense* culture and inoculum

*Ganoderma boninense* PER71 cultures were kindly provided by *Ganoderma* & Diseases Research of Oil Palm Unit Laboratory, MPOB. They were maintained onto PDA at Crop Protection Unit, Sime Darby Research Sdn Bhd, Banting, Selangor (Figure 4.1). After subculture, RWBs measuring 6 cm x 6 cm x 6 cm were used as a source of inoculum for fungal colonization. Once the RWBs were fully colonized, they were then used for artificial infection of oil palm seedlings (Figure 4.2).

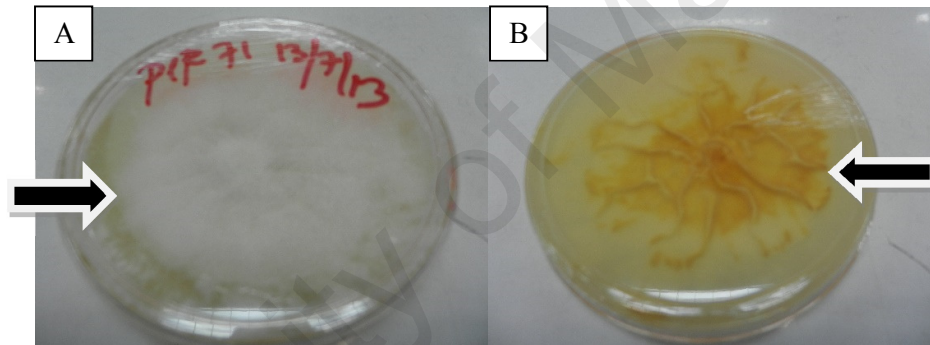


**Figure 4.1:** *Ganoderma boninense* cultures were maintained on PDA plates. They were incubated at 37°C in the dark for ten days. Mature cultures were then cut into smaller pieces and inoculated into RWBs. (A) Top view of the fungal culture showing mature mycelia covering the surface of the agar. (B) Bottom view of a mature fungal culture. Arrows indicate growth of fungus.



**Figure 4.2:** RWBs were inoculated with mature *G. boninense* and incubated in the dark for three months until the blocks were fully colonized by the fungus. These fully colonised RWBs are ready for artificial inoculation of germinated oil palm seedlings. The white mycelium of the fungus is seen covering the whole surface of the RWB.

## 4.2 Nursery trial set-up

Germinated *DxP* seedlings were used as planting materials. The fully colonized RWBs were placed in a polybag half-filled with soil. After which, more soil was used to fill up the bag. The germinated seedlings were then sowed approximately 2 cm below the surface of the soil. A total of 120 germinated seedlings each was treated with *G. boninense* inoculated and non-inoculated RWBs over a six-month time course study. In this time course study, destructive sampling commenced when the plants were two-months old (two-months post inoculation, 2-mpi) until they were seven-months old (7-mpi).

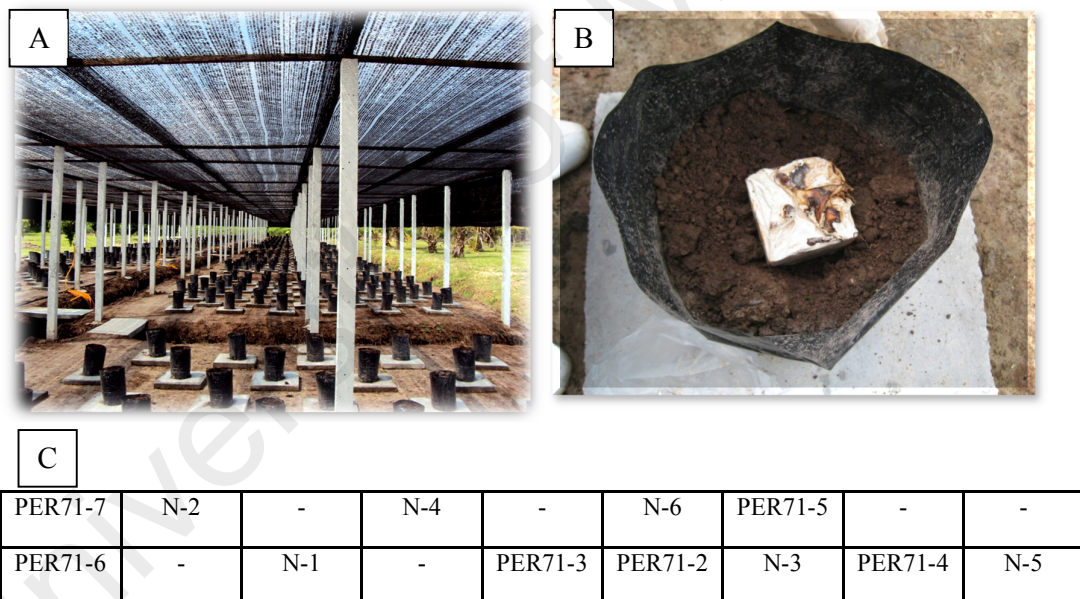


**Figure 4.3:** Nursery set-up for *Ganoderma boninense* trial. Germinated commercial *DxP* oil palm seedlings were used as planting materials. The trial was run for seven months where leaf tissues were collected at monthly intervals for 2D-PAGE. (A) Randomized block design that was used to set-up the arrangements of the oil palm seedlings. (B) Artificial infection of germinated oil palm seedlings. (C) Nursery trial layout: PER71-7 indicates inoculated palms where leaf tissues were sampled at 7-mpi; N-1 indicates non-inoculated palms where leaf tissues were sample at month 2.

### 4.3 Destructive sampling of oil palm seedlings

To observe the architecture of the whole plant, the oil palm seedlings were uprooted to expose their root systems. The overall vegetative growth and the root mass of both non-inoculated and inoculated plants were compared (Figure 4.4). The physical appearance of both non-inoculated and inoculated seedlings looked similar at 2-mpi, without much differences in height, nor the number of fronds. This condition was similar for 3-mpi and 4-mpi oil palm seedlings. However, chlorosis was observed on the leaves of 5-mpi oil palm seedlings without the presence of basidiocarp. Chlorotic leaves were obvious on 6-mpi and 7-mpi seedlings and at times, with the presence of basidiocarp at the bole (Figure 4.5). Some seedlings were also found to be dead at 6-mpi without the presence of basidiocarp. The inoculated seedlings appeared stunted in growth and with fewer numbers of fronds when compared to the non-inoculated seedlings.

At a closer look, basidiocarp can be seen emerging from the base of the trunk of a dying seedling (Figure 4.6A). In some cases, the basidiocarp emerged only after the seedling is dead (Figure 4.6B). The overall physical appearances of seedlings were documented and compared (Figure 4.7). The leaf foliar and the root mass of non-inoculated seedlings were visibly more dense than inoculated seedlings.

To investigate further, cross sections of stems from both non-inoculated and inoculated seedlings were performed (Figure 4.8). It is obvious that the stems of non-inoculated seedlings were clear and showed no signs of lesions compared to the stems inoculated seedlings. At a closer look at the area where lesions are visible, the signs of dark, rotten tissues indicate the disease has made its way to the base of the stem.

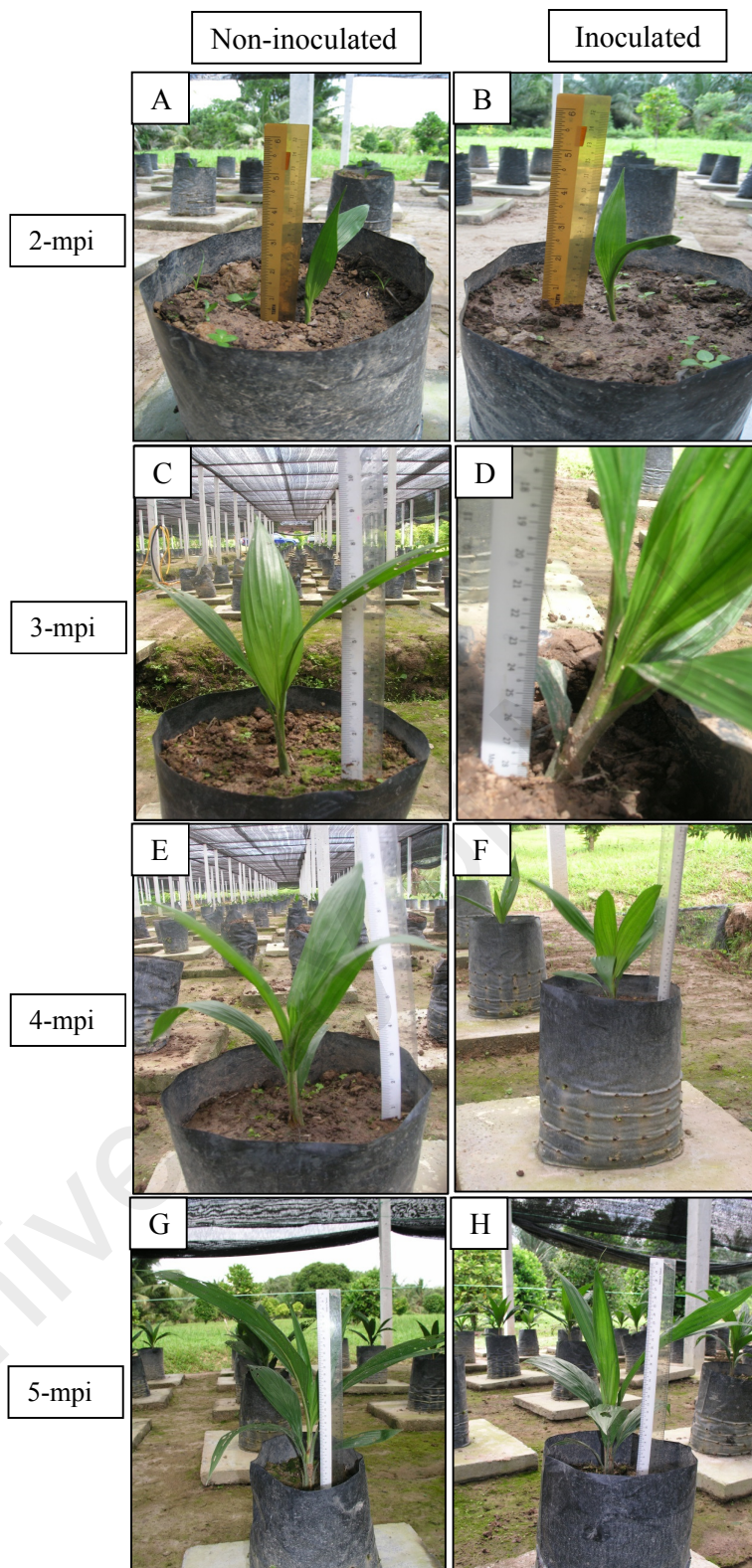


**Figure 4.4:** The overall vegetative growth of both non-inoculated and inoculated oil palm seedlings (2mpi to 5mpi). Upkeep of the plants was carried out according to Good Agricultural Practices (Sime Darby Plantation). (A) Non-inoculated, 2-months old (B) Inoculated, 2mpi (C) Non-inoculated, 3-months old (D) Inoculated, 3mpi (E) Non-inoculated, 4-months old (F) Inoculated, 4mpi (G) Non-inoculated, 5-months old (H) Inoculated, 5mpi. No signs of the BSR disease symptoms can be observed.

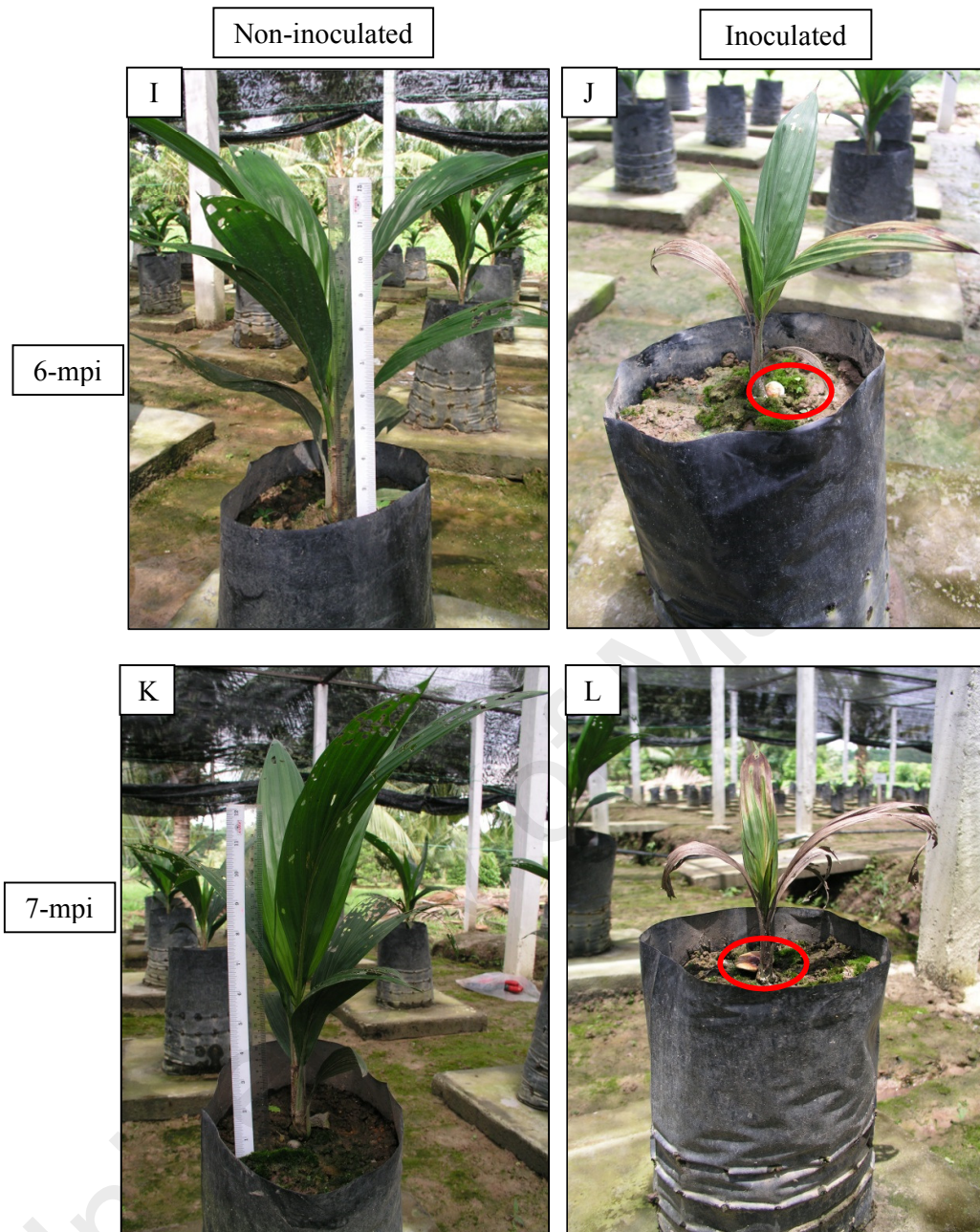


**Figure 4.5:** The overall vegetative growth of both non-inoculated and inoculated oil palm seedlings (6mpi to 7mpi). Red circles indicate the appearance of mature, brown basidiocarps at the base of inoculated oil palm seedlings. Chlorosis can be seen appearing on all the leaves. Growth of inoculated seedlings appeared stunted compared to the non-inoculated seedlings. (I) Non-inoculated, 6-months old (J) Inoculated, 6mpi. (K) Non-inoculated, 7-months old (L) Inoculated, 7mpi.

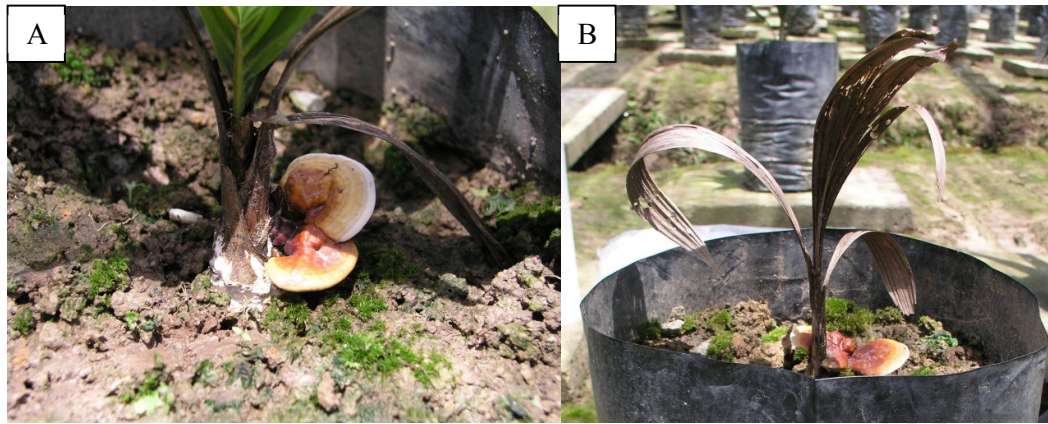


**Figure 4.6:** Basidiocarp can be seen emerging from the boles of 6-mpi seedlings. White mycelia have colonized basal stem of inoculated oil palm seedlings. (A) Although basidiocarp can be seen attached to the bole, the plant is still able to grow. (B) Basidiocarp at the bole with the remaining leaves undergone chlorosis, rendering the seedling dead at the point of sampling.

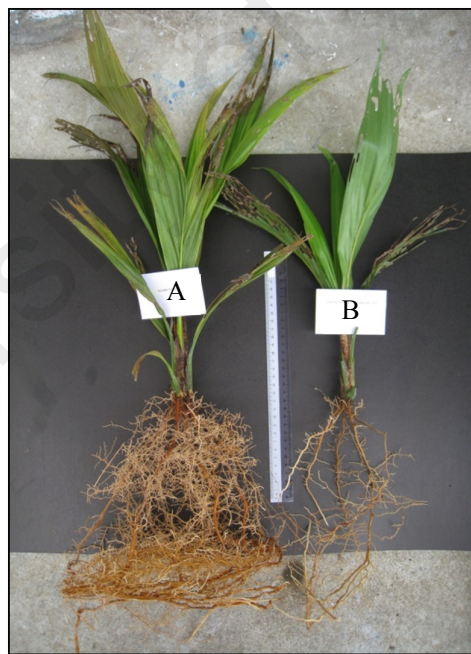


**Figure 4.7:** The overall physical appearances of 6-mpi oil palm seedlings were compared. Seedling A has not been inoculated with *G. boninense* while seedling B has been artificially inoculated with *Ganoderma* fungus. The number of fronds in seedling A is higher than seedling B. The overall root mass of seedling A was visibly more dense than seedling B.

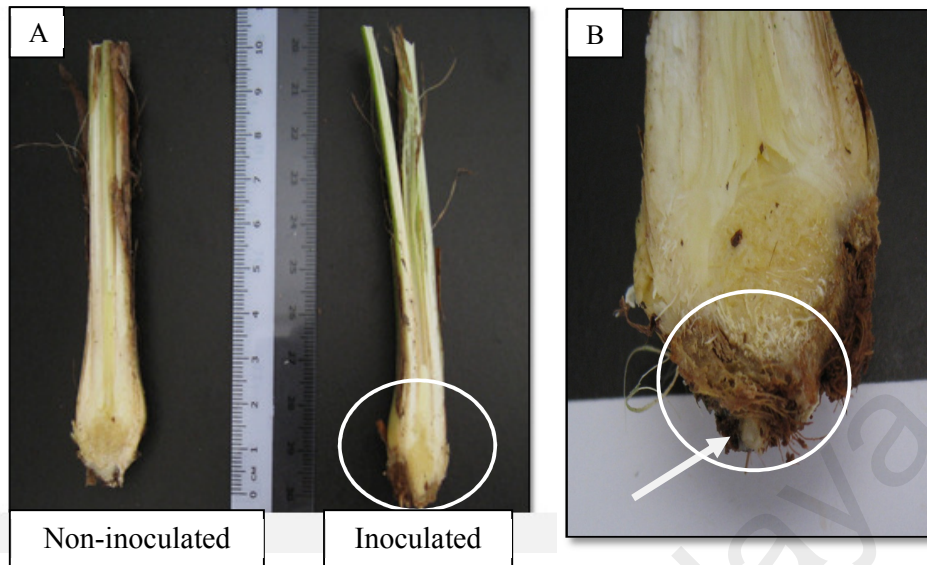


**Figure 4.8:** The cross section of the stems of 6-mpi oil palm seedlings. The oil palm seedlings were destructed to collect leaf tissues for proteomics studies. Fronds and roots were removed to investigate the conditions of the stems after germinated seedlings were inoculated with *G. boninense*. (A) The bole of non-inoculated) appeared clean without any signs of lesions whereas the bole of inoculated seedling had a brownish lesion on the left. (B) The arrow indicates the point of entry of *G. boninense* into the bole.

#### 4.4 Evaluation of protein extraction protocols

Four protein extraction protocols were evaluated for oil palm leaf tissues from young (less than one year old) and mature (five years old) palms. The four protocols that were tested are as follows: Phenol-guanidine isothiocyanate method (M1), TCA-acetone precipitation method (M2), Sucrose method (M3) and TCA-acetone-phenol method (M4). The extracted proteins were first run through SDS-PAGE to visualize the protein profiles of each extraction method. They were then run through 2D-PAGE to determine which extraction method yielded the best 2-DE image. The protocol would then be used to extract proteins from leaf tissues of non-inoculated and inoculated oil palm seedlings.

Different extraction methods yielded different amounts of proteins based on the same amounts of starting materials. Protein yield obtained from TCA-acetone precipitation (M2) was considerably higher, followed by sucrose (M3) and TCA-acetone-phenol

method (M4). The phenol-guanidine isothiocyanate method (M1) yielded the least amount of proteins (Table 4.1). The protein yield from young leaves was comparatively lower than those from mature leaves.

SDS-PAGE was performed (Figure 4.9) to evaluate the complexity of the proteins extracted using the four different extraction methods. Proteins within the range of 20 - 212 kDa were successfully resolved. Proteins extracted using the TCA-acetone-phenol method (M4) managed to be resolved into higher molecular weight proteins and showed a higher number of bands compared to other extraction methods.

The protein profiles of phenol-guanidine isothiocyanate method (M1), however, resolved low molecular weight proteins. Figures 4.10A and 4.10B are representations of the two-dimensional gels of proteins from young and mature palm leaves extracted via the methods discussed. Protein spots were found to distribute evenly across the gels, while the more abundant spots concentrated at the acidic end.

The 2D gel image of TCA-acetone precipitation (M2) showed the lowest number of protein spots although the protein yield was the highest. In both 2D gels of mature and young leaf tissues, the spots were not properly focused with the presence of smearing and horizontal streaking. Sucrose (M3) and TCA-acetone-phenol (M4) methods produced comparable 2D gels that were better than TCA-acetone precipitation (M2). Protein extraction using the phenol-guanidine isothiocyanate method (M1) resulted in the most focused and well resolved 2D gels with 1455 protein spots detected in mature leaf. However, its' SDS-PAGE profile was unfavourable, with the higher molecular weight proteins aggregated at the top of the gel.

**Table 4.1:** Four different extraction methods were used to extract proteins from oil palm leaf tissues. The yield obtained was calculated based on one g of starting material. Values indicate the mean of three independent extraction replicates per method with the standard deviation.

Extraction method	Young leaf	Mature leaf
	Protein yield (mg/g starting material)	Protein yield (mg/g starting material)
Phenol-guanidine isothiocyanate (M1)	0.05±0.00	0.04±0.01
TCA-acetone (M2)	3.47±0.23	7.73±0.84
Sucrose (M3)	1.40±0.40	1.88±0.72
TCA-acetone-phenol (M4)	1.20±0.13	3.60±0.53

**Table 4.2:** The total number of detectable spots varied among different extraction methods. More spots could be detected in young oil palm leaf tissues compared to mature tissues. The Image Master Platinum 7 (GE Healthcare) software was used to detect and analyse protein spots. Values indicate the mean of three independent gel image analysis per method with the standard deviation.

Extraction method	Young leaf	Mature leaf
	Total number of detectable spots	Total number of detectable spots
Phenol-guanidine isothiocyanate (M1)	1562 ± 522.26	1455 ± 210.80
TCA-acetone (M2)	1269 ± 39	1223 ± 348
Sucrose (M3)	1428 ± 259.41	1299 ± 525.51
TCA-acetone-phenol (M4)	1576 ± 45.24	1266 ± 95.50

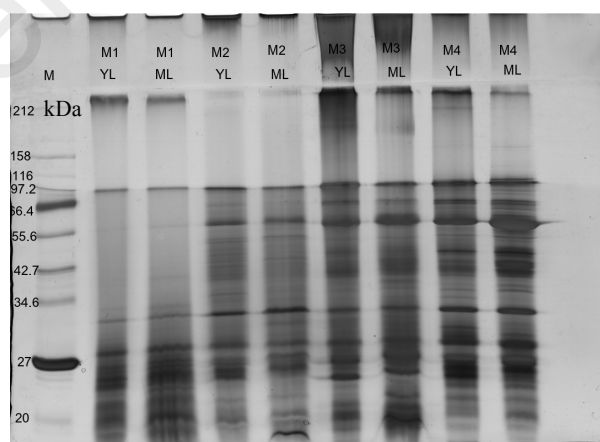


**Figure 4.9:** SDS-PAGE profiles of oil palm leaf tissues from young (YL) and mature (ML) oil palms. Tissues were extracted using phenol-guanidine isothiocyanate (M1), TCA-acetone (M2), sucrose (M3) and TCA-acetone-phenol (M4) methods. Five µg of each protein was separated on polyacrylamide gels and stained using silver nitrate. M: Protein marker (NEB).

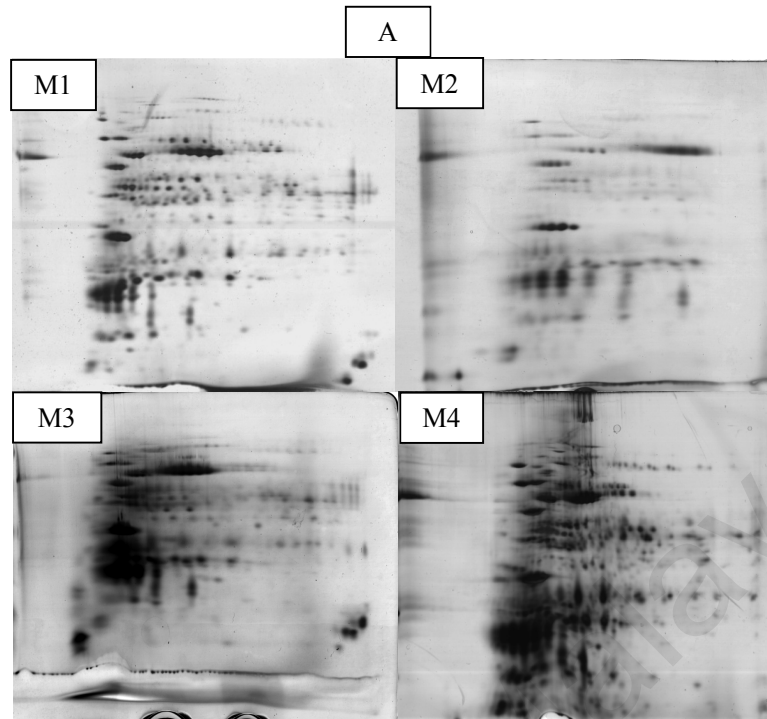


**Figure 4.10A:** 2-DE protein profiles of leaf tissues extracted from young oil palms. Proteins were focused on 7 cm pH3-10NL IPG strips. The four different extraction methods are phenol-guanidine isothiocyanate method (M1), TCA-acetone method (M2), sucrose method (M3) and TCA-acetone-phenol method (M4). A: young leaf; B: mature leaf.

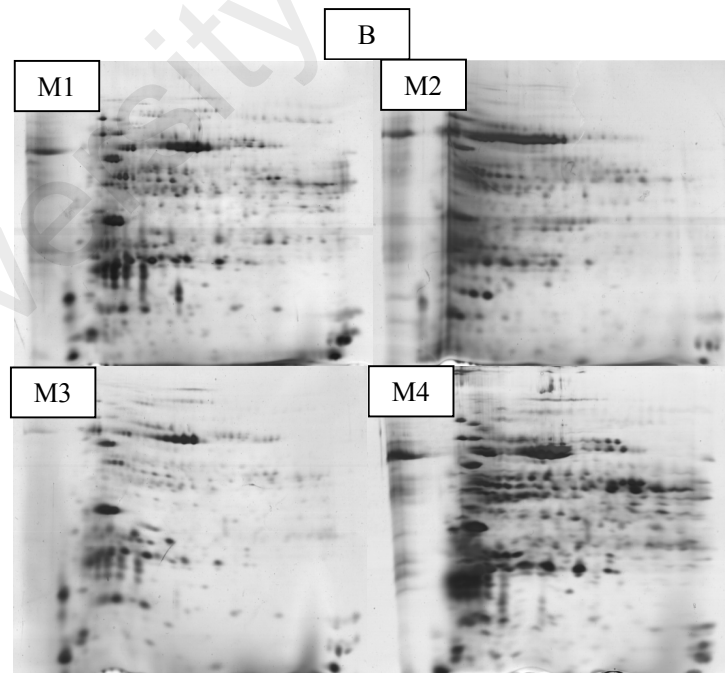


**Figure 4.10B:** 2-DE protein profiles of leaf tissues extracted from mature oil palms. Proteins were focused on 7 cm pH3-10NL IPG strips. The four different extraction methods are phenol-guanidine isothiocyanate method (M1), TCA-acetone method (M2), sucrose method (M3) and TCA-acetone-phenol method (M4). A: young leaf; B: mature leaf.

The phenol-guanidine isothiocyanate extraction (M1) was shown to be better in producing well focused 2D gels, with 1562 spots. Two extraction methods – TCA-acetone precipitation (M2) and sucrose (M3) - resulted in similar quality 2D gels with comparable number of spots (Table 4.2). The TCA-acetone-phenol method (M4) when used in young leaf tissues, managed to yield 1576 spots. Although the protein spots produced using TCA-acetone-phenol method (M4) were not distinct, they were still considered suitable for 2D-PAGE analysis.

In terms of 2-DE gel separation, detection and analysis of protein spots of oil palm leaf tissues, the TCA-acetone-phenol extraction method (M4) was found to be the most consistent and reliable. With this method, higher number of spots, greater spot resolution, cleaner backgrounds and minimal spot streaking were observed.

Among the four protein extraction methods that had been tested, the TCA-acetone-phenol method (M4) managed to give a more comprehensive profile of proteins on SDS-PAGE, where both low and high molecular weight proteins were resolved. The protein yield that was obtained using M3 was approximately 3 mg/g of starting material, which was sufficient to run a complete 2D-PAGE analysis. Therefore, the TCA-acetone-phenol method (M4) is a comprehensive protein extraction protocol that can be used for both 2D-PAGE and western blotting.

#### **4.5 2-DE analyses**

The protein profiles of leaf tissues were compared between non-inoculated (healthy) and inoculated (diseased) oil palm seedlings to identify proteins that change in abundance with fungal infection at different time points. An experimental outline describing the process workflow is shown in Figure 4.12.

A total of 48 gels (6 time points × 2 treatments × 4 technical gel replicates) were run in this analysis. The number of proteins that changed in abundance varied between time points. After image analysis using the IMP7 software, hundreds of protein spots with different abundance were subjected to the Benjamini-Hochberg analysis to remove false positives. This drastically reduced the number of spots to work with. Fold changes were manually generated from the analysis to indicate the changes in expression of individual protein at every time point. Protein spots with fold changes of more than 2.0 were considered to be significant. The number of protein spots that changed in abundance was found to be the highest at 3-mpi with 52 spots. This was followed by significant changes that were detected at 6-mpi with 46 spots, 5-mpi with 10 spots, 7-mpi with six spots and 2-mpi with two spots. However, no spots were found to be significant in protein abundance in leaf tissues of 4-mpi (Table 4.3).

**Table 4.3:** Image and statistical analyses were performed to determine the number of protein spots that changed in abundance between inoculated and non-inoculated tissues. The highest number of spots that changed in abundance were detected in 3-mpi while none were present in 4-mpi.

Months-post-inoculation	Number of spots that changed in abundance
2-mpi	2
3-mpi	52
4-mpi	0
5-mpi	10
6-mpi	46
7-mpi	6
Total	116

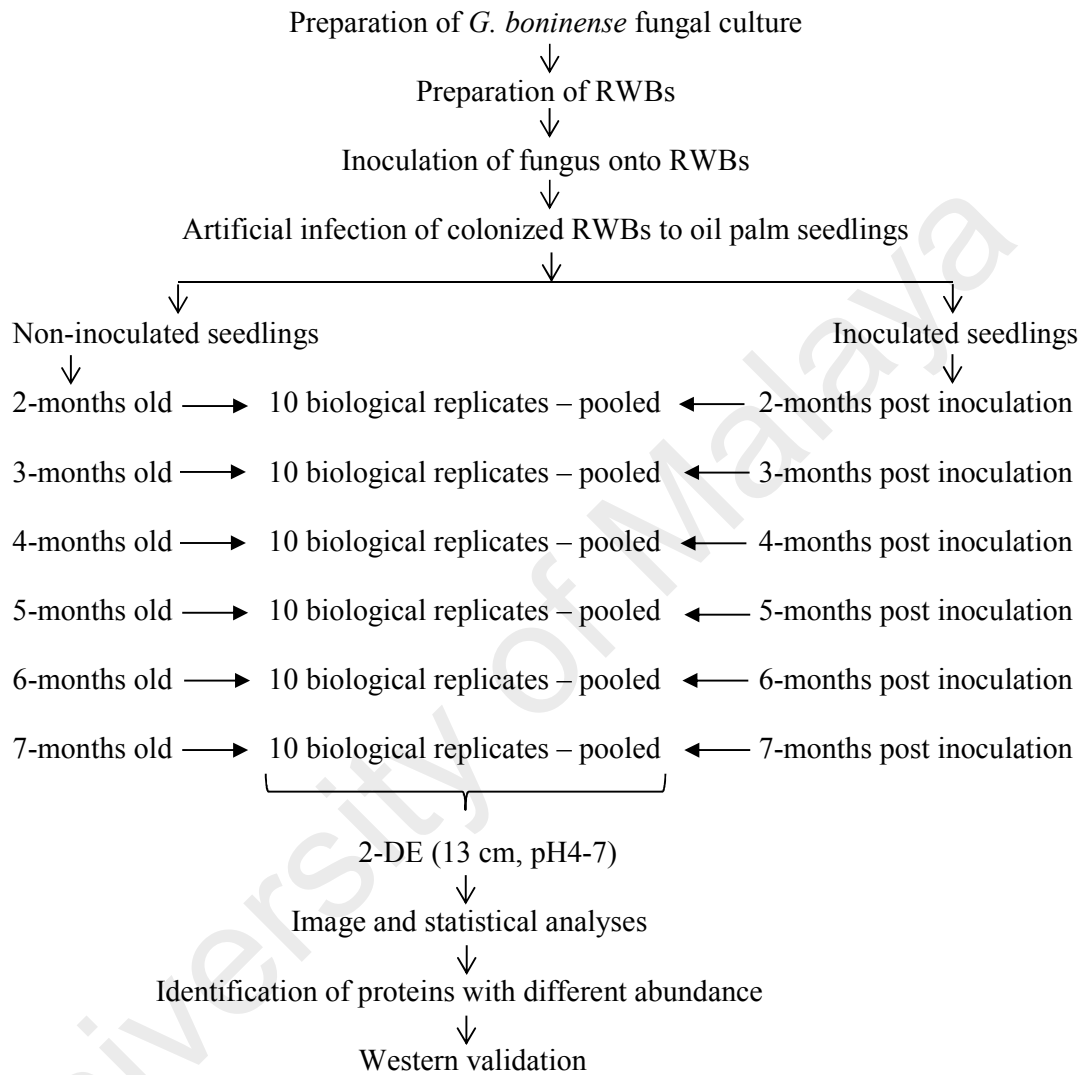


**Figure 4.11:** A diagrammatic representation of the proteomics workflow to detect differences in the proteome of leaf tissues of inoculated and non-inoculated oil palm seedlings. The RWBs were inoculated with *G. boninense* fungal culture which were then used as inoculums for germinated oil palm seedlings. Leaf samples were collected for six time points, starting from 2-mpi to 7-mpi. The leaves from 10 individual seedlings were sampled every month for each treatment, which were subsequently pooled prior to 2-DE. Protein samples from each time point were run in four technical replicates before image and statistical analyses. Significant protein spots that changed in abundance were excised from the gels and identified using mass spectrometry. Plant based antibodies were commercially purchased to validate the expression of these significant proteins.

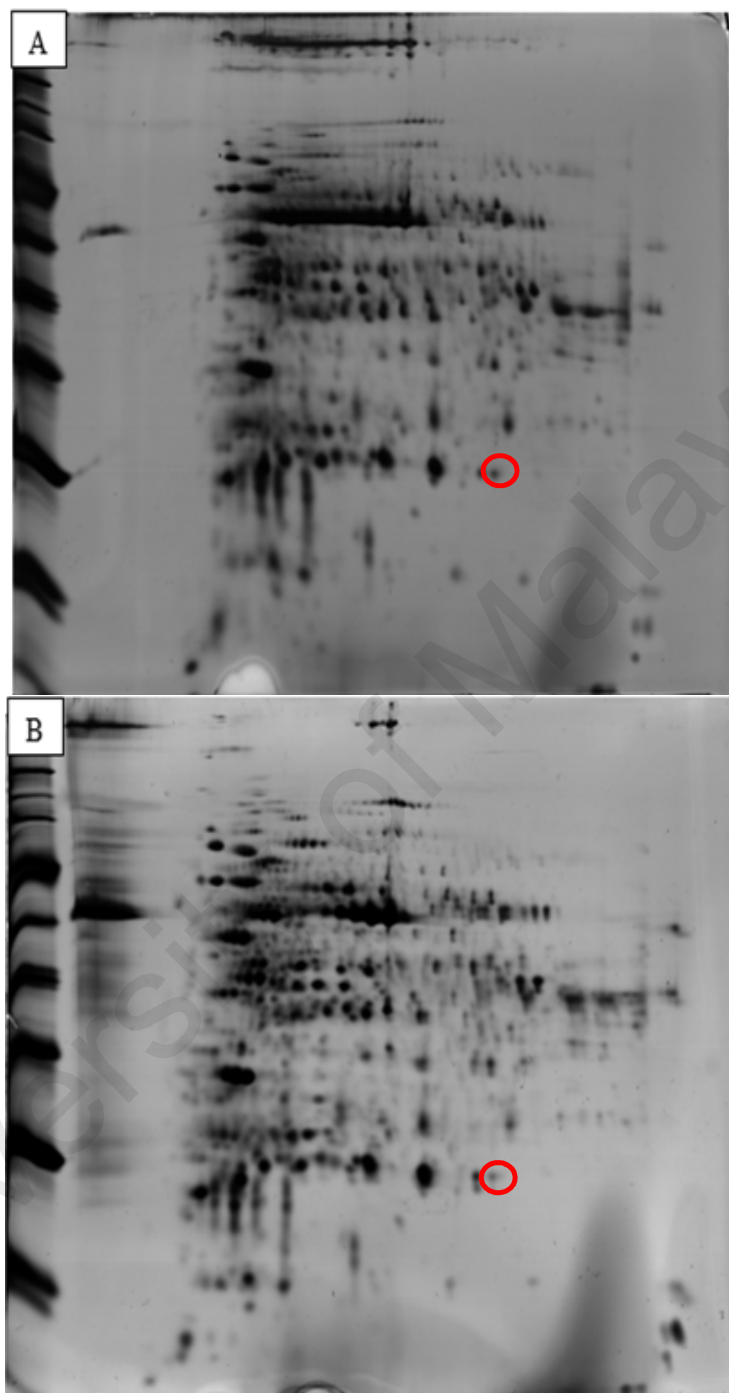


**Figure 4.12a:** Representative 2D-PAGE gel images of 2 month-old oil palm leaf tissues from non-inoculated (A) and inoculated seedlings (B). The proteins were focused on 13 cm pH4-7 IPG strips. Each protein sample was run as four technical replicates prior to image and statistical analyses. Red circles indicate prominent protein spots with different abundance at different time points that were picked for identification. The remaining spots were identified but their positions were not highlighted in the gels.

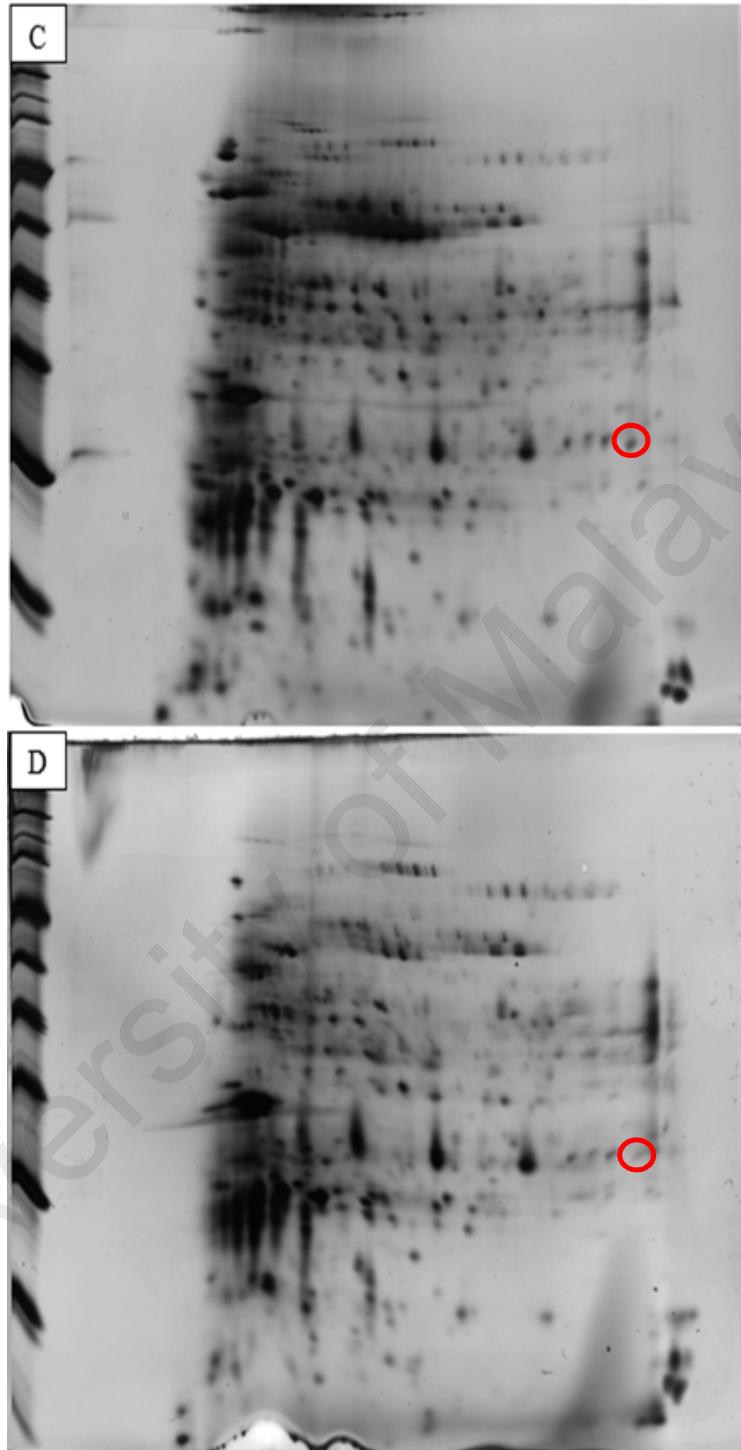


**Figure 4.12b:** Representative 2D-PAGE gel images of 3 month-old oil palm leaf tissues from non-inoculated (C) and inoculated seedlings (D). The proteins were focused on 13 cm pH4-7 IPG strips. Each protein sample was run as four technical replicates prior to image and statistical analyses. Red circles indicate prominent protein spots with different abundance at different time points that were picked for identification. The remaining spots were identified but their positions were not highlighted in the gels.

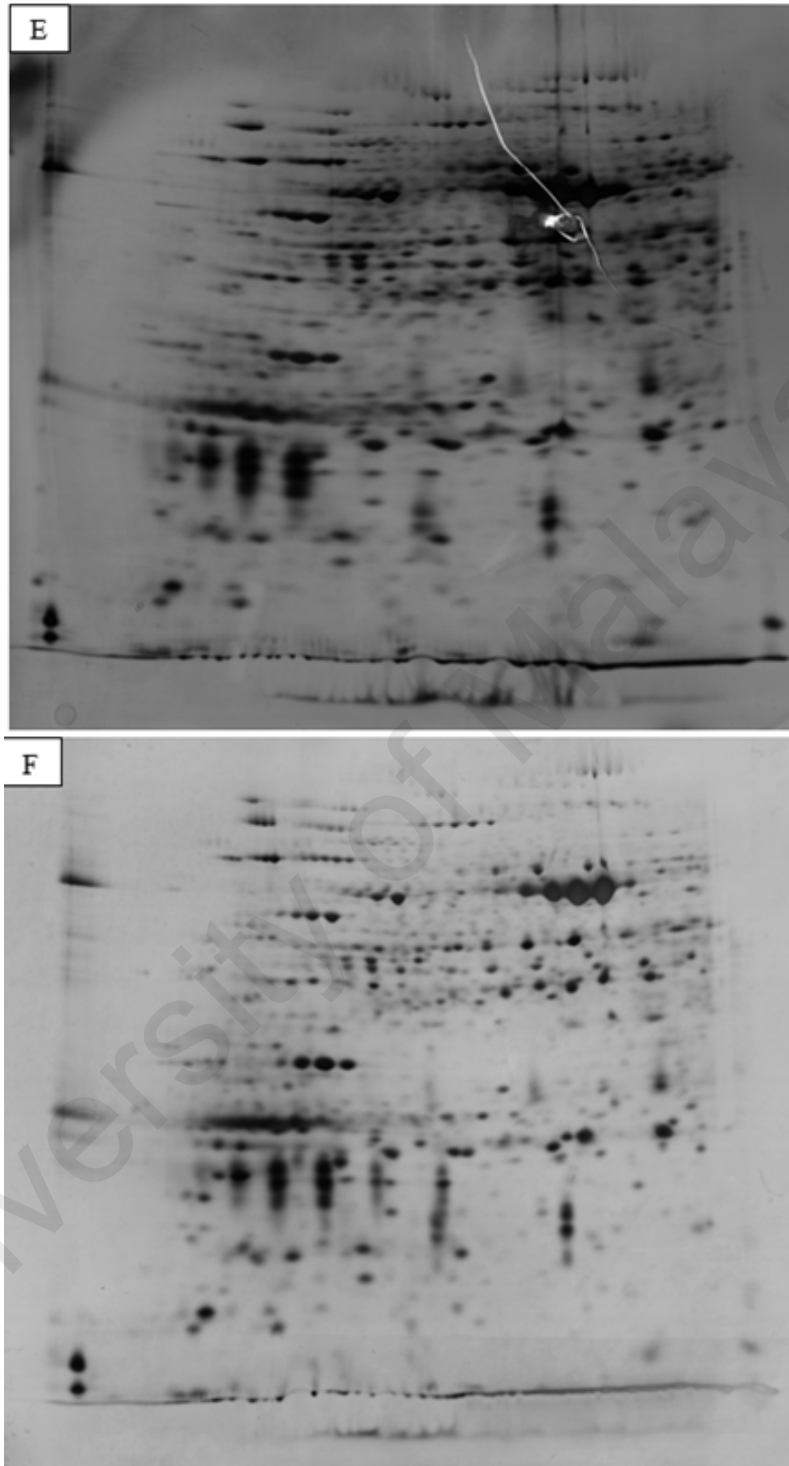


**Figure 4.12c:** Representative 2D-PAGE gel images of 4 month-old oil palm leaf tissues from non-inoculated (E) and inoculated seedlings (F). The proteins were focused on 13 cm pH4-7 IPG strips. Each protein sample was run as four technical replicates prior to image and statistical analyses. Protein spots that changed in abundance were not detected to be significant in this pair of leaf samples. The minimum fold-change was set at 2-fold.

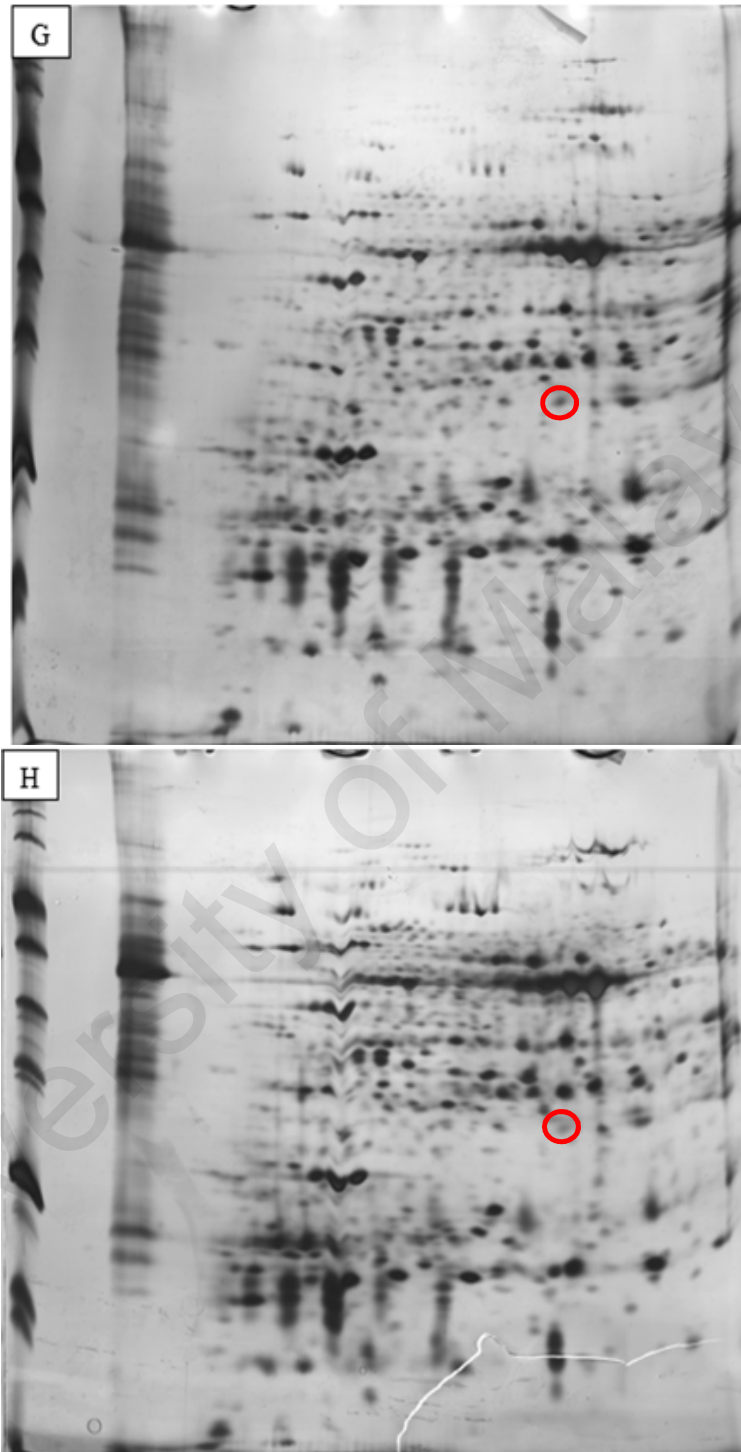


**Figure 4.12d:** Representative 2D-PAGE gel images of 5 month-old oil palm leaf tissues from non-inoculated (G) and inoculated seedlings (H). The proteins were focused on 13 cm pH4-7 IPG strips. Each protein sample was run as four technical replicates prior to image and statistical analyses. Red circles indicate prominent protein spots with different abundance at different time points that were picked for identification. The remaining spots were identified but their positions were not highlighted in the gels.

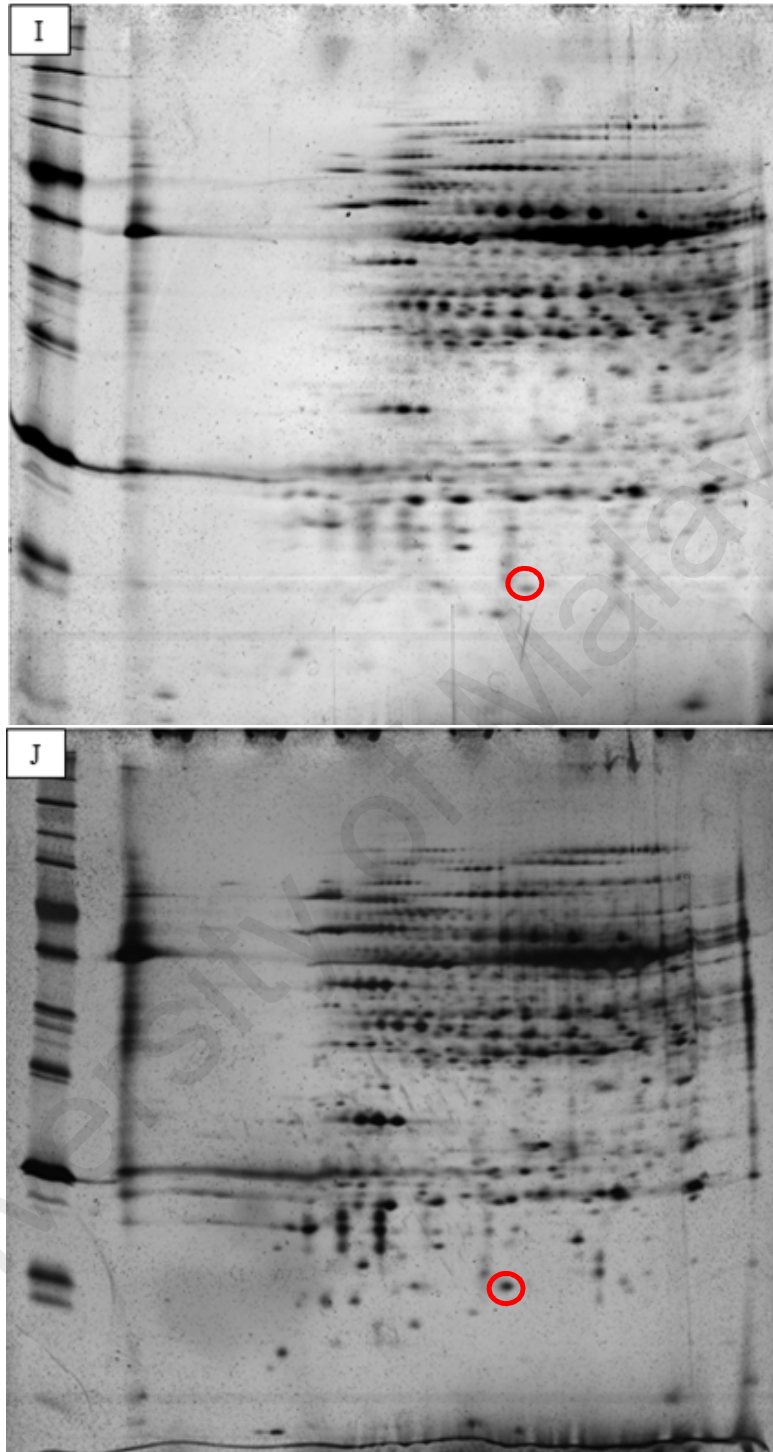


**Figure 4.12e:** Representative 2D-PAGE gel images of 6 month-old oil palm leaf tissues from non-inoculated (I) and inoculated seedlings (J). The proteins were focused on 13 cm pH4-7 IPG strips. Each protein sample was run as four technical replicates prior to image and statistical analyses. Red circles indicate prominent protein spots with different abundance at different time points that were picked for identification. The remaining spots were identified but their positions were not highlighted in the gels.

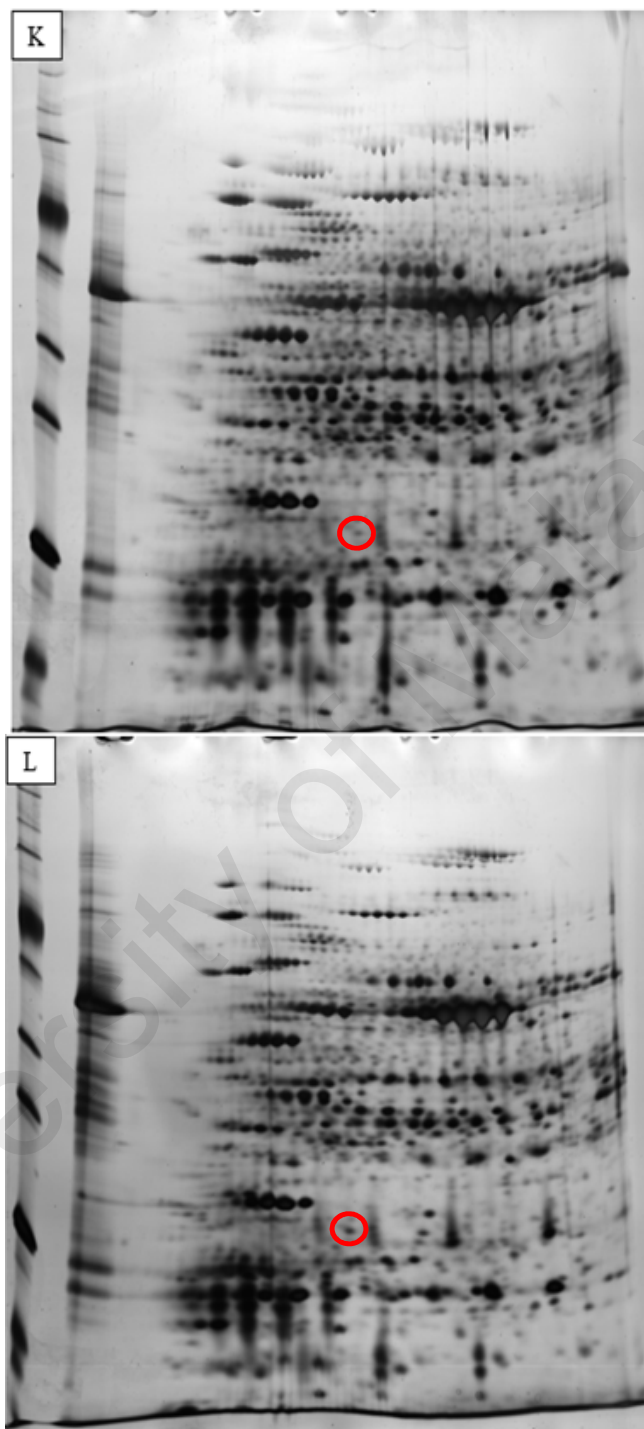


**Figure 4.12f:** Representative 2D-PAGE gel images of 7 month-old oil palm leaf tissues from non-inoculated (K) and inoculated seedlings (L). The proteins were focused on 13 cm pH4-7 IPG strips. Each protein sample was run as four technical replicates prior to image and statistical analyses. Red circles indicate prominent protein spots with different abundance at different time points that were picked for identification. The remaining spots were identified but their positions were not highlighted in the gels.

**Table 4.4:** List of proteins with different abundance, according to time points, in leaf tissues of inoculated oil palm seedlings. A total of 107 spots were identified using mass spectrometry. This gave rise to 76 proteins with different UniProt entries. The proteins were grouped into ten functional categories – carbohydrate metabolism, cellular component, energy production, fatty acid biosynthesis, immunity and defence, nitrogen metabolism, protein metabolism, stress response, transport, and photosynthesis.

Spot ID	Protein	Fold change	MW (Da)	pI (pH)	PLGS score	No of unique peptides	Peptide coverage (%)
<b>2-mpi</b>							
Protein metabolism							
2-127	Thiamine thiazole synthase, chloroplastic ( <i>Citrus sinensis</i> , O23787)	7.93, ↑ E2	37570	5.28	4419.86	19	23.60
Photosynthesis							
2-317	Ribulose biphosphate carboxylase/oxygenase activase, chloroplastic ( <i>Oryza sativa Japonica</i> , P93431)	5.42, ↑ E2	47826	5.75	8351.38	12	14.12
<b>3-mpi</b>							
Carbohydrate metabolism							
3-139	Glyceraldehyde-3-phosphate dehydrogenase A, chloroplastic ( <i>Pisum sativum</i> , P12858)	3.23, ↓ E3	15426	5.70	536.64	1	8.50
3-138, 3-162	Phosphoribulokinase, chloroplastic ( <i>Triticum aestivum</i> , P26302)	2.48, ↑ E3, 4.56, ↓ E3	26785	9.35	129.95	4	7.11
3-130, 3-135	Glyceraldehyde-3-phosphate dehydrogenase, cytosolic ( <i>Dianthus caryophyllus</i> , P34921)	2.09, ↑ E3, 2.49, ↑ E3	22744	5.52	1407.98	6	22.55
3-141	Phosphoglycerate kinase 2, chloroplastic ( <i>Arabidopsis thaliana</i> , P50318)	2.76, ↑ E3	39082	5.36	923.34	16	17.42
3-116, 3-118, 3-136	Fructose-bisphosphate aldolase, chloroplastic ( <i>Oryza sativa Japonica</i> , Q40677)	2.17, 2.10, 2.26, all ↑ E3	52347	4.57	9534.88	39	24.85
Energy production							
3-002	ATP synthase epsilon chain, chloroplastic ( <i>Arabidopsis thaliana</i> , P09468)	3.42, ↓ E3	62945	5.72	2219.77	57	29.24

3-195	ATP synthase subunit alpha, chloroplastic ( <i>Arabidopsis thaliana</i> , P56757)	4.37, ↓ E3	14463	4.78	301.86	1	8.33
3-013	ATP synthase subunit b, chloroplastic ( <i>Phalaenopsis aphrodite</i> , Q3BAQ6)	6.48, ↑ E3	40168	8.55	3824.21	19	22.78
3-014	ATP synthase subunit d, mitochondrial ( <i>Arabidopsis thaliana</i> , Q9FT52)	6.42, ↓ E3	25488	8.45	636.64	5	3.51
Immunity and defence							
3-004	Superoxide dismutase [Cu-Zn], ( <i>Solidago canadensis</i> , O04996)	3.04, ↓ E3	26557	5.78	722.66	4	8.94
3-029	Superoxide dismutase [Mn], mitochondrial ( <i>Nicotiana plumbaginifolia</i> , P11796)	2.21, ↓ E3	43311	8.85	766.90	6	9.88
3-015	2-Cys peroxiredoxin BAS1, chloroplastic ( <i>Oryza sativa Japonica</i> , Q6ER94)	5.30, ↓ E3	34925	5.71	87114.62	31	23.10
3-018, 3-020, 3-024, 3-025	2-Cys peroxiredoxin BAS1, chloroplastic ( <i>Hordeum vulgare</i> , Q96468)	5.14, 4.33, 8.06, 3.60, all ↓ E3	45112	5.64	3057.50	23	23.02
3-035	L-ascorbate peroxidase 2, cytosolic ( <i>Oryza sativa Japonica</i> , Q9FE01)	2.72, ↓ E3	35366	5.67	509.86	2	8.41
Nitrogen metabolism							
3-142	Glutamine synthetase cytosolic isozyme ( <i>Medicago sativa</i> , P04078)	2.11, ↑ E3	52672	6.29	4868.45	14	22.27
Photosynthesis							
3-000	Ribulose biphosphate carboxylase small chain, chloroplastic ( <i>Capsicum annuum</i> , O65349)	2.96, ↓ E3	21185	7.10	674.16	2	8.56
3-197	RuBisCO large subunit-binding protein subunit alpha ( <i>Ricinus communis</i> , P08824)	29.21, ↓ E3	36876	6.50	1677.01	10	15.98
3-192	RuBisCO large subunit-binding protein subunit beta, chloroplastic ( <i>Pisum sativum</i> , P08927)	2.24, ↑ E3	19674	5.91	312.43	1	8.06

3-100	Ferredoxin--NADP reductase, leaf isozyme, chloroplastic ( <i>Pisum sativum</i> , P10933)	1.97, ↑ E3	35051	8.67	583.30	6	8.33
3-019, 3-021	Chlorophyll a-b binding protein 6A, chloroplastic (i, P12360)	3.75, ↓ E3, 6.76, ↓ E3	28589	4.46	3547.68	18	30.98
3-085, 3-087, 3-089, 3-090, 3-098	Oxygen-evolving enhancer protein 1, chloroplastic ( <i>Solanum lycopersicum</i> , P23322)	2.14, ↑ E3, 2.72, ↑ E3, 2.46, ↓ E3, 2.21, ↑ E3, 2.71, ↓ E3	52476	6.34	3179.99	31	18.79
3-094	Oxygen-evolving enhancer protein 1, chloroplastic ( <i>Solanum tuberosum</i> , P26320)	2.69, ↓ E3	49893	6.23	3653.51	23	22.59
3-189	Ribulose bisphosphate carboxylase large chain ( <i>Barnadesia caryophylla</i> , P28381)	3.12, ↓ E3	55294	4.99	7103.26	32	22.29
3-027, 3-030, 3-032	Carbonic anhydrase, chloroplastic ( <i>Hordeum vulgare</i> , P40880)	8.76, 3.82, 3.27, all ↓ E3	1392	7.06	4790.01	1	91.67
3-093	Ribulose bisphosphate carboxylase large chain ( <i>Isophysis tasmanica</i> , P92463)	4.76, ↓ E3	51734	5.84	1701.62	23	27.90
3-109	Ribulose bisphosphate carboxylase large chain ( <i>Hyophorbe lagenicaulis</i> , Q9BA49)	8.16, ↓ E3	21120	6.20	110.37	3	9.78
Protein metabolism							
3-049	20 kDa chaperonin, chloroplastic ( <i>Arabidopsis thaliana</i> , O65282)	4.92, ↓ E3	42121	7.80	3701.30	23	18.30
3-026	Proteasome subunit beta type-3-B ( <i>Arabidopsis thaliana</i> , O81153)	4.34, ↓ E3	28079	5.58	998.30	16	19.54
3-005	50S ribosomal protein L12, chloroplastic ( <i>Nicotiana sylvestris</i> , P36688)	3.41, ↓ E3	23284	5.34	2624.57	12	20.00
3-060	Proteasome subunit alpha type-5 ( <i>Oryza sativa Japonica</i> , Q9LSU1)	4.94, ↓ E3	52928	6.12	23859.75	65	42.77

3-066	Proteasome subunit alpha type-6 ( <i>Oryza sativa</i> Japonica, Q9LSU3)	3.54, ↓ E3	27100	5.03	5167.43	6	11.16
Stress response							
3-084	14-3-3-like protein GF14 psi ( <i>Arabidopsis thaliana</i> , P42644)	6.75, ↓ E3	19573	4.89	869.67	4	22.62
3-140	Elongation factor Tu, chloroplastic ( <i>Glycine max</i> , P46280)	2.57, ↑ E3	25976	4.50	3705.23	9	43.46
<b>5-mpi</b>							
Photosynthesis							
5-154	Oxygen-evolving enhancer protein 1, chloroplastic ( <i>Solanum lycopersicum</i> , P23322)	6.34, ↓ E5	34925	5.71	52163.47	42	19.76
5-135	Ribulose biphosphate carboxylase/oxygenase activase, chloroplastic ( <i>Oryza sativa</i> Japonica, P93431)	2.44, ↓ E5	42034	6.00	725.84	44	18.32
5-053	Ribulose biphosphate carboxylase large chain ( <i>Dioscorea elephantipes</i> , A6MML5)	2.72, ↓ E5	52907	6.12	1972.52	7	3.56
Carbohydrate metabolism							
5-391, 5-394	Transketolase, chloroplastic ( <i>Spinacia oleracea</i> , O20250)	2.19, ↑ E5, 2.90, ↑ E5	80230	6.20	350.16	10	4.45
5-202	Sedoheptulose-1,7-biphosphatase, chloroplastic ( <i>Triticum aestivum</i> , P46285)	9.39, ↓ E5	70529	5.03	11656.17	25	26.36
Stress response							
5-390	Heat shock 70 kDa protein ( <i>Zea mays</i> , P11143)	2.00, ↑ E5	51421	5.26	10242.90	57	24.68
<b>6-mpi</b>							
Carbohydrate metabolism							
6-280, 6-283, 6-284	Transketolase, chloroplastic ( <i>Spinacia oleracea</i> , O20250)	2.06, 3.93, 2.21, all ↓ E6	52928	6.12	11417.46	78	42.35

6-214	Glyceraldehyde-3-phosphate dehydrogenase B, chloroplastic ( <i>Pisum sativum</i> , P12859)	7.22, ↓ E6	25649	0.15	58	1	1
6-076	Triosephosphate isomerase, cytosolic ( <i>Zea mays</i> , P12863)	3.54, ↓ E6	16611	0.87	134	3	3
6-139, 6-147, 6-155, 6-166	Glyceraldehyde-3-phosphate dehydrogenase GAPA1, chloroplastic ( <i>Arabidopsis thaliana</i> , P25856)	16.65, ↓ E6, 3.53, ↑ E6, 2.25, ↓ E6, 4.83, ↓ E6,	80230	6.20	318.42	12	4.45
6-138	Sedoheptulose-1,7-bisphosphatase, chloroplastic ( <i>Triticum aestivum</i> , P46285)	2.34, ↑ E6	23516	0.16	77	1	1
6-141	Fructose-bisphosphate aldolase, chloroplastic ( <i>Oryza sativa Japonica</i> , Q40677)	2.18, ↓ E6	22061	1.22	253	5	3
6-136, 6-176, 6-177	Phosphoglycerate kinase, chloroplastic ( <i>Nicotiana tabacum</i> , Q42961)	3.04, 10.42, 4.19, all ↓ E6	40048	5.85	4391.31	17	14.56
Cellular component							
6-171	Actin-101 ( <i>Solanum tuberosum</i> , P30173)	2.04, ↓ E6	35148	5.39	2605.41	8	18.07
Energy production							
6-125	ATP synthase gamma chain, chloroplastic ( <i>Spinacia oleracea</i> , P05435)	2.09, ↓ E6	48066	7.53	476.73	3	9.09
6-240, 6-241	ATP synthase subunit alpha, chloroplastic ( <i>Nymphaea alba</i> , Q6EW63)	2.25, ↓ E6, 5.94, ↑ E6	26876	5.38	635.85	13	20.24
Fatty acid biosynthesis							
6-013	Putative uncharacterized protein ( <i>Selaginella moellendorffii</i> , D8R975)	2.38, ↓ E6	34925	5.71	4086.17	16	20.06
Immunity and defence							
6-020	Superoxide dismutase [Cu-Zn], chloroplastic ( <i>Zantedeschia aethiopica</i> , O65175)	4.59, ↑ E6	42463	7.74	2152.24	15	13.64

6-034	2-Cys peroxiredoxin BAS1, chloroplastic ( <i>Oryza sativa Japonica</i> , Q6ER94)	3.41, ↓ E6	34488	6.43	291.03	3	6.54
Photosynthesis							
6-092	Oxygen-evolving enhancer protein 1, chloroplastic ( <i>Spinacia oleracea</i> , P12359)	2.51, ↑ E6	41616	5.08	19441.40	34	36.87
6-091, 6-093	Oxygen-evolving enhancer protein 1, chloroplastic ( <i>Solanum lycopersicum</i> , P23322)	2.68, ↑ E6, 2.70, ↑ E6	22706	9.89	671.77	12	21.74
6-058	Carbonic anhydrase, chloroplastic ( <i>Nicotiana tabacum</i> , P27141)	3.11, ↑ E6	40552	8.75	1502.09	5	10.19
6-077, 6-011, 6-029	Photosystem I reaction center subunit II, chloroplastic ( <i>Cucumis sativus</i> , P32869)	16.08, ↓ E6, 9.01, ↑ E6, 2.00, ↑ E6	42034	6.00	526.10	11	15.27
6-106, 6-111	Ferredoxin--NADP reductase, chloroplastic ( <i>Vicia faba</i> , P41346)	2.22, 15.02, all ↓ E6	57013	8.96	2497.04	16	17.99
6-027	Thylakoid lumenal 19 kDa protein, chloroplastic ( <i>Arabidopsis thaliana</i> , P82658)	3.50, ↑ E6	44257	8.72	463.24	5	14.46
6-003	Ribulose biphosphate carboxylase large chain ( <i>Isophysis tasmanica</i> , P92463)	3.03, ↓ E6	24964	0.15	93	1	1
6-153, 6-197, 6-200, 6-201	Ribulose biphosphate carboxylase/oxygenase activase, chloroplastic ( <i>Oryza sativa Japonica</i> , P93431)	2.15, 2.80, 2.05, 2.02, all ↑ E6	51734	5.84	1064.37	24	11.16
6-032	Oxygen-evolving enhancer protein 2, chloroplastic ( <i>Solanum tuberosum</i> , P93566)	3.89, ↓ E6	51421	5.26	14043.03	33	18.03
6-219	Ribulose biphosphate carboxylase large chain ( <i>Hyophorbe lagenicaulis</i> , Q9BA49)	6.94, ↑ E6	27987	0.14	63	2	1
Protein metabolism							
6-239	Serine hydroxymethyltransferase 1, mitochondrial ( <i>Flaveria pringlei</i> , P49357)	6.45, ↓ E6	27079	0.14	27	1	1

6-180	Aminomethyltransferase, mitochondrial ( <i>Pisum sativum</i> , P49364)	2.44, ↓ E6	37040	5.30	2239.21	10	21.88
6-022	30S ribosomal protein S3, chloroplastic ( <i>Oltmannsiellopsis viridis</i> , Q20F10)	3.49, ↑ E6	42121	7.80	671.72	14	14.95
6-115	Thiamine thiazole synthase, chloroplastic ( <i>Alnus glutinosa</i> , Q38709)	6.80, ↓ E6	50145	8.68	2517.63	22	21.21
Transport							
6-024	NAD(P)H-quinone oxidoreductase subunit M, chloroplastic ( <i>Oryza sativa</i> Indica, A2XVZ1)	3.37, ↓ E6	28079	0.66	161	5	4
6-042	Ras-related protein RABC1 ( <i>Arabidopsis thaliana</i> , O23657)	2.47, ↓ E6	55482	5.43	14105.94	118	34.91
<b>7-mpi</b>							
Carbohydrate metabolism							
7-297	Sedoheptulose-1,7-bisphosphatase, chloroplastic ( <i>Triticum aestivum</i> , P46285)	9.66, ↓ E7	22706	9.89	1334.91	25	32.37
Immunity and defence							
7-036	Superoxide dismutase [Cu-Zn], chloroplastic ( <i>Zantedeschia aethiopica</i> , O65175)	8.04, ↑ E7	22061	6.19	1993.32	11	15.74
Photosynthesis							
7-088	Photosystem I reaction center subunit II, chloroplastic ( <i>Cucumis sativus</i> , P32869)	2.62, ↓ E7	40552	8.75	760.06	13	17.63
7-220	Ferredoxin--NADP reductase, chloroplastic ( <i>Vicia faba</i> , P41346)	2.18, ↑ E7	42034	6.00	1871.33	13	19.85
7-007	Cytochrome b6-f complex iron-sulfur subunit, chloroplastic ( <i>Arabidopsis thaliana</i> , Q9ZR03)	2.46, ↑ E7	24350	8.69	1124.59	6	14.41

#### **4.6 Leaf proteins that changed in abundance during *G. boninense* infection**

The significant protein spots that were detected were picked, trypsin digested and identified using an LC-QToF mass spectrometer. The resulting mass spectra were searched against the Swissprot plant database (downloaded on 9<sup>th</sup> May 2014). Information such as the UniProtKB/Swissprot entry identifier, the organisms from which the proteins were identified, predicted molecular weight (Da), isoelectric point (pI) and the PLGS score were retrieved from the PLGS software (Waters Corporation). A list of proteins, complete with their respective identifications, UniProt entry, molecular weight (kDa), pI, PLGS score, peptide coverage, number of unique peptides and fold changes is provided in Appendix A.

A total of 116 protein spots were detected to have changed in abundance in leaf tissues of inoculated oil palm seedlings. However, only 107 were identified using mass spectrometry, indicating a 92% identification rate (Table 4.4). Nine spots were not picked for identification due to the difficulty in correctly picking the desired spot. These spots were not properly focused and they were too close to each other. Out of these 9 spots, 3 were from 3-mpi (3-017, 3-028, 3-037), 3 from 5-mpi (5-061, 5-095, 5-134), 2 from 6-mpi (6-036, 6-252) and 1 from 7-mpi (7-104).

After excluding these nine spots, protein spots with the same UniProt entries were removed. These numbers were further reduced to remove proteins that had the same identities, as well as to remove redundancies in the protein identities. The final number of protein spots was grouped based on time points. The number of protein candidates unique to 2-mpi was 2, 3-mpi was 29, 5-mpi was 6, 6-mpi was 27 while 5 were unique to 7-mpi.

**Table 4.5:** The numbers of unique proteins that were expressed in leaf tissues of inoculated oil palm seedlings (based on time points) were obtained by removing proteins with the same UniProt entries and identities.

Time points	Number of spots detected	Number of identified spots	Number of spots not identified	Number of unique proteins
2-mpi	2	2	0	2
3-mpi	52	49	3	29
4-mpi	0	0	0	0
5-mpi	10	7	3	6
6-mpi	46	44	2	27
7-mpi	6	5	1	5
Total	116	107	9	69

The proteins were then categorised based on their functions. They were grouped into ten functional categories – carbohydrate metabolism, cellular component, energy production, fatty acid biosynthesis, immunity and defence, nitrogen metabolism, protein metabolism, stress response, transport, and photosynthesis. Table 4.5 lists the identities of the unique proteins based on their functions, according to time points. Appendix B lists down the unique proteins with different expression patterns and abundances in leaf tissues of inoculated oil palm seedlings.

In leaf tissues of 2-mpi, two proteins were found to be higher in abundance compared to leaf tissues of non-inoculated oil palm seedlings. Thiamine thiazole synthase, which is involved in protein metabolism, was found to be 7.9-fold higher in abundance while ribulose biphosphate carboxylase/oxygenase activase, which is involved in the activation of ribulose-1,5-biphosphate carboxylase/oxygenase (RuBisCO) during photosynthesis, was 5.4-fold higher.

In leaf tissues of 3-mpi, proteins involved in immunity and defence, carbohydrate metabolism, energy production, nitrogen metabolism, photosynthesis, protein metabolism and stress response were found to have changed in abundance. The level of

protein abundance in chloroplastic phosphoribulokinase, phosphoglycerate kinase 2 and fructose-bisphosphate aldolase was higher while glyceraldehyde-3-phosphate dehydrogenase (GAPDH) A was lower. Cytosolic GAPDH A was also found to be higher in abundance in leaf tissues of inoculated oil palm seedlings. Proteins involved in energy production are ATP synthase subunit alpha, chloroplastic ATP synthase epsilon chain, ATP synthase subunit b and mitochondrial ATP synthase subunit d. All the proteins categorised under energy production were found to be higher in abundance except ATP synthase subunit alpha, which was lower in abundance.

Under immunity and defence, superoxide dismutase [Cu-Zn] (CuZnSOD), mitochondrial superoxide dismutase [Mn] (MnSOD), chloroplastic 2-cysteine peroxiredoxin BAS1 (2-cys Prx) and cytosolic L-ascorbate peroxidase 2 (cAPX) were found to be down-regulated. Stress response proteins, 14-3-3-like protein GF14 was 6.75-fold lower in expression while chloroplastic elongation factor Tu (EF-Tu) was 2.57-fold higher in leaf tissues of 3-mpi oil palm seedlings. Glutamine synthetase cytosolic isozyme under the nitrogen metabolism group was also found to be up-regulated at 2.1-fold.

Eight different proteins were functionally categorised under photosynthesis. Five proteins including chloroplastic ribulose bisphosphate carboxylase small chain, ribulose bisphosphate carboxylase large chain, RuBisCO large subunit-binding protein subunit alpha, chloroplastic chlorophyll a-b binding protein 6A and chloroplastic carbonic anhydrase were down-regulated. The remaining three proteins that were up-regulated in the chloroplasts consisted of RuBisCO large subunit-binding protein subunit beta, ferredoxin-NADP reductase leaf isozyme and oxygen-evolving enhancer protein 1. All five proteins that are involved in protein metabolism (chloroplastic 20 kDa chaperonin,

50S ribosomal protein L12, proteasome subunit beta type-3-B, proteasome subunit alpha type-5 and proteasome subunit alpha type-6) were down-regulated.

In leaf tissues of 4-mpi oil palm seedlings, no proteins were found to be significant in terms of expression. However, in leaf tissues of 5-mpi oil palm seedlings, proteins involved in photosynthesis (ribulose biphosphate carboxylase large chain, chloroplastic ribulose biphosphate carboxylase/oxygenase activase and chloroplastic oxygen-evolving enhancer protein 1) were all down-regulated. The stress response protein, heat shock 70kDa protein, was up-regulated 2-fold. Proteins categorised under carbohydrate metabolism were located in the chloroplast and they comprised of transketolase and sedoheptulose-1,7-bisphosphatase.

In leaf tissues of 6-mpi oil palm seedlings, the most number of proteins detected to be differentially expressed fell under photosynthesis. Chloroplast proteins including oxygen-evolving enhancer protein 1 (OEE1), ribulose biphosphate carboxylase/oxygenase activase, carbonic anhydrase, thylakoid lumenal 19 kDa protein and photosystem I reaction centre (PSI) subunit II were found to be up-regulated while oxygen-evolving enhancer protein 2 (OEE2), ferredoxin-NADP reductase and ribulose biphosphate carboxylase large chain were down-regulated. All six proteins that were functionally grouped in carbohydrate metabolism were found to be down-regulated. They comprised of chloroplast proteins (GAPDH B, GAPDH GAPA1, transketolase, fructose-bisphosphate aldolase and phosphoglycerate kinase) and the cytosolic protein, triosephosphate isomerase (TPI).

Under protein metabolism, chloroplastic 30S ribosomal protein S3 was 3.49-fold higher in leaf tissues of 6-mpi oil palm seedlings. Chloroplastic thiamine thiazole synthase was

6.8-fold lower in expression; while mitochondrial proteins, serine hydroxymethyltransferase 1 and aminomethyltransferase, were 6.45- and 2.44-fold lower, respectively. ATP synthase gamma chain and its subunit alpha, functionally categorised under energy production, were found to be down-regulated. Immunity and defence proteins, CuZnSOD was 4.59-fold higher while 2-cys Prx was 3.41-fold lower in expression. Proteins that are involved in transportation were down-regulated 3.37-fold in NAD(P)H-quinone oxidoreductase subunit M while ras-related protein RABC1 was also 2.47-fold lower. Actin-101, grouped under cellular components, was 2.04-fold higher in expression while a putative uncharacterized protein, grouped under fatty acid biosynthesis, was found to be 2.38-fold lower in expression.

CuZnSOD, ferredoxin-NADP reductase and cytochrome b6-f complex iron-sulfur subunit were 8.04-, 2.18- and 2.46-fold higher in leaf tissues of 7-mpi oil palm seedlings, respectively. On the other hand, sedoheptulose-1,7-bisphosphatase and PS1 subunit II were 9.66- and 2.62-fold lower in expression, respectively.

#### **4.7 Validation of protein abundance by Western blotting**

Western blotting was carried out to validate protein spots that changed in abundance generated from 2-DE analysis of *G. boninense* inoculated and non-inoculated oil palm seedlings. Three individual plants were each sampled from non-inoculated and inoculated oil palm seedlings. Proteins were extracted from leaf tissues of 3-mpi seedlings. The protein expression ratio between non-inoculated and inoculated tissue samples was also generated.

With 69 unique protein candidates to work with, only five were able to be validated using Western hybridization. This was due to the easy accessibility of commercial

antibodies that were available. The selected proteins were 14-3-3-like protein GF14, MnSOD, CuZnSOD, cAPX 2 and RuBisCO large subunit-binding protein as the loading control. The immunogens were derived from plants.

The molecular weights of the proteins that were detected using commercially available polyclonal antibodies were in accordance with the expected results provided by the manufacturer (Table 4.6). All antibodies detected a major band at a position close to the predicted molecular weights, except for 14-3-3 which accounted for three bands (Figure 4.13). After the blots have been analysed, the protein expression ratio between non-inoculated and inoculated samples was calculated by dividing the normalised values obtained from inoculated samples with normalised values obtained from non-inoculated samples.

The Western blot results obtained for 14-3-3 and CuZnSOD were consistent with the 2-DE data (Table 4.7). In both analyses, the levels of protein abundance for 14-3-3 and CuZnSOD from inoculated samples were lower compared to non-inoculated samples. However, the protein abundance ratio from both analyses differed significantly. In the case of MnSOD and cAPX, the levels of protein abundance were detected to be higher in Western blots compared to 2-DE. The abundance ratios for these two proteins calculated from Western blot were higher than data obtained for 2-DE.

**Table 4.6:** Five antibodies were used to detect the presence of candidate proteins in leaf tissues and RbcL was used as a loading control. The predicted molecular weights were in accordance with the experimental data.

Primary antibody	Organism	Host	Predicted size (kDa)	Experimental size (kDa)
14-3-3 GRF (14-3-3 like protein)	Arabidopsis thaliana	Rabbit polyclonal	20-28	30
MnSOD (manganese superoxide dismutase)	Arabidopsis thaliana	Rabbit polyclonal	25	21.5
CSD2 (Cu/Zn superoxide dismutase)	Arabidopsis thaliana	Rabbit polyclonal	19-22	15
cAPX (ascorbate peroxidase)	Zea mays	Rabbit polyclonal	28	22
RbcL (control)	Arabidopsis thaliana	Rabbit monoclonal	52	50

**Table 4.7:** The abundance ratio obtained from Western blots were compared to the ratios obtained from 2-DE. The protein candidates identified from 2-DE analysis were found to be lower in abundance compared to the ones detected using Western blots. Arrows indicate that the level of protein abundance were either lower or higher in inoculated samples compared to non-inoculated samples.

Protein candidate	Abundance ratio (2-DE)	Abundance ratio (Western)
14-3-3	6.75, ↓	0.82, ↓
CuZnSOD	3.04, ↓	0.86, ↓
MnSOD	2.21, ↓	1.80, ↑
cAPX	2.72, ↓	1.95, ↑

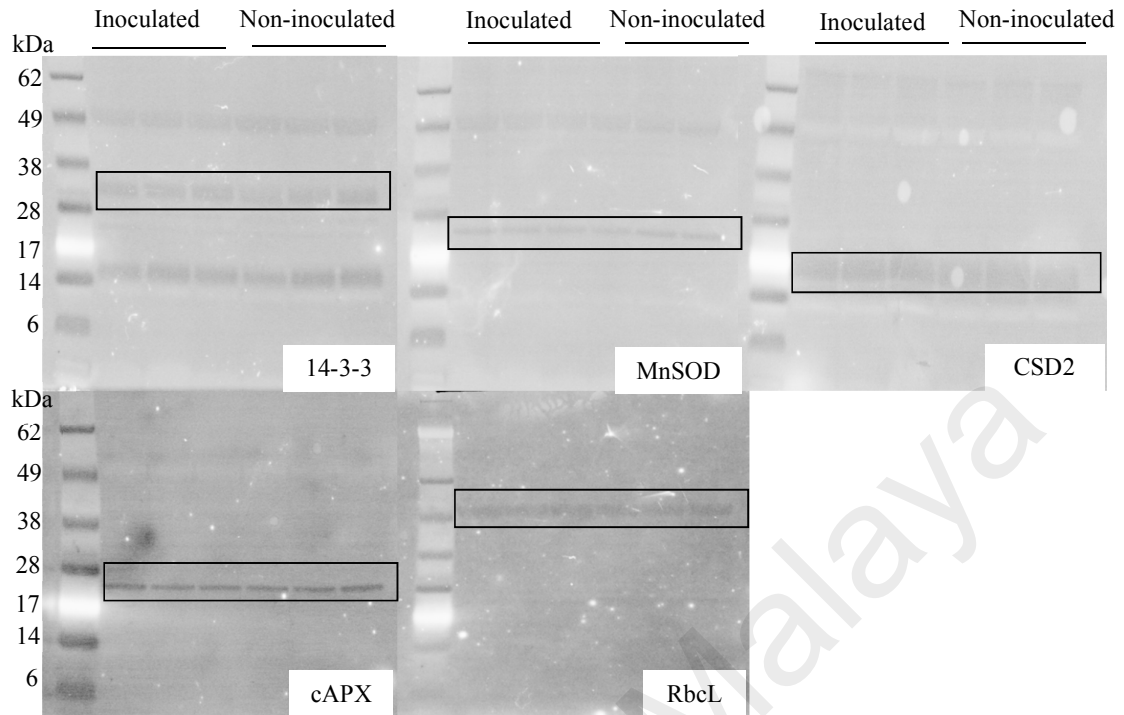


**Figure 4.13:** Western blotting detection of leaf proteins in non-inoculated and inoculated oil palm seedlings. The protein sizes (boxed area) of the detected candidate proteins are in concordance with the predicted weights. Protein marker: SeeBlue Plus2 (Novex).

#### 4.8 Bioinformatic analysis of 2-cys peroxiredoxin

The 2-cys Prx candidate protein obtained from 2D-PAGE was searched against the nucleic acid sequence of the oil palm root transcriptome. Blast result showed that it hit a list of several full length isotig sequences with isotig46827 being the highest score of 485. Isotig46827 has a length of 1240 bp, an open reading frame (ORF) of 822 bp and 274 amino acids. An InterProScan search revealed that this protein belongs to the thioredoxin-like superfamily, with an alkyl hydroperoxide reductase subunit C (thiol specific antioxidant) domain. A blast search against the NCBI database showed that the candidate protein shared the highest homology (85%) with 2-cys Prx-like protein mRNA (*Hyacinthus orientalis*).

#### 4.9 RNA extraction and cloning of cDNA encoding 2-cys peroxiredoxin

Total RNA was extracted from the leaves of oil palm seedlings. The purity of the extracted RNA was determined by electrophoresis on agarose gels (Figure 4.14). The RNA was quantified using a spectrophotometer (NanoDrop) with the 260/280 ratio of 1.8 and yield of 210.9 ng/ $\mu$ L. The cDNA has a concentration of 753.7 ng/ $\mu$ L with the 260/230 ratio of 1.6.

A total of 200 ng of cDNA template was used for cDNA amplification. The expected size of cyclophilin was approximately 200 bp. The amplified cDNA of 2-cys Prx gene has an ORF of 822 bp long with 274 aa with an approximate molecular weight of 30 kDa (Figure 4.15).

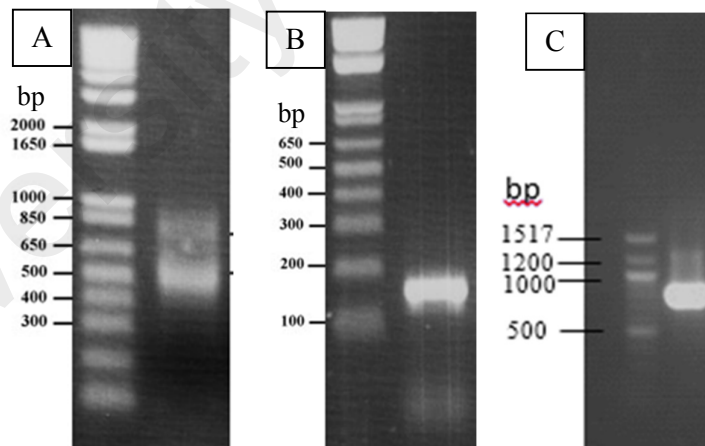


**Figure 4.14:** Total RNA extracted from leaves of oil palm seedlings and PCR products of cyclophilin and 2-cys peroxiredoxin were run on agarose gels. (A) Total RNA with bands indicating the presence of 28S and 18S rRNA, (B) cDNA that has been reverse-transcribed from RNA was used to amplify the cyclophilin gene, (C) cDNA of 2-cys peroxiredoxin was successfully amplified at approximately 800 bp.

**ATG** GCT TGC TCC GTT CCT TCC ATT GTC TCC TCG AAC CCT AGG GTT TTC CCT TCC  
**M** A C S V P S I V S S N P R V F P S

AAG CCC TTG ACT CCC ACA GCG TCT TTG CCT CCC GCC CCG GGG CTT CTC TCC CTA  
 K P L T P T A S L P P A P G L L S K

AAA ACC GCC GTC CCG AAG AGC TTC CAC GGC CTC CGG AAG AGC TTC CAC CCT CGC  
 A T L V P K S F H G L R K S F H P R

TCC GCT CCG ATG GTC TCT TCT CCT AGA TCC TCC CGA AGA AGC TTC GTC GTG AAT  
 S A P M V S S P R S S R R S F V V N

GCC GTC AGC GGG AGT GAG CTG CCG CTG GTT GGA AAT CGA GCA CCA GAT TTT GAG  
 A V S G S E L P L V G N R A P D F E

GCT GAA GCA GTC TTT GAT CAG GAG TTC ATC AAT GTG AAA CTC TCT GAT TAT ATT  
 A E A V F D Q E F I N V K L S D Y I

GGG AAG AAG TAT GTG ATT TTG TTT TTC TAC CCA CTG GAT TTT ACA TTT GTT TGC  
 G K K Y V I L F F Y P L D F T F V C

CCC ACT GAG ATA ACT GCT TTC AGT GAT CGG TAC TCA GAA TTT GAG CAG CTG AAT  
 P T E I T A F S D R Y S E F E Q L N

ACA GAA ATA TTG GGT GTT TCA ATC GAC AGT GTG TTC TCC CAT CTT GCA TGG GTT  
 T E I L G V S I D S V F S H L A W V

CAA ACA GAC AGG AAG TCA GGG GGA CTT GGT GAT CTG AAG TAT CCG TTG ATT TCT  
 Q T D R K S G G L G D L K Y P L I S

GAT GTT ACC AAG TCA ATT TCA AAA TCT TTT GGA GTT TTG ATT CCT GAT CAG GGA  
 D V T K S I S K S F G V L I P D Q G

ATT GCA TTG CGA GGA CTG TTC ATC ATT GAC AAG GAA GGA GTG ATT CAG CAT TGT  
 I A L R G L F I I D K E G V I Q H C

ACT ATT AAC AAC CTT GCC ATT GGA CGG AGT GTT GAT GAA ACC ATG AGG ACC CTT  
 T I N N L A I G R S V D E T M R T L

CAG GCG TTG CAA TAT GTC CAA GAT AAC CCA GAT GAG GTC TGC CCT GCC GGA TGG  
 Q A L Q Y V Q E N P D E V C P A G W

AAG CCT GGG GAG AAG TCT ATG AAG CCA GAC CCT AAA CTC AGC AAG GAA TAC TTC  
 K P G E K S M K P D P K L S K E Y F

GCA GCT ATA **TAA**  
 A A I \*

**Figure 4.15:** The 822 bp ORF sequence for 2-cys peroxiredoxin has 274 amino acids. The start and stop codons are highlighted in red. The nucleic acid sequence is represented in three alphabets while the amino acid sequence is represented in a single alphabet.

#### 4.10 Protein expression

Once the cDNA amplification of 2-cys peroxiredoxin gene has been completed, it was sequenced to confirm its orientation. The amplified product was then subcloned into the pET49b expression vector. Fig 4.16 illustrates agarose gel images that were run to confirm that sizes of amplified products were indeed correct before proceeding to the following steps. The vector was then sequenced to confirm that the peroxiredoxin gene is in the correct reading frame and orientation in the vector (Fig 4.17). The expression vector containing the sequence of the 2-cys peroxiredoxin gene was transformed into *E. coli* and the recombinant protein was expressed in the soluble form. The expressed recombinant protein contains a GST-tag (22 kDa), a 1 kDa His-tag and the 30 kDa 2-cys peroxiredoxin protein. The predicted size of the recombinant protein was approximately 53 kDa. The expressed recombinant protein separated on the SDS-PAGE had a size of approximately 50 kDa.  $\beta$ -galactosidase protein (119 kDa) was used as an induction control (Fig 4.18).

The recombinant protein was identified to be the oil palm (*Elaeis guineensis* var *tenera*) thioredoxin peroxidase, with a predicted molecular weight of 31.6 kDa and a pI of 7.74. The PLGS score was high, at 16,072, indicating that the statistical measure of accuracy of assignment was significant, with a peptide coverage of 49.65% (Table 4.8).

The 2-cys Prx recombinant protein was purified using an immobilized metal affinity chromatography purification system (Thermo Scientific). The molecular weight of the purified protein was approximately 50 kDa, as determined using SDS-PAGE (Figure 4.19).

After purification, the recombinant protein was run through a pull-down polyHis

protein-protein interaction column to identify its' interacting partner. The recombinant bait protein (2-cys Prx) was immobilized to the cobalt resin column. The prey proteins used were stem and leaf proteins sampled from *Ganoderma*-inoculated oil palm seedlings. After the prey protein was eluted, it was then separated on SDS-PAGE (Figure 4.20). These bands containing prey proteins were individually cut and subsequently identified using an ESI-Quad-ToF mass spectrometer. The identities of the peptides were searched against the Viridiplantae database. Protein identification results showed that the prey proteins from L560 and L351 were uncharacterized proteins from *Oryza brachyantha*. Further investigation against the oil palm database (Sime Darby Technology Centre Sdn Bhd) found that the identification points to disease resistance protein RPM1 (*Arabidopsis thaliana*) with a UniProt ID of Q39214.

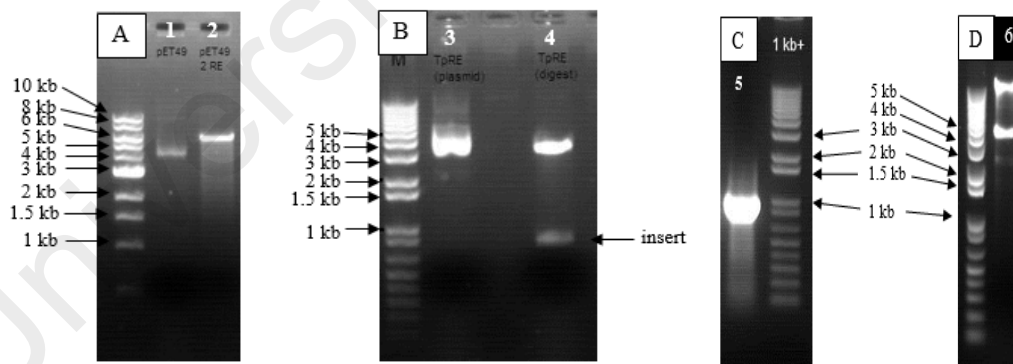


**Figure 4.16:** Agarose gel images of the pET-49b expression vector and gene insert prior to protein expression. (A) Lane 1: Circular, undigested pET-49b vector; Lane 2: Linearized pET-49b that has been digested with *EcoRI* and *NotI*; Marker: 1 kb DNA Ladder (NEB). (B) Lane 3: Plasmid containing the insert with the restriction enzymes sites incorporated; Lane 4: Digested pET-49b vector with the insert at approximately 800 bp; Marker: GeneRuler 1 kb Plus DNA Ladder (Invitrogen). (C) Lane 5: Colony PCR of the pET-49b expression vector containing the insert with restriction enzymes sites; Marker: GeneRuler 1 kb Plus DNA Ladder (Invitrogen); Lane 6: Extracted pET-49b/*tpx* plasmid containing vector and insert; Marker: GeneRuler 1 kb Plus DNA Ladder (Invitrogen).

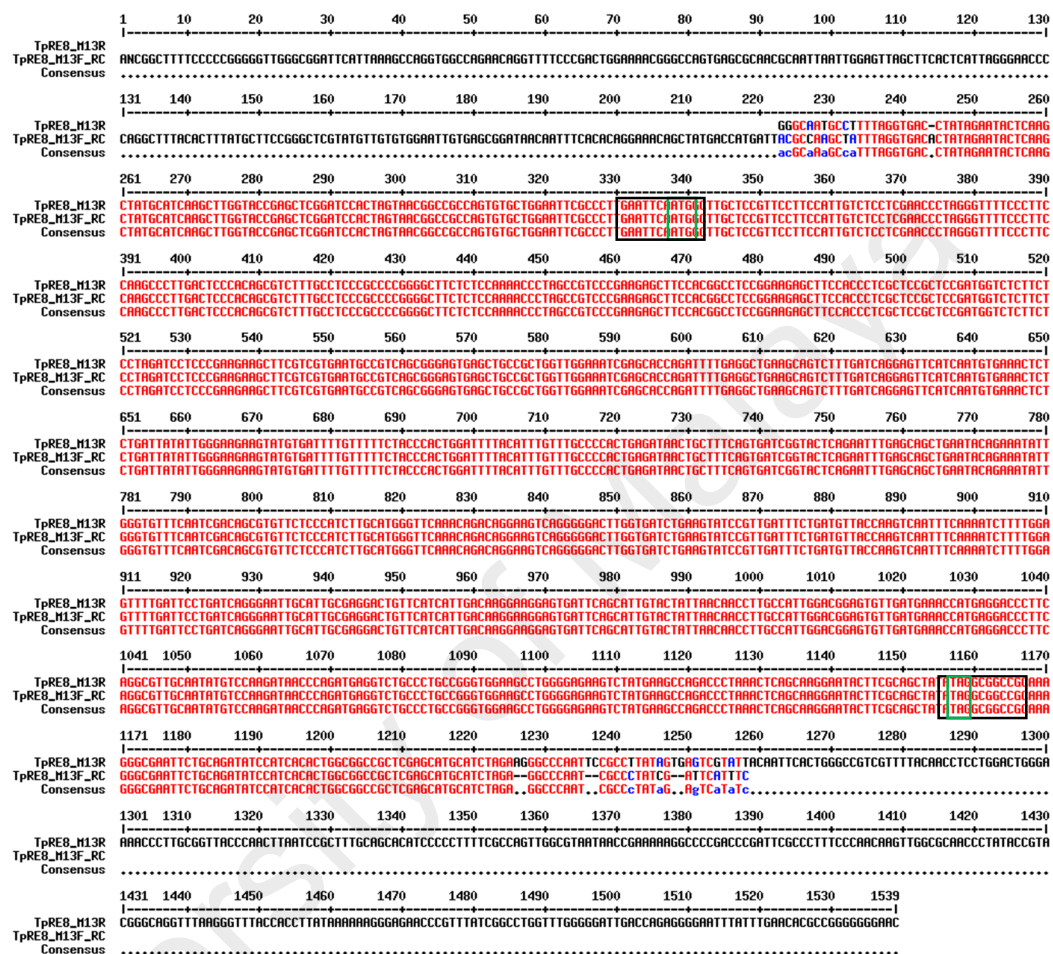


**Figure 4.17:** Aligned sequence consensus of the 2-cys peroxiredoxin gene with restriction enzymes cutting sites. Black boxes represent the primer sequences that were used for amplification while green boxes indicate the start and stop codons.

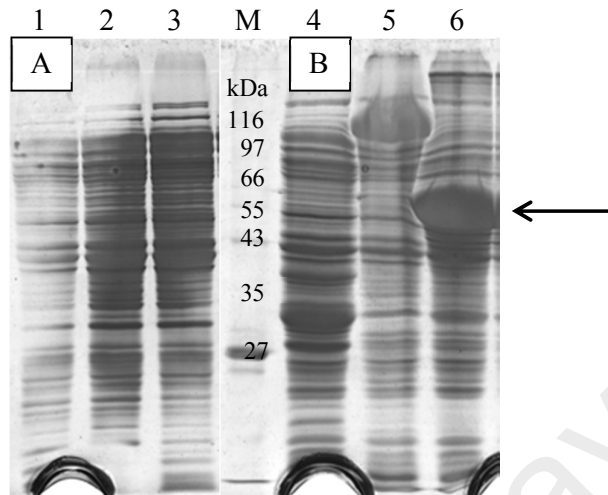


**Figure 4.18:** Expression of the target gene in the soluble cytoplasmic fraction before and after induction was accessed on SDS-PAGE. (A) Before induction: Lane 1: pET-49b expression vector without insert; Lane 2: β-galactosidase as an induction control; Lane 3: recombinant 2-cys peroxiredoxin protein. (B) After induction: Arrow indicates the presence of expressed recombinant 2-cys peroxiredoxin at approximately 53 kDa. Lane M: Prestained Broad Range Marker (NEB); Lane 4: pET-49b expression vector without insert; Lane 5: β-galactosidase as an induction control (119 kDa); Lane 6: recombinant protein with a size of approximately 53 kDa.

**Table 4.8:** The recombinant 2-cys peroxiredoxin protein was identified using an LC-qToF mass spectrometry. The resulting peptides were searched against the oil palm database (Sime Darby Technology Centre) for analogs.

Description	mW (Da)	pI (pH)	PLGS Score	Peptides	Theoretical Peptides	Coverage (%)
Thioredoxin peroxidase OS <i>Elaeis guineensis</i> var tenera	31,609	7.7452	16,072.82	85	23	49.6528

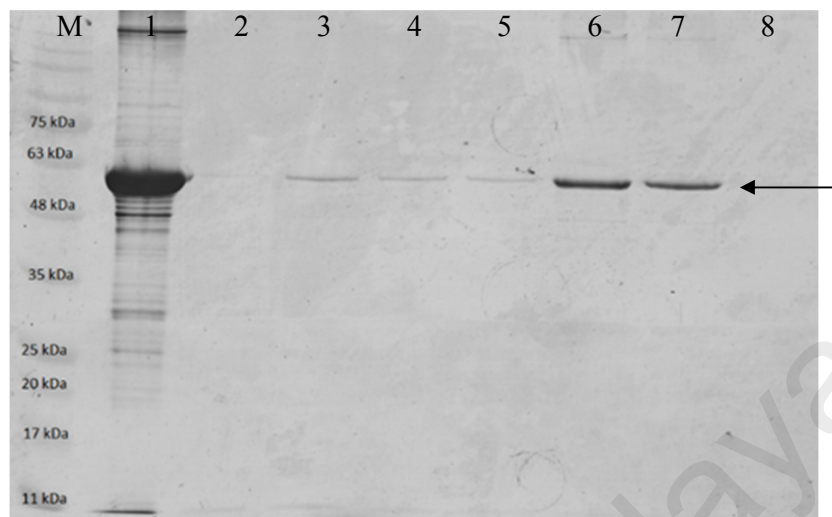


**Figure 4.19:** The recombinant 2-cys peroxiredoxin protein was purified using a polyhistidine-tagged nickel column. The purified protein (as indicated by an arrow) was eluted with an elution buffer containing 250 mM imidazole. The eluted protein was identified using the LC-QToF mass spectrometer. Marker: Prism Ultra Protein Ladder (Abcam), Lane 1: Unpurified protein; Lane 2: Flow-through; Lane 3: Wash 1; Lane 4: Wash 2; Lane 5: Wash 3; Lane 6: Eluant 1; Lane 7: Eluant 2; Lane 8: Eluant 3.

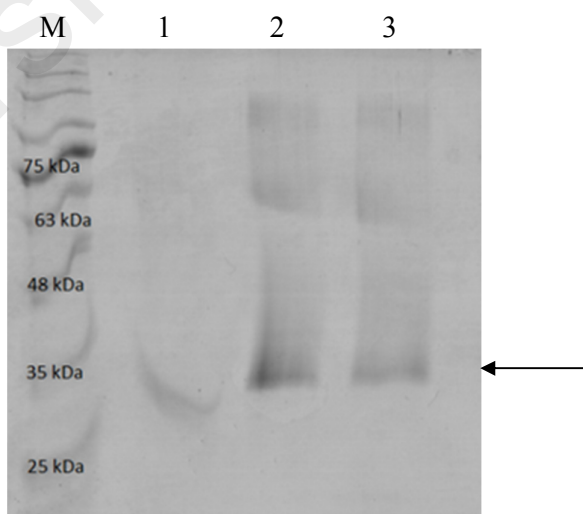


**Figure 4.20:** Prey proteins were detected in the first elution in the leaf tissues (L560 and L351) of *Ganoderma*-inoculated oil palm seedlings but not in the stem (S560). Arrow indicates the presence of the prey proteins. Marker: Prism Ultra Protein Ladder (Abcam); Lane 1: Stem (S560); Lane 2: Leaf (L560); Lane 3: Leaf (L351).

## CHAPTER 5: DISCUSSION

*Ganoderma boninense* is a basidiomycete fungal pathogen. It causes the incurable BSR disease in oil palm. Although efforts have been made to find cures for the disease, there is still no effective method to control and eliminate the disease. Currently there is also no molecular marker that can precisely detect the presence of the disease. The mode of infection of the BSR disease is primarily via the root system, however, detection of the disease through the root system is very invasive. It is also not practical to sample root tissues from adult palms as we may not correctly sample them. This is because of the presence of a large complex belowground root network of a mature palm. The root network may span across and include those from neighbouring palms. Furthermore, the results of this study could be used as potential biomarkers to detect oil palms that are infected with *Ganoderma boninense*, and the use of leaf tissues as starting materials seemed to be the easiest and least invasive method of sampling.

Therefore, in order to understand the changes in protein profiles of diseased palms, global protein expression profiles of both healthy and diseased palms using 2-DE were compared. These changes were observed in the leaf tissues of oil palm seedlings inoculated with and without the *Ganoderma* fungus. Leaf tissues were used as the source of global protein profiling because leaves are easily accessible. This mode of comparison diminishes the possibilities of wounding the roots and further exposing them to potential pathogen invasion.

Not much information has been reported regarding the specific molecular interactions that occur during BSR infection. The global protein expression of a diseased palm has also not been extensively profiled. This is especially so since the mode of infection is in

the roots, but the mode of detection is in the leaves. Several reports contemplated that when plant roots come into contact with belowground pathogens, the plant host defence responses are activated (Bezemer *et al.*, 2003; Bezemer *et al.*, 2004). These defence responses are channelled to the aboveground foliar through a series of signalling molecules. This mode of signalling transfer has been shown to occur in other plant studies where these signalling molecules were transported from belowground to aboveground. The same was also reported to occur from aboveground to belowground (Bezemer and van Dam, 2005; Kumar and Bais, 2012; van Geem *et al.*, 2013). The same situation also occurs in oil palm. The expression of defence-related genes can be detected in both root and leaf tissues of *Ganoderma*-inoculated seedlings (Alizadeh *et al.*, 2011; Tan *et al.*, 2013). It is this aboveground-belowground relationship that has provided us with evidence to proceed with identification of changes in plant proteins that may be associated with *Ganoderma* infection.

### **5.1 Protein extraction and analysis**

Four methods were used to extract total proteins from the leaf tissues of oil palm seedlings, namely the phenol-guanidine isothiocyanate, TCA-acetone precipitation, sucrose and TCA-acetone-phenol methods. The profiles of leaf proteins from both inoculated and non-inoculated oil palms were presented by accessing these four extraction methods. Among these methods, the TCA-acetone-phenol method managed to extract proteins that could be consistently run on SDS-PAGE and 2D-PAGE. By using this method, a broad range of proteins from low to high molecular weights were extracted and this has been proven useful for Western validation work. The 2D-PAGE profiles that were produced using proteins extracted using this method clearly showed a uniform coverage of spots across a wide pH range.

### **5.1.1 Phenol-guanidine isothiocyanate method**

Based on the SDS-PAGE profiles of leaf proteins, this method seemed to be able to extract proteins below 100 kDa. However, it yielded the least amount of extracted proteins compared to other extraction methods. This may be due to the fact that leaf tissues were subjected to several chemical processes prior to protein extraction. Cell debris was removed, followed by different precipitation steps for RNA and DNA. Contaminants were removed before protein pellets were finally precipitated. A significant proportion of proteins may be lost as a consequence of these manipulations. Furthermore, chloroform was added to the phenol extract and this caused hydrophilic proteins to be precipitated into the organic phase. This organic phase was discarded together with DNA since chloroform does not precipitate hydrophobic proteins (D'Andréa *et al.*, 2007). This could also be the cause of low protein yield.

The SDS-PAGE profile showed that low molecular weight proteins were not extracted since they were not visible in the gel images. However, 2D gels of proteins extracted from young and mature leaves using this method yielded distinct spots, although they were not clear.

### **5.1.2 TCA-acetone precipitation method**

The TCA-acetone precipitation method yielded the highest amount of extracted proteins. However, this did not include any steps to remove carbohydrates and polysaccharides. Therefore, a lot of protein seemed to be precipitated into pellets. Approximately 3.5 mg extracted proteins per g of starting material were obtained compared to other extraction methods. The incomplete removal of interfering compounds during protein extraction could contribute to the increase in yield.

These compounds/substances may block gel pores and cause proteins to be precipitated during IEF. This may result in streaking, smearing or even loss of resolution (Carpentier *et al.* 2005). An overestimation of the protein content could also be caused by the presence of these interfering compounds during protein quantitation (Bradford, 1976). Moreover, the SDS-PAGE profile of this protein did not show any presence of high molecular weight proteins. This could impede future Western validation work which requires the validation of high molecular weight proteins. The 2D-PAGE profiles that were generated using proteins extracted from this method produced gel images with the least number of detectable spots.

### **5.1.3 Sucrose method**

The sucrose method showed the second highest protein yield among four methods that were tested. This could be due to the addition of PVPP and  $\beta$ -mercaptoethanol to the extraction buffer where both were used to remove phenolic compounds and polyphenols. Sucrose was added so that the mixture of proteins could be separated on top of the solution (Berg *et al.*, 2002). Moreover, the SDS-PAGE profiles for both young and mature leaf tissues were well resolved.

However, this method produced gel images with the highest background. The 2D-PAGE gel images of young leaves contained many unresolved spots that concentrated on the acidic end. Gel images of mature leaves showed many spots that were not clearly stained. Although addition of DTT was to reduce the disulfide bonds of proteins to prevent them from forming cysteine residues, this did not allow a better separation of proteins on the polyacrylamide gels.

#### 5.1.4 TCA-acetone-phenol method

The TCA-acetone-phenol method yielded 1.2 mg protein for young leaves and 3.6 mg protein for mature leaves. Lower protein yield from young leaves could indicate that mature leaves contained more proteins. The SDS-PAGE profile showed extracted proteins from both high and low molecular weights. Moreover, its 2D profiles of young and mature leaves managed to produce gel images with distinct spots. The gel images were easily reproducible, indicating that the extraction method is robust.

This extraction method produced 1D gels that are suitable for downstream validation work (eg Western hybridization). The 1D profile managed to separate a broad range of proteins and many visible spots could be detected from its' 2-DE profiles. This is because a 1-D profile with protein bands that cover most of the molecular weight range is an added advantage for validation using Western blotting when compared to a protein profile with fewer numbers of bands. It can be potentially used for further downstream studies of the oil palm leaf tissue proteome.

Kiskini *et al.* (2016) reported that there was no effect of plant age to the amount of protein extracted in sugar beet. Within the same variety of sugar beet, the protein content from young and mature leaves were similar. They concluded that variations in the final protein isolation yield were mostly due to variations in nitrogen extractability (28–56%). However, in the case of oil palm, more mature leaf proteins were extracted compared to young leaf tissues.

In short, the TCA–acetone–phenol extraction method was consistent in extracting proteins from oil palm leaf tissues. It is evident in the 1D- and 2-DE gel separation, detection and analysis of protein spots. This method incorporates phenol in the

extraction protocol where it efficiently recovers proteins and effectively removes non-protein components from plant tissues (Faurobert *et al.*, 2007). This method was used in subsequent protein extractions from leaf tissues.

## **5.2 Leaf protein candidates that changed in abundance in relation to BSR**

An investigation into the global view of the proteome from leaves of both inoculated and non-inoculated oil palm seedlings was performed. Proteins that changed in abundance were identified and it is possible to exploit them for the detection of the BSR disease. This may also shed some light into the biological changes that occurred in the host plant in relation to *G. boninense* attack. Although stress and defence responses play important roles in understanding plant-pathogen interaction, other responses may also suggest crucial changes that are related to disease infection. Currently, no known biological markers can be directly linked to BSR disease.

From the list of protein candidates that changed in abundance, nine spots were not picked for identification because they were difficult to be picked (neighbouring spots were too close to each other) or that the amount required for detection using mass spectrometry was not sufficient. After removing redundant identities, the remaining 69 unique protein spots were then categorised based on their functions. They were grouped into nine functional categories – photosynthesis, carbohydrate metabolism, protein metabolism, immunity and defence, energy production, stress response, transport, cellular component, fatty acid biosynthesis and nitrogen metabolism.

### **5.2.1 Photosynthesis**

Plants are constantly invaded by pathogens such as bacteria, fungus and viruses. The plant's immune system subsequently undergoes non-stop reinforcement to protect

themselves from further damage. To be able to withstand this situation, more resources from growth are allocated to defence responses. Therefore, a global reduction of photosynthetic capacity can be observed in leaf tissues (Bilgin *et al.*, 2010). The following proteins were grouped under photosynthesis: chlorophyll a-b binding protein 6A, ferredoxin-NADP reductase, Photosystem I reaction centre (PSI) subunit II, cytochrome b6-f complex iron-sulfur subunit, oxygen evolving enhancer protein 1 (OEE1), oxygen evolving enhancer protein 2 (OEE2), ribulose biphosphate carboxylase large and small chains, ribulose biphosphate carboxylase/oxygenase activase, RuBisCO large subunit-binding protein subunit  $\alpha$  and  $\beta$ , thylakoid luminal 19 kDa protein and carbonic anhydrase.

During photosynthesis, plants convert carbon dioxide and water into sugar (food) and oxygen by absorbing light energy from the sun. This process occurs in the chloroplast, where the main organelles are thylakoid membranes and stroma (aqueous liquid). Photosynthesis goes through two main reactions: photosystem II (light dependent reaction) and photosystem I (light independent reaction). Photosystem II is the first step of photosynthesis where chlorophyll, which gives leaves their green colour, absorbs energy from light and transfers this energy to the reaction centres of the photosystems.

In the light reaction, energy emitted by the sun is utilized to synthesize ATP and NADPH. ATP is the source of cellular energy while NADPH is a cellular reducing agent. In the dark reaction, carbon dioxide ( $\text{CO}_2$ ) is fixed and converted to carbohydrates where ATP and NADPH are consumed (Suga *et al.*, 2015). Most of the proteins that were found to be different in abundance were found to function in both Photosystem I and II.

The role of photosynthesis in plant defence is still not clear. Garavaglia *et al.* (2007) observed that the expression of sugar-regulated photosynthetic proteins, such as Rubisco, Rubisco activase and ATP synthase, decreased during citrus canker infection. This indicates that at the onset of disease infection, the biosynthesis of defence-related compounds are a priority for the survival of the plant. Other growth related cellular activities are reduced, thereby diminishing photosynthetic rates until pathogenic growth has been controlled (Berger *et al.*, 2007; Bolton, 2009; Bilgin *et al.*, 2010).

Some photosynthetic proteins may be induced for expression during interactions between apple leaves and *Marssonina coronaria*. The involvement of light-sensing mechanisms has been implicated in the induction of plant disease defence signalling (Li *et al.*, 2014). Several proteins related to photosynthesis were changed and this suggested that the dynamic influence of pathogen on host photosynthetic machinery (Berger *et al.*, 2007).

A decrease in the photosynthetic activity was obvious in some plants following pathogen infection (Li *et al.*, 2014). The higher abundance in photosynthetic proteins at 2-mpi can be explained by the rapid defence response to the fungus. However, a decline can be detected following 3-, 5- and 6-mpi. As the disease progresses, it is possible that the gradual decline in the rate of photosynthesis in infected areas of the plants is caused by pathogens. At 7-mpi, the photosynthetic protein activities could be seen to increase slightly in abundance but this trend could not be investigated further as no further leaf samples were collected. The gradual decline of photosynthetic proteins starting from 3-mpi may indicate that the fungal infection could have possibly inhibited the rate and extent of photosynthetic processes. This down-regulation of proteins involved in photosynthesis during pathogen infection may be due to the allocation of more energy

and resources from growth to defence in the roots, hence a global reduction of photosynthetic capacity in leaf tissues can be observed.

### 5.2.2 Carbohydrate metabolism

The following two groups of proteins were grouped under carbohydrate metabolism. Proteins involved in glycolysis include triose phosphate isomerase (TPI), phosphoglycerate kinase, phosphoglycerate kinase 2, glyceraldehyde-3-phosphate dehydrogenase (GAPDH), glyceraldehyde-3-phosphate dehydrogenase A (GAPDH A), glyceraldehyde-3-phosphate dehydrogenase B (GAPDH B), glyceraldehyde-3-phosphate dehydrogenase GAPA1 (GAPDH GAPA1) and fructose-bisphosphate aldolase. Proteins associated with the Calvin cycle include phosphoribulokinase, sedoheptulose-1,7-bisphosphatase and transketolase,

The Calvin cycle is a series of chemical reactions that takes place in the chloroplast during photosynthesis. Energy is generated by photosynthesis and CO<sub>2</sub> is converted into organic compounds (Michelet *et al.*, 2013). Glycolysis is a process where carbohydrates and sugar are broken down to release energy in the form of ATP. It takes place during cellular respiration in the cytoplasm. Both chemical reactions result in the production of energy. The differential protein analysis indicates that most of the proteins found to be involved in the carbohydrate metabolism have decreased in abundance. This could be due to the channelling of energy towards other factors including defence responses.

However, fructose-bisphosphate aldolase was found to be of higher abundance in 3-mpi. Fructose 1,6-bisphosphate aldolase is thought to be potential to control photosynthetic carbon flux through the Calvin cycle (Uematsu *et al.*, 2012). An increase in aldolase activities showed enhanced growth and increased biomass in tobacco plants. In the case

of oil palm artificially inoculated with *G. boninense*, the increase in fructose 1,6-bisphosphate aldolase could potentially push the photosynthetic carbon flux towards increased photosynthetic rates. This can be seen in the differential analysis of 7-mpi where proteins involved in photosynthesis were seen to increase in abundance.

One report has suggested an increase in the accumulation of cytosolic GAPDH in response to biotic stresses or elicitors in maize (Chivasa *et al.*, 2005). Abiotic stresses are also known to affect the protein abundance of GAPDH. Transketolase was also found to be involved in carbohydrate metabolism. For example, transketolase has been shown to be involved in the formation of a sugar, octulose, in *Craterostigma plantagineum* (Zhang *et al.*, 2016). Octulose is localized in the cytosol and then transported from the leaves to the roots. Protein phosphorylation has been reported in leaf blades, leaf sheaths and roots of young rice seedlings under various stress conditions (Khan *et al.*, 2005). GAPDH have also been found as targets of phosphorylation cascades in rice under stressed conditions.

### **5.2.3 Protein metabolism**

The following proteins were grouped under protein metabolism: 20 kDa chaperonin, 30S ribosomal protein S3, 50S ribosomal protein L12, aminomethyltransferase, proteasome subunit alpha type-5, proteasome subunit alpha type-6, proteasome subunit beta type-3-B, serine hydroxymethyltransferase 1 and thiamine thiazole synthase. Many biochemical processes are involved in protein metabolism. These processes are responsible for the synthesis of amino acids and proteins as well as the breakdown of proteins by catabolism. Changes in the rate of protein synthesis, including accumulation and degradation in connection with plant growth and function are also involved during protein metabolism.

A 20 kDa chaperonin, 50S ribosomal protein, proteasomes and thiazole biosynthetic enzyme were found to be different in abundance in BSR-inoculated oil palm leaf tissue. All these proteins were found to have decreased abundance except thiazole biosynthetic enzyme.

Molecular chaperones control the folding and assembly of newly synthesized proteins where they are usually present in the form of linear chains of amino acids (Evstigneeva *et al.*, 2001). Chaperonins usually fold these linear chains into three-dimensional forms. They are responsible for correctly folding these amino acid chains. Chaperonins belong to a large class of molecules called chaperones. The levels of chaperonins are known to be influenced in plant–pathogen interactions (Cui *et al.*, 2005; Garg *et al.*, 2013).

In plants, abnormal or non-functional polypeptides are selectively removed by proteasomes through proteolysis. This is to maintain homeostasis and control the development, growth and physiology of plants (Santner and Estelle, 2010). However, the ubiquitin/proteasome system mediates the selective proteolysis in plants. During defence against pathogens, damaged proteins may be harmful to the cell if they experience translational errors or form aggregates. Proteasomes then remove these damaged proteins.

The biosynthesis of thiamine involves the thiazole biosynthetic enzyme. This enzyme is associated with mitochondrial DNA damage tolerance (Godoi *et al.*, 2006; Ribeiro *et al.*, 2005). It is detected at different stages in the organs throughout a plant's lifecycle. However, it is more active in shoots where its expression is affected by different stresses (Ribeiro *et al.*, 2005). Rapala-Kozik *et al.* (2012) discovered that thiamine indirectly participates in the plant adaptation processes to oxidative stress. It has been

suggested that during the early phase of *Arabidopsis* seedlings response to salt and osmotic stresses, the thiamine biosynthesis processes were quickly activated (Rapala-Kozik *et al.*, 2012).

#### **5.2.4 Immunity and defence**

The following proteins were grouped under immunity and defence: chloroplastic 2-cysteine peroxiredoxin BAS1 (2-cys Prx), cytosolic L-ascorbate peroxidase 2 (cAPX), chloroplastic superoxide dismutase [Cu-Zn] (CuZnSOD) and mitochondrial superoxide dismutase [Mn] (MnSOD). These proteins were found to be lower in abundance in leaf tissues of artificially inoculated oil palms.

The production of reactive oxygen species (ROS) increases and can cause significant damage to the cells when plants are exposed to stressful environmental conditions (Caverzan *et al.*, 2012). Plants deploy many defence mechanisms when attacked by pathogens. One such mechanism is the oxidative burst. Oxidative bursts occur with rapid production of ROS, especially hydrogen peroxide (H<sub>2</sub>O<sub>2</sub>). H<sub>2</sub>O<sub>2</sub> is important in signalling processes that lead to the strengthening of defence-related genes (Faize *et al.*, 2012). The production of ROS is one way to recognize successful pathogen infection followed by activation of plant defence (Torres, 2010; Espinosa *et al.*, 2014). ROS play many signalling functions. They mediate the establishment of multiple responses and also act as local toxins (Torres, 2010; O'Brien *et al.*, 2012).

2-cys Prx regulates the intracellular concentration of H<sub>2</sub>O<sub>2</sub>. This regulation of H<sub>2</sub>O<sub>2</sub> then controls gene transcription and cell signalling through phosphorylation cascades (Wagner *et al.*, 2002). The sudden surge of ROS in the early defence responses in oil palm could have caused its defence mechanisms to be compromised. As a consequence,

certain defence proteins are down-regulated. If not rapidly processed, this sudden surge of ROS could cause oxidative damage to proteins and other components of the cell.

Antioxidant defences can detoxify ROS, and they are present in plants. Prx and ascorbate peroxidase are some of the most important H<sub>2</sub>O<sub>2</sub> detoxifying antioxidants in plant cells. The Prx enzymes use thioredoxin as a specific electron donor in catalysing the conversion of H<sub>2</sub>O<sub>2</sub> into water (Ohdate *et al.*, 2010). Ascorbate peroxidase uses ascorbate as its specific electron donor (Caverzan *et al.*, 2012).

2-cys Prx belong to a family of peroxide detoxifying enzymes (König *et al.*, 2002; Dietz, 2003). Prxs can be regulated by changes to phosphorylation, redox and possibly oligomerisation states (Wood *et al.*, 2003, Muthuramalingam *et al.*, 2009). The metabolisms of ROS can be regulated by antioxidants through oxidative bursts (Nowogórska and Patykowski, 2015).

Superoxide dismutase (SOD) is part of the first line of defence against ROS (Alscher *et al.*, 2002). They are responsible for the efficient removal of superoxides that are formed during photosynthetic electron transport by catalysing the dismutation of superoxide into oxygen and H<sub>2</sub>O<sub>2</sub>. SODs are also involved in ROS metabolism (Pilon *et al.*, 2011). Since SOD is the first defence mechanism to be activated when the oil palm is under attack by the fungus, its abundance was found to be higher compared to other antioxidant enzymes.

### **5.2.5 Energy production**

Chloroplastic ATP synthase epsilon ( $\epsilon$ ) chain, ATP synthase gamma ( $\gamma$ ) chain, ATP synthase subunit alpha ( $\alpha$ ), ATP synthase subunit b and the mitochondrial ATP synthase

subunit d were grouped together under energy production.

Chloroplasts and mitochondria act as power plants of living cells. Both organelles use ATP synthase in the electron transport chain to create an electro-chemical gradient. The flow of hydrogen ions through the ATP synthase channel combines ADP with phosphate group to produce ATP as energy (von Ballmoos *et al.*, 2008; von Ballmoos *et al.*, 2009). Although the majority of spots were from the chloroplastic ATP synthase, mitochondrial ATP synthase subunits were also identified. These ATP synthases were found to be lower in abundance in diseased oil palms. ATP synthase was down-regulated in the interaction between *Xanthomonas axonopodis* pv. citri and citrus plants, which causes citrus canker (Zimaro *et al.*, 2011). In the proteomic analysis of Arabidopsis, a homozygous gene knockout mutants of ATP synthase  $\beta$ -subunit was identified as a plant cell death regulator (Chivasa *et al.*, 2011). Plants in which the gene for ATP synthase was knocked out by insertion of a transfer-DNA sequence became resistant to fumonisin B1-induced cell death.

#### **5.2.6 Stress response**

Stress response proteins, 14-3-3 like protein and plant elongation factor Tu, were also found to change in abundance in BSR inoculated oil palm seedlings. The 14-3-3 like proteins were found to regulate cellular signal transduction and primary metabolism. The 14-3-3 protein encoding gene, GF14, has been found to be regulated between rice and *Xanthomonas oryzae* (Chen *et al.*, 2006; Manosalva *et al.*, 2011). During the effector-triggered immunity associated with pathogens, the GF14 gene was believed to be induced. As evident in barley in the non-host hypersensitive response with *Blumeria graminis*, the 14-3-3 protein encoding gene was identified to be involved.

Hydrolases are activated when they are bound to the 14-3-3 proteins. This creates a binding site for the fungal phytotoxin fusicochin. Upon fungal attack, this fusicochin-binding activity increases through activating the proton pump to stimulate the defence response.

One of the key proteins that play a major role in the elongation phase of protein synthesis is the protein synthesis elongation factor Tu (EF-Tu). The EF-Tu protein can be found in bacteria and organelles including mitochondria, and plastids in plants (Fu *et al.*, 2012). The N-terminal part of the EF-Tu protein was identified as the elicitor. This was based on studies conducted on the immune responses of the plant cells to different fragments of EF-Tu. The first 18 amino acids of the protein contains the N-terminal acetylated peptide which was then subsequently identified to be the fully active inducer of defence responses (Kunze *et al.*, 2004; Zipfel *et al.*, 2006). This implies that EF-Tu is regulated in biotic stress in plants. The mechanisms of disease resistance may involve crosstalk at the molecular level.

### **5.2.7 Transport**

The following proteins were grouped under transport: NAD(P)H-quinone oxidoreductase subunit M and Ras-related protein RABC1.

The NAD(P)H:quinone acceptor oxidoreductase (NQO) gene belongs to the family of flavoproteins (Vasiliou *et al.*, 2006). The NAD(P)H-quinone oxidoreductase subunit M is an ortholog of NADH dehydrogenase (EC 1.6.5.3). They are involved in removing radicals contributing to oxidative stress (Sollner and Macheroux, 2009). Plant NAD(P)H-quinone oxidoreductase can use either NADPH or NADH as an electron donor and hydrophilic quinones as acceptors (Sparla *et al.*, 1996). However, this

enzyme prefers the short-chain acceptor quinones, such as ubiquinone and benzoquinone. The main function of NAD(P)H-quinone oxidoreductase is to reduce quinones to quinols, which prevents the production of potentially harmful semiquinones and oxygen radicals (Sparla *et al.*, 1996; Ryan *et al.*, 2014).

The Ras-related protein RABC1, a small Rab-related GTPase, functions in regulating vesicle trafficking. It regulates the formation of vesicles on donor membranes and facilitates vesicle docking on target membranes (Zerial and McBride, 2001; Gillingham and Munro, 2007). There are five major families of the Ras superfamily: Ras, Rho, Arf/Sar, Ran, and Rab. The Ras family regulates intracellular signalling and also functions as signalling molecules that are activated by extracellular stimuli (Rojas *et al.*, 2012). This signalling essentially controls gene transcription where cell growth and differentiation are eventually influenced. Plant Rab homologs were found to play functional roles in vesicle trafficking (McElver *et al.*, 2000; Lu *et al.*, 2001). Vesicle trafficking has been shown to be involved in the plant's immune response towards pathogens (Robatzek, 2007). During vesicle trafficking, vesicles are used transport intermediaries by which proteins and other macromolecules are distributed throughout the cell. The expression of Rab11 antisense RNA was found to cause defects in the secretion of cell wall-degrading enzymes in ripening tomatoes (Lu *et al.*, 2001).

### **5.2.8 Cellular component**

Under cellular component, actin-101 was found to have changed in abundance. Actin is a major component of the plant cytoskeleton where it supports cell shape and function. There are two forms of action: filamentous actin (F-actin) and globular action (G-actin). F-actin is involved in cell division and regulates the maintenance of the internal architecture of the cell (Deeks and Hussey, 2009). G-actin is the monomer from where

the F-actin is produced. Actins are also involved in many well documented functions. They support vesicle trafficking and coordinates the complex cytoplasmic responses to extra- and intracellular signals (Dominguez and Holmes, 2011).

### **5.2.9 Fatty acid biosynthesis**

A putative uncharacterized protein was grouped under fatty acid biosynthesis. A search through the UniProt database showed that this protein is coded by the selmodraft\_68476 gene. A more thorough search against the oil palm database found that this protein belongs to the thioesterase superfamily protein with a function in hydro-lyase activity and is expressed during growth stages. The heterologous expression of thioesterases has been found to influence the lipid profile of oilseed plants (Voelker *et al.*, 1992) and this has led to the engineering of plant thioesterases into other variety of plant species to alter their oil content (Thelen and Ohlrogge, 2002; Blatti *et al.*, 2012).

### **5.2.10 Nitrogen metabolism**

Glutamine synthetase (GS) cytosolic isozyme was grouped under nitrogen metabolism. It is involved in the primary assimilation of ammonia in all living organisms. It is also the key enzyme in nitrogen metabolism where the synthesis of glutamine is catalysed from glutamic acid, ATP and  $\text{NH}_4^+$ . The major isoforms of GS in plants are GS1 (cytosolic) and GS2 (chloroplastic) (Oliveira *et al.*, 2002). GS2 assimilates ammonia which is produced by nitrate reduction and photorespiration. GS1 assimilates  $\text{NH}_3$  which is produced during symbiotic nitrogen fixation in the nodules (Morey *et al.*, 2002).

### **5.2.11 Main proteins of importance to changes in leaf proteome**

The highest number of identified proteins was found to have functions in

photosynthesis. Since proteins were extracted from leaf tissues, naturally the highest number of proteins was found to be those involved in photosynthesis. However, the two main groups of proteins that are of interest to this study are those of immunity and defence as well as stress response. By studying proteins from these two categories, the fundamental mechanisms of plant/host response towards disease infection could be understood.

### **5.3 Protein validation, expression and characterization**

Proteins from leaf tissues sampled from 3-mpi seedlings were used for western hybridization. This is because most of the protein candidates (immunity and defence, stress response) were detected from this time point. After profiling of the leaf proteome via 2-DE, a list of protein candidates that differ in abundance was identified. The presence of these protein candidates has to be verified to ensure that these protein spots do change in abundance and that their trends are in concordance with results obtained from 2D-PAGE. These five proteins (including RbcL as loading control) were chosen due to the easy accessibility of commercial antibodies that were available.

A major band at a position close to the predicted molecular weights was detected by all four antibodies, except 14-3-3; where three bands were found to be present. The expected target is clearly visible at approximately 30 kDa. The band present at approximately 15 kDa could be an isoform of the 14-3-3 delta/zeta protein (UniProt P63104). According to the UniProt database, this smaller isoform is produced by alternative splicing of the 14-3-3 protein. The 50 kDa band could be a calcium-dependent protein kinase (CDPK). The 14-3-3 protein is known to bind and activate CDPK (Camoni *et al.*, 1998). In this case, the 14-3-3 polyclonal antibody could have bound to the plant CDPK in the leaf tissues, thus emitting a signal on the western blot.

The protein abundance ratio between non-inoculated and inoculated tissue samples was also generated. This is to ascertain that the presence of protein candidates could be differentiated between non-inoculated and inoculated leaf samples. Western hybridization results indicated that the protein spots do change in abundance but the trends of only two out of four proteins were in concordance with each other. This is probably due to the nature of pooling of ten individuals at the start of the 2-DE experiment. When samples are pooled, the biological variance can potentially be masked and a false confidence concerning data significance may be given (Sadiq and Agranoff, 2008; Karp and Lilley, 2009). Pooling samples also average the biological variance of individual samples. Although the true abundance ratios could not be obtained in the current analysis, it is nevertheless important to validate the protein candidates. From this semi-quantitative analysis, although trends appear prominent to the eye, the results for quantification indicate insignificant difference.

The aim of profiling the leaf proteome was to generate a list of protein candidates to work with. Western validation was the fastest and cheapest way to verify the presence of these candidate proteins in a biological sample. Other modes of validation, such as ELISA (enzyme-linked immunosorbent assay) and MRM (multiple reaction monitoring) could be some better alternatives (Ling *et al.*, 2000; Loei *et al.*, 2013). These techniques are quantitative and are sensitive enough to detect small amounts of proteins.

The oil palm 2-cys Prx protein homolog was subsequently expressed in a bacterial system to characterize the recombinant protein. As mentioned in Section 5.2.4, peroxiredoxins are detoxifying enzymes that act as primary sensors in regulating the concentration of hydrogen peroxide. The expression of peroxiredoxin was found to be low in leaves of diseased oil palm seedlings: it was low in both leaves of 3- and 6-mpi.

By identifying the interacting partner of peroxiredoxin, the roles of this protein could be studied to explain the biochemical mechanisms that caused the changes in expression.

Pull-down assay is a form of affinity purification (i.e. affinity chromatography). This technique is similar to immunoprecipitation, except that a "bait" protein is used instead of an antibody (Morris *et al.*, 2014; Xing *et al.*, 2016). Following protein-protein interaction study, an RPM1 disease resistance protein was found to interact with 2-cys Prx. In Arabidopsis, the RPM1 disease resistance protein confers resistance against the AvrRpm1 or the AvrB type III effector proteins expressed by *Pseudomonas syringae* (Boyes *et al.*, 1998, Mackey *et al.*, 2002). RPM1 is a nucleotide-binding-site leucine-rich-repeats protein (NBS-LRR) that confers resistance to plant disease (Boyes *et al.*, 1998; DeYoung and Innes, 2006). Another type of resistance gene product has been found to interact with 2-cys Prx. In *P. syringae*, the VirPphA effector protein identified several putative and promising 2-cys Prx-like proteins (Ammounh *et al.*, 2005).

The low protein abundance of peroxiredoxin in leaf tissues of 3- and 6-mpi could be due to the effects of oxidation in response to mild H<sub>2</sub>O<sub>2</sub> stress. These oxidized proteins were then degraded where active proteins are newly synthesized during recovery (Song *et al.*, 2016). Thioredoxin peroxidase is a thiol specific anti-oxidant, with thioredoxin as the immediate electron donor. This was later renamed to peroxiredoxin (2-cys peroxiredoxin was named based on the location of the cysteine residue on the enzyme) (König *et al.*, 2002; Dietz, 2003; Muthuramalingam *et al.*, 2009). This could be the reason why signals were undetected in 2D-PAGE.

#### **5.4 Functions of the known protein homologs in relation to disease infection**

The biological functions of known protein homologs that were found to change in

abundance in the leaf tissues of inoculated oil palms were described in Section 5.2. This section describes the relationship between the functions of these proteins with respect to fungal infection, as well as the plant immune system.

Plants do not have mobile defender cells or a somatic adaptive immune system. Alternatively, they rely on the detection of systemic signals emitted from infection sites and depend on the innate immunity of each cell for defence (Dangl and Jones, 2001; Jones and Dangl, 2006; Chisholm *et al.*, 2006). Basically, there are two branches in the plant immune system. In the first, transmembrane pattern recognition receptors (PRRs) identify microbial- or pathogen-associated molecular patterns (MAMPs or PAMPs), such as flagellin (Zipfel and Felix, 2005; Amil-Ruiz *et al.*, 2011). In the second, R genes are activated to target specific nucleotide binding site-leucine rich repeat (NBS-LRR) protein products (Dangl and Jones, 2001). These NBS-LRR proteins recognize pathogen effectors from diverse kingdoms, and similar defence responses are thereby activated. NBS-LRR-mediated disease resistance is effective against obligate biotrophs or hemibiotrophs. However, they are ineffective against necrotrophs (Glazebrook, 2005). A model proposed by Jones and Dangl (2006), can be used to illustrate the findings obtained from this proteomics work.

The 'zigzag' model (Fig 5.1) illustrates the quantitative output of the plant immune system. This model is used to explain the changes in protein abundance that were found to occur at different time points of disease infection. The number of proteins that changed in abundance was found to increase from 2-mpi to 3-mpi. Proteins with functions in immunity and defence as well as stress response were detected in leaf tissues of 3-mpi. This could be due to the activation of the oil palm immune system. In the first branch of defence, PAMP-triggered immunity may have been initiated when

the oil palm roots came into contact with *Ganoderma* mycelia. The plant recognized these pathogen effectors and sent signalling molecules from the roots to the leaves. The increase in number of detected proteins could be due to the identification of these signalling molecules from the host. The activities that occurred at these two time points could be summarized as ‘phase 1’ of the zigzag model.

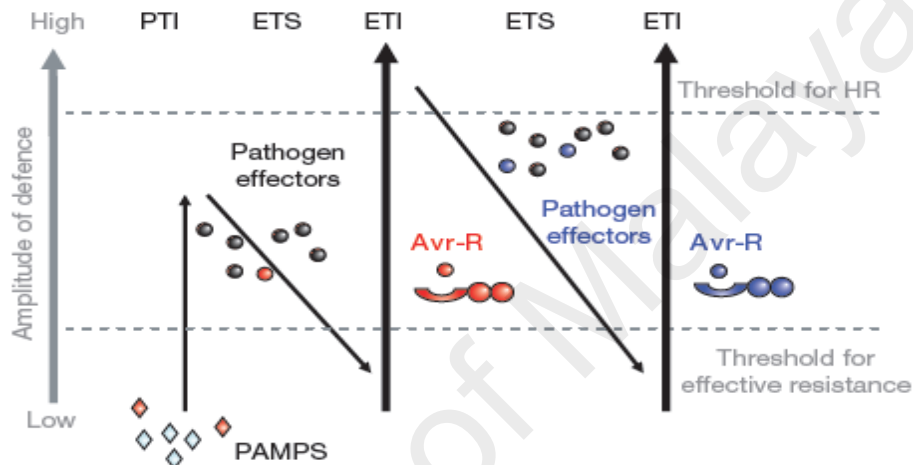


**Figure 5.1:** A zigzag model illustrating the quantitative output of the plant immune system (Jones & Dangl, 2006). This model consists of two branches of the plant immune system. The first branch recognizes and responds to molecules common to many classes of microbes, including non-pathogens. The second responds to pathogen virulence factors, either directly or through their effects on host targets. These plant immune systems and the pathogen molecules to which they respond, provide insights into molecular recognition, cell biology and evolution across biological kingdoms. By thoroughly understanding the plant immune function, this will serve as a foundation for crop improvement, especially for food. PTI: PAMP triggered immunity; PAMP: pathogen associated molecular patterns; ETS: effector triggered susceptibility; ETI: effector triggered immunity; Avr-R: avirulence protein; PRR: pattern recognition receptor; HR: hypersensitive response.

At 4-mpi, no significant changes were detected in protein abundance in the leaves of inoculated oil palm seedlings. Upon analysing the leaf proteome of 4-mpi, changes were detected but they were not significant. In this phase, termed phase 2, pathogen effectors could potentially interfere with PTI. Pathogen nutrition and pathogen dispersal are enabled, thus activating effector-triggered susceptibility (ETS). The *Ganoderma* fungus could be actively acquiring nutrition from colonized roots and at the same time

dispersing spores for further propagation. This could be the reason why no significant changes were detected in the host plant.

The same gradual increase in the detection of significant proteins that changed in abundance was found in 5-mpi and 6-mpi. A higher number of proteins with functions in photosynthesis and carbohydrate metabolism were found to have changed in abundance. The *Ganoderma*-inoculated oil palm could be relocating its resources from the leaves to the roots, as indicated by the reduction in abundance of proteins with functions in carbohydrate metabolism and photosynthesis in leaf tissues of 5-mpi. In leaf tissues of 6-mpi, proteins with functions in immunity and defence were found to experience significant changes. The occurrence of this phase is similar to phase 1 of the zigzag model. In this phase 3, the effectors elicited by the fungus could be recognized by resistance proteins or other signalling molecules. This situation may activate the effector-triggered immunity (ETI), where ETI is an amplified and accelerated version of PTI. These signalling molecules may have been sent to the leaves of oil palm and subsequently detected using 2D-PAGE.

In leaf tissues of 7-mpi, three main groups of proteins were detected: immunity and defence, carbohydrate metabolism and photosynthesis. The presence of these groups of proteins could indicate that the oil palm is still trying to defend and protect itself from further harmful attack by the invading pathogen. At this time point, several *Ganoderma*-inoculated oil palm seedlings in the nursery were observed to show symptoms of disease infection, while others have already succumbed to the disease. This situation could be described using the final phase of the zigzag model. In this final phase, if the amplitude of defence exceeds the threshold for HR, the host-plant could succumb to the

disease and eventually die. However, if the amplitude of defence exceeds the threshold for effective resistance, the host-plant could resist the disease and eventually survive.

The findings by Floerl *et al.* (2012) on roots of *Arabidopsis thaliana* infected with *Verticillium longisporum* showed that this fungal infection affects the leaf apoplastic proteome, metabolome and cell wall properties of the host plant. These results were supported by gene expression studies of *V. longisporum*-responsive proteins, lignin and cell wall studies and metabolite fingerprinting analysis.

Other similar examples include leaf proteome analysis of *Fagus sylvatica* with the root pathogen *Phytophthora citricola* (Valcu *et al.*, 2009). In this case, protein functions related to energy, primary and secondary metabolism and stress and defence were identified. The authors found that the plant response to *P. citricola* was weak and unspecific. This was evident with the changes in protein abundance of energy and primary metabolism. They hypothesized that the invading pathogen could have suppressed the host plant's defence reaction by observing changes that were specific to the wounded roots.

## **5.5 Future prospects**

Although the findings of this proteomic experiment has enhanced our knowledge on the aboveground leaf foliar activities, more in-depth research could be done to close the current knowledge gaps. The time course study could be further extended to include profiling of 8- to 12-month old oil palms. The current findings could only explain half of the zigzag model, as no further data was available to show the on-going activities in phases 3 and 4. Phases 3 and 4 explain the susceptibility and resistance nature of a plant host towards its virulent pathogen.

### 5.5.1 Resistant planting materials

Partial resistant or BSR tolerant planting materials could be bred as alternatives to a cure for the disease. Many oil palm plantation companies are currently looking for *Ganoderma* resistant planting materials. Mass screening of oil palms with different genetic backgrounds by artificially inoculating them with *G. boninense* is one of the methods to discover resistant crosses. Planting *Ganoderma* resistant oil palms in the estates could potentially be the most cost-effective means for BSR management.

At the same time, it is also important to understand the resistance mechanisms of oil palm to *G. boninense*. Disease progression and histological studies of the fungus itself would greatly improve the understanding of the mechanisms of infection.

As evident in the research of *Sclerotinia sclerotiorum* infection of *Brassica napus*, the microarray studies conducted in the leaf/seedling stage of *B. napus* are similar to the protein expression profiles in cotyledon tissues (Yang *et al.*, 2007; Zhao *et al.*, 2007; Garg *et al.*, 2013). These proteins could also be found at the stem stage (Zhao *et al.*, 2009), and in other host species of this pathogen such as soybean (Calla *et al.*, 2009). Based on this information, Garg *et al.* (2013) found that the transcription of various phytoalexins and pathogenesis-related proteins were likely stimulated during defence to prevent further spread of the pathogen within the host cell tissue. They suggested that by overexpressing the defence-related enzymes that were up-regulated in the resistance variety, the resistance against *S. sclerotiorum* would be further enhanced.

Najihah *et al.*, (2015) found that silicon-treated oil palms were resistant to *G. boninense*. In their study, silicon was incorporated into fertilizers and these were added at monthly intervals. They found that rates of transpiration in uninoculated oil palm seedlings were

significantly associated with different silicon concentrations. Different concentrations of silicon treatment seemed to assist in the survival of these infected seedlings.

Conventional breeding for tolerant oil palms is a long term goal and can be time consuming. On the other hand, the molecular approach to produce tolerant palms could be the way forward. Screening of potential tolerant varieties and the manipulation of resistance genes could arm us with information to improve current practices of producing resistant planting materials.

University of Malaysia

## CHAPTER 6: CONCLUSION

In order to elucidate the changes in the global expression of proteins and to understand the mechanisms of defence against fungal pathogens, proteomic analyses were conducted on leaf tissues of *Ganoderma* inoculated- and non-inoculated oil palms. Leaf tissues were sampled for this analysis as it is believed that defence responses from the roots could be transported to the aboveground foliar via a series of signalling molecules. The indirect detection of these responses in the leaves could be used to further investigate signalling mechanisms or signal transduction processes of the plant defence mechanism. Proteomic profiling of leaf tissues from *Ganoderma* inoculated- and non-inoculated oil palms revealed changes in carbohydrate metabolism, cellular component, energy production, fatty acid biosynthesis, immunity and defence, nitrogen metabolism, protein metabolism, stress response, transport, and photosynthesis. These changes in the leaf could indicate similar changes in the root of inoculated palms. Antioxidant enzymes, particularly peroxiredoxins, are important in the detoxification of hydrogen peroxides and reactive oxygen species. The elevated levels of these enzymes could indicate that the peroxide levels in inoculated palm have drastically increased. Elevated levels of peroxiredoxins could potentially be used as biomarkers of oxidative stress. Protein-protein interaction studies between peroxiredoxin and leaf proteins extracted from inoculated oil palms revealed the presence of an RPM1 resistance protein. This may indicate that antioxidant enzymes could interact with resistance proteins but the mechanisms behind it are not clear. However, further investigations and validation into the functions of these proteins must be performed to understand the underlying mechanisms of infection. If the functions of these proteins can be shown to be specific to cause *ganoderma* infection, they could possibly be developed into markers for early detection of BSR.

## REFERENCES

- Abadi, A.L. (1987). Biologi *Ganoderma boninense* Pat. pada kelapa sawit (*Elaeis guineensis* Jacq.) dan pengaruh beberapa mikroba tanah antagonistik terhadap pertumbuhannya. PhD thesis, IPB, Bogor.
- Abdullah, A. H., Adom, A.H., Md. Shakaff, A.Y., Ahmad, M.N., Saad, M.A., Tan, E.S., Fikri, N.A., Markom, M.A. & Zakaria, A. (2011). Electronic nose system for *Ganoderma* detection. *Sensor Letters*, 9(1): 353-358.
- Abdullah, A.H., Shakaff, A.Y.M., Zakaria, A., Saad, F.S.A., Abdul Shukor, S.A. & Mat, A. (2014). Application specific electronic nose (ASEN) for *Ganoderma boninense* detection using artificial neural network. *International Conference on Electronic Design* (pp.148-152). Penang, Malaysia: IEEE Xplore.
- Abdullah, F. (2000). Spatial and sequential mapping of the incidence of basal stem rot of oil palms (*Elaeis guineensis*) on a former coconut (*Cocos nucifera*) plantation. In: Flood, J., Bridge, P.D., Holderness, M. (Eds.), *Ganoderma Diseases of Perennial Crops* (pp. 183-194). Oxon: CABI Publishing.
- Adaskaveg, J.E. & Ogawa, J.M. (1990). Wood decay pathology of fruit and nut trees in California. *Plant Disease*, 74: 341-352.
- Adaskaveg, J.E., Blanchette, R.A. & Gilbertson, R.L. (1991). Decay of date palm wood by white-rot and brown-rot fungi. *Canadian Journal of Botany*, 69: 615-629.
- Adaskaveg, J.E., Miller, R.W. & Gilbertson, R.L. (1993). Wood decay, lignicolous fungi and decline of peach trees in South Carolina. *Plant Disease*, 77: 707-711.
- Ahuja, I., Kissen, R. & Bones, A.M. (2012). Phytoalexins in defense against pathogens. *Trends in Plant Science*, 17(2): 73-90.
- Alizadeh, F., Siti Nor Akmal, A., Khodavandi, A., Faridah, A., Umi Kalson, Y. & Chong, P. (2011). Differential expression of oil palm pathology genes during interactions with *Ganoderma boninense* and *Trichoderma harzianum*. *Journal of Plant Physiology*, 168: 1106-1113.
- Alscher, R.G., Erturk, N. & Heath, L.S. (2002). Role of superoxide dismutases (SODs) in controlling oxidative stress in plants. *Journal of Experimental Botany*, 53(372): 1331-1341.

- Amil-Ruiz, F., Blanco-Portales, R., Muñoz-Blanco, J. & Caballero, J.L. (2011). The strawberry plant defense mechanism: A molecular review. *Plant & Cell Physiology*, 52(11): 1873–1903.
- Ammounh, A., Al-Daoude, A. & Mansfield, J.W. (2005). Protein-protein interaction studies revealed genes associated with plant disease resistance and drought tolerance. The International Conference on Biotechnology for Salinity and Drought Tolerance in Plants. Islamabad, Pakistan. 28-31 March 2005.
- Ariffin, D. (2005). Progress of research on Ganoderma basal stem rot at MPOB. Paper presented at the Workshop on Prioritising Ganoderma Research in Oil Palm, 28 March 2005, Bangi.
- Ariffin, D., Idris, A.S. & Singh, G. (2000) Status of Ganoderma in Oil Palm. In: Flood. J., Bridge. P.D. and Holderness. M. (Eds.), *Ganoderma Diseases of Perennial Crops* (pp. 49-68). Egham, UK: CABI Publishing.
- Ariffin, D., Singh, G. & Lim, T.K. (1989). Ganoderma in Malaysia – current status and research strategy. In: Jalani, S. *et al.* (Eds), *Proceedings of the 1989 PORIM International Palm Oil Development Conference* (pp. 249-247). Selangor, Malaysia: Palm Oil Research Institute of Malaysia.
- Asemota, O. & Shah, F.H. (2004). Detection of mesocarp oleoyl-thioesterase gene of the South American oil palm *Elaeis oleifera* by reverse transcriptase polymerase chain reaction. *African Journal of Biotechnology*, 3(11): 595-598.
- Baietto, M., Wilson, A.D., Bassi, D. & Ferrini, F. (2010). Evaluation of three electronic noses for detecting incipient wood decay. *Sensors*, 10: 1062-1092.
- Baracat-Pereira, M.C., Barbosa, M.dO., Magalhães, M.J.J., Carrijo, L.C., Games, P.D., Almeida, H.O., Netto, J.F.S., Pereira, M.R. & de Barros, E.G. (2012). Separomics applied to the proteomics and peptidomics of low-abundance proteins: Choice of methods and challenges – A review. *Genetics and Molecular Biology*, 35(1): 283–291.
- Barcelos, E., de Almeida Rios, S., Cunha, R.N.V., Lopes, R., Motoike, S.Y., Babiychuk, E., Skiryecz, A. & Kushnir, S. (2015). Oil palm natural diversity and the potential for yield improvement. *Frontiers in Plant Science*, 6:190. doi: 10.3389/fpls.2015.00190.
- Barracough, D., Obenland, D., Laing, W. & Carroll, T. (2004). A method for quick and easy two-dimensional electrophoresis of plant samples. *Postharvest Biology and Technology*, 32: 175-181.

- Bashir, Z., Ahmad, A., Shafique, S., Anjum, T., Shafique, S. & Akram, W. (2013). Hypersensitive response – A biophysical phenomenon of producers. *European Journal of Microbiology and Immunology*, 3(2): 105–110.
- Berg, J.M., Tymoczko, J.L. & Stryer, L. (2002). Chapter 29: Protein synthesis. *Biochemistry* (5th ed.). New York: W H Freeman.
- Berger, S., Sinha, A.K. & Roitsch, T. (2007). Plant physiology meets phytopathology: plant primary metabolism and plant-pathogen interactions. *Journal of Experimental Botany*, 58: 4019-4026.
- Bernoux, M., Ve, T., Williams, S., Warren, C., Hatters, D., Valkov, E., Zhang, X., Ellis, J.G., Kobe, B. & Dodds, P.N. (2011). Structural and functional analysis of a plant resistance protein TIR domain reveals interfaces for self-association, signaling, and autoregulation. *Cell Host and Microbe*, 9(3): 200–211.
- Bezemer, T.M. & van Dam, N. (2005). Linking aboveground and belowground interactions via induced plant defenses. *Trends in Ecology and Evolution*, 20: 617–624.
- Bezemer, T.M., Wagenaar, R., van Dam, N.M. & Wäckers, F.L. (2003). Interactions between above- and belowground insect herbivores as mediated by the plant defense system. *Oikos*, 101: 555–562.
- Bezemer, T.M., Wagenaar, R., van Dam, N.M., van der Putten, W.H. & Wäckers, F.L. (2004). Above- and below-ground terpenoid aldehyde induction in cotton, *Gossypium herbaceum*, following root and leaf injury. *Journal of Chemical Ecology*, 30: 53–67.
- Bhuiyan, N., Selvaraj, G., Wei, Y.D. & King, J. (2009) Gene expression profiling and silencing reveal that monolignol biosynthesis plays a critical role in penetration defence in wheat against powdery mildew invasion. *Journal of Experimental Botany*, 60: 509–521.
- Bilgin, D.D., Jorge, A.Z., Zhu, J., Clough, S.J., Ort, D.R. & DeLucia, E.H. (2010). Biotic stress globally downregulates photosynthesis genes. *Plant, Cell and Environment*, 33: 1597–1613.
- Blanchette, R.A. (1984). Screening wood decayed by white rot fungi for preferential lignin degradation. *Applied Environmental Microbiology*, 48: 647-653.

- Blatti, J.L., Beld, J., Behnke, C.A., Mendez, M., Mayfield, S.P. & Burkart, M.D. (2012). Manipulating fatty acid biosynthesis in microalgae for biofuel through protein-protein interactions. *PLoS ONE*, 7(9): e42949.
- Blum, H., Beier, H. & Gross, H. (1987). Improved silver staining of plant proteins, RNA and DNA in polyacrylamide gels. *Electrophoresis*, 8(2): 93-99.
- Bolton, M.D. (2009). Primary metabolism and plant defense fuel for the fire. *Molecular Plant-Microbe Interactions Journal*, 22: 487-97.
- Boyes, D.C., Nam, J. & Dangl, J.L. (1998). The *Arabidopsis thaliana* RPM1 disease resistance gene product is a peripheral plasma membrane protein that is degraded coincident with the hypersensitive response. *Proceedings of the National Academy of Sciences*, 95(26): 15849-15854.
- Bozhkov, P.V. & Lam, E. (2011). Green death: revealing programmed cell death in plants. *Cell Death and Differentiation*, 18(8): 1239-1240.
- Bradford, M.M. (1976). A rapid and sensitive method for the quantitation of microgram quantities of protein utilizing the principle of protein-dye binding. *Analytical Biochemistry*, 72: 248-254.
- Breton, F., Hasan, Y., Hariadi, S., Lubis, Z. & De Franqueville, H. (2006). Characterization of parameters for the development of an early screening test for basal stem rot tolerance in oil palm progenies. *Journal of Oil Palm Research, Special issue*: 24-36.
- Bridge, P.D., Singh, T. & Arora, D.K. (2004). The application of molecular markers in epidemiology of plant pathogenic fungi. In: Arora, D.K. (Ed.) *Fungal Biotechnology in Agriculture, Food and Environmental Applications* (pp. 57-68). New York: CRC Press.
- Calla, B., Vuong, T., Radwan, O., Hartman, G.L. & Clough, S.J. (2009). Gene expression profiling soybean stem tissue early response to *Sclerotinia sclerotiorum* and in silico mapping in relation to resistance markers. *Plant Genome*, 2: 149-166.
- Camoni, L., Harper, J.F. & Palmgren, M.G. (1998). 14-3-3 proteins activate a plant calcium-dependent protein kinase (CDPK). *FEBS Letters*, 430(3): 381-384.
- Carpentier, S.C., Witters, E., Laukens, K., Deckers, P., Swennen, R. & Panis, B. (2005). Preparation of protein extracts from recalcitrant plant tissues: an evaluation of

different methods for two-dimensional gel electrophoresis analysis. *Proteomics*, 5(10): 2497-2507.

Cary, J.W., Rajasekaran, K., Brown, R.L., Luo, M., Chen, Z-Y. & Bhatnagar, D. (2011). Developing resistance to aflatoxin in maize and cottonseed. *Toxins*, 3: 678-696.

Caverzan, A., Passaia, G., Rosa, S.B., Ribeiro, C.W., Lazzarotto, F. & Margis-Pinheiro, M. (2012). Plant responses to stresses: Role of ascorbate peroxidase in the antioxidant protection. *Genetics and Molecular Biology*, 35(4): 1011-1019.

Chang, J.H., Goel, A.K., Grant, S.R. & Dangl, J.L. (2004). Wake of the flood: ascribing functions to the wave of type III effector proteins of phytopathogenic bacteria. *Current Opinion in Microbiology*, 7: 11–18.

Chen, F., Li, Q., Sun, L. & He, Z. (2006). The rice 14-3-3 gene family and its involvement in responses to biotic and abiotic stress. *DNA Research*, 13: 53–63.

Chi, F., Yang, P., Han, F., Jing, Y. & Shen, Y. (2010). Proteomic analysis of rice seedlings infected by *Sinorhizobium meliloti* 1021. *Proteomics*, 10: 1861–1874.

Chichkova, N.V., Shaw, J., Galiullina, R.A., Drury, G.E., Tuzhikov, A.I., Kim, S.H., Kalkum, M., Hong, T.B., Gorshkova, E.N., Torrance, L., Vartapetian, A.B. & Taliansky, M. (2010). Phytaspase, a relocatable cell death promoting plant protease with caspase specificity. *EMBO Journal*, 29: 1149–1161.

Chisholm, S.T., Coaker, G., Day, B. & Staskawicz, B.J. (2006). Host–microbe interactions: shaping the evolution of the plant immune response. *Cell*, 124: 803–814.

Chivasa, S., Simon, W.J., Yu, X.L., Yalpani, N. & Slabas, A.R. (2005). Pathogen elicitor-induced changes in the maize extracellular matrix proteome. *Proteomics*, 5: 4894–4904.

Chivasa, S., Tomé, D.F.A., Hamilton, J.M. & Slabas, A.R. (2011). Proteomic analysis of extracellular ATP-regulated proteins identifies ATP synthase  $\beta$ -subunit as a novel plant cell death regulator. *Molecular and Cellular Proteomics*, 10(3):M110.003905.

Chong, K.P., Lum, M.S., Foong, C.P., Wong, C.M.V.L., Atong, M. & Rossall, S. (2011). First identification of *Ganoderma boninense* isolated from Sabah based on PCR and sequence homology. *African Journal of Biotechnology*, 10(66): 14718-14723.

- Chung, G.F. (2011). Management of *Ganoderma* diseases in oil palm plantations. *The Planter*, 87(1022): 325-339.
- Coleman, J.J., White, G.J., Rodriguez-Carres, M. & Vanetten, H.D. (2011). An ABC transporter and a cytochrome P450 of *Nectria haematococca* MPVI are virulence factors on pea and are the major tolerance mechanisms to the phytoalexin pisatin. *Molecular Plant Microbe Interaction*, 24: 368–376.
- Coll, N.S., Vercammen, D., Smidler, A., Clover, C., Van Breusegem, F., Dangl, J.L. & Epple, P. (2010). Arabidopsis type I metacaspases control cell death. *Science*, 330: 1393–1397.
- Collinge, D.B. (2009). Cell wall appositions: the first line of defence. *Journal of Experimental Botany*, 60(2): 351-352.
- Comte, I., Colin, F., Whalen, J.K., Gru, O. & Caliman J-P. (2012). Agricultural practices in oil palm plantations and their impact on hydrological changes, nutrient fluxes and water quality in Indonesia: A review. In: Sparks, D.L. (Ed.), *Advances in Agronomy* (pp. 71-124). Burlington, US: Academic Press
- Cooper, R.M., Flood, J. & Rees, R.W. (2011). *Ganoderma boninense* in oil palm plantations: current thinking on epidemiology, resistance and pathology. *The Planter*, 87: 515-526.
- Corley, R.H.V. & Tinker, P.B.H. (2016). The origin and development of the oil palm industry. *The oil palm* (5th ed.) (pp. 133–199). Blackwell Science Ltd.
- Cui, S., Huang, F., Wang, J., Ma, X., Cheng, Y. & Liu J. (2005). A proteomic analysis of cold stress responses in rice seedlings. *Proteomics*, 5(12): 3162-3172.
- D'Andréa, S., Jolivet, P., Boulard, C., Larré, C., Froissard, M. & Chardot, T. (2007). Selective one-step extraction of *Arabidopsis thaliana* seed oleosins using organic solvents. *Journal of Agricultural and Food Chemistry*, 55(24): 10008–10015.
- Dangl, J.L. & Jones, J.D.G. (2001). Plant pathogens and integrated defence responses to infection. *Nature*, 411: 826–833.
- de Franqueville, H., Asmady, H., Jacquemard, J.C., Hayun, Z. & Durand-Gasselín, T. (2001). Indication on sources of oil palm (*Elaeis guineensis* Jacq.). Genetic resistance and susceptibility to *Ganoderma* sp., that cause basal stem rot. In:

Proceedings of the 2001 International Palm Oil Congress, Kuala Lumpur, Malaysia. p. 420-431.

Deeks, M.J. & Hussey, P.J. (2009). Plant Actin Biology. *Encyclopedia of Life Sciences*. New Jersey, United States: Wiley.

DeYoung, B. & Innes, R.W. (2006). Plant NBS-LRR proteins in pathogen sensing and host defense. *Nature Immunology*, 7(12): 1243-1249.

de León, I.P. & Montesano, M. (2013). Activation of defense mechanisms against pathogens in mosses and flowering plants. *International Journal of Molecular Sciences*, 14: 3178-3200.

Dietz, K-J. (2003). Plant peroxiredoxins. *Annual Review of Plant Biology*, 54: 93–107.

Dominguez, R. & Holmes, K.C. (2011). Actin structure and function. *Annual Review of Biophysics*, 9(40): 169–186.

Durand-Gasselin, T., Asmady, H., Flori, A., Jacquemard, J.C., Hayun, Z., Breton, F. & de Franqueville, H. (2005). Possible sources of genetic resistance in oil palm (*Elaeis guineensis* Jacq.) to basal stem rot caused by *Ganoderma boninense* – prospects for future breeding. *Mycopathologia*, 159: 93-100.

Dziedzic, M., Hill, R. & Hansen, K.C. (2014). GeLC-MS/MS analysis of complex protein mixtures. *Methods in Molecular Biology*, 1156: 53–66.

Ellinger, D., Naumann, M., Falter, C., Zwikowics, C., Jamrow, T., Manisseri, C., Somerville, S.C. & Voigt, C.A. (2013). Elevated early callose deposition results in complete penetration resistance to powdery mildew in Arabidopsis. *Plant Physiology*, 161(3): 1433–1444.

Espinosa, F., Garrido, I., Ortega, A., Casimiro, I. & Alvarez-Tinaut, M. (2014). Redox activities and ROS, NO and phenylpropanoids production by axenically cultured intact olive seedling roots after interaction with a mycorrhizal or a pathogenic fungus. *PLoS One*, 9: e100132.

Evstigneeva, Z.G., Solov'eva, N.A. & Sidel'nikova, L.I. (2001). Structures and functions of chaperones and chaperonin. *Applied Biochemistry and Microbiology*, 37(1): 1-13.

- Faize, M., Burgos, L., Faize, L., Petri, C., Barba-Espin, G., D'iaz-Vivancos, P., Clemente-Moreno, M.J., Albuquerque, N. & Hernandez, J.A. (2012). Modulation of tobacco bacterial disease resistance using cytosolic ascorbate peroxidase and Cu,Zn-superoxide dismutase. *Plant Pathology*, 61: 858–866.
- Faurobert, M., Pelpoir, E. & Chaib, J. (2007). Phenol extraction of proteins for proteomic studies of recalcitrant plant tissues. *Methods in Molecular Biology*, 355: 9-14.
- Ferrari, S., Savatin, D.V., Sicilia, F., Gramegna, G., Cervone, F. & Lorenzo, G.D. (2013). Oligogalacturonides: plant damage-associated molecular patterns and regulators of growth and development. *Frontiers in Plant Science*, 4:49. doi.org/10.3389/fpls.2013.00049.
- Floerl, S., Majcherczyk, A., Possienke, M., Feussner, K., Tappe, H., Gatz, C., Feussner, I., Kües, U. & Polle, A. (2012) *Verticillium longisporum* infection affects the leaf apoplastic proteome, metabolome, and cell wall properties in *Arabidopsis thaliana*. *PLoS ONE*, 7(2): e31435.
- Flood, J., Hasan, Y., Turner, P.D. & O'Grady, E.B. (2000). The spread of Ganoderma from infective sources in the field and its implications for the management of the disease in oil palm. In: Flood, J., Bridge, P.D. and Holderness, M (Eds.), *Ganoderma Diseases of Perennial Crops* (pp. 101-112). Oxon: CABI Publishing.
- Flood, J., Keenan, L., Wayne, S. & Hasan, Y. (2005). Studies on oil palm trunks as sources of infection in the field. *Mycopathologia*, 159(1): 101–107.
- Fornace, K.M., Drakeley, C.J., William, T., Espino, F & Cox, J. (2014). Mapping infectious disease landscapes: unmanned aerial vehicles and epidemiology. *Trends in Parasitology*, 30(11): 514-519.
- Fröhlich, A., Gaupels, F., Sarioglu, H., Holzmeister, C., Spannagl, M., Durner, J. & Lindermayr, C. (2012). Looking deep inside: Detection of low-abundance proteins in leaf extracts of *Arabidopsis* and phloem exudates of pumpkin. *Plant Physiology*, 159(3): 902–914.
- Fu, J., Momcilovic, I. & Vara Prasad, P. (2012). Roles of protein synthesis elongation factor EF-Tu in heat tolerance in plants. *Journal of Botany*, Article ID 835836.
- Garavaglia, B.S., Thomas, L., Gottig, N., Zimaro, T., Garofalo, C.G., Gehring, C. & Ottado, J. (2007). Shedding light on the role of photosynthesis in pathogen

colonization and host defense. *Communicative & Integrative Biology*, 3(4): 382-384.

Garcion, C., Lamotte, O. & Métraux, J.P. (2007). Mechanisms of defence to pathogens: biochemistry and physiology. In: Walters, D., Newton, A. and Lyon, G. (Eds.) *Induced Resistance for Plant Defence: A Sustainable Approach to Crop Protection* (pp. 109-132). Oxford: Blackwell.

Garg, H., Li, H., Sivasithamparam, K. & Barbetti, M. (2013). Differentially expressed proteins and associated histological and disease progression changes in cotyledon tissue of a resistant and susceptible genotype of *Brassica napus* infected with *Sclerotinia sclerotiorum*. *PLoS ONE*, 8: e65205.

Getzin, S., Wiegand, K. & Schöning, I. (2012) Assessing biodiversity in forests using very high resolution images and unmanned aerial vehicles. *Methods in Ecology and Evolution*, 3: 397–404.

Geyer, P.E., Kulak, N.A., Pichler, G., Holdt, L.M., Teupser, D. & Mann, M. (2016). Plasma proteome profiling to assess human health and disease. *Cell Systems*, 2: 185–195.

Gillingham, A.K. & Munro, S. (2007). The small G proteins of the Arf family and their regulators. *Annual Review of Cell and Developmental Biology*, 23: 579-611.

Glazebrook, J. (2005). Contrasting mechanisms of defense against biotrophic and necrotrophic pathogens. *Annual Review of Phytopathology*, 43: 205–227.

Godoi, P., Galhardo, R., Luche, D., Van Sluy, M.-A., Menck, C. & Oliva, G. (2006). Structure of the thiazole biosynthetic enzyme THI1 from *Arabidopsis thaliana*. *Journal of Biological Chemistry*, 281: 30957–30966.

Hamrita, B., Nasr, H.B., Chahed, K., Kabbage, M. & Chouchane, L. (2010). Proteomic analysis of human breast cancer: New technologies and clinical applications for biomarker profiling. *Journal of Proteomics and Bioinformatics*, 3: 91-98.

Han, X., Aslanian, A. & Yates, J.R. III. (2008). Mass spectrometry for proteomics. *Current Opinion in Chemical Biology*, 12: 483–490.

Hasan, Y. & Turner, P.D. (1998). The comparative importance of different oil palm tissues as infection sources for basal stem rot in replantings. *The Planter*, 74: 119-135.

- He, C., Zhang, J., Duan, A., Yin, J. & Zhou, D. (2005). Comparison of methods for protein extraction from pine needles. *Forestry Studies in China*, 7(4): 20-23.
- Ho, C.L. & Tan, Y.C. (2015). Molecular defense response of oil palm to *Ganoderma* infection. *Phytochemistry*, 114: 168-177.
- Ho, C.L., Tan, Y.C., Yeoh, K.A., Ghazali, A.K., Yee, W.Y. & Hoh, C.C. (2016). De novo transcriptome analyses of host-fungal interactions in oil palm (*Elaeis guineensis* Jacq.). *BMC Genomics*, 17: 66-84.
- Ho, Y.W. & Nawawi, A. (1985). *Ganoderma boninense* Pat. from basal stem rot of oil palm in peninsular Malaysia. *Pertanika*, 8 (3): 424-428.
- Hofius, D., Schultz-Larsen, T., Joensen, J., Tsitsigiannis, D.I., Petersen, N.H.T., Mattsson, O., Jørgensen, L.B., Jones, J.D.G., Mundy, J. & Petersen, M. (2009). Autophagic components contribute to hypersensitive cell death in Arabidopsis. *Cell*, 137: 773-783.
- Hushiarian, R., Yusof, N.A. & Dutse, S.W. (2013). Detection and control of *Ganoderma boninense*: strategies and perspectives. *SpringerPlus*, 2: 555. DOI: 10.1186/2193-1801-2-555.
- Idris, A.S., Kushairi, D., Ismail, S. & Ariffin, D. (2004). Selection for partial resistance in oil palm progenies to *Ganoderma* basal stem rot. *Journal of Oil Palm Research*, 16(2): 12-18.
- Ingle, R.A., Carstens, M. & Denby, K.J. (2009). PAMP recognition and the plant-pathogen arms race. *BioEssays*, 28(9): 880-889.
- Jollands, P. (1983). Laboratory investigations on fungicides and biological agents to control three diseases of rubber and oil palm and their potential applications. *Tropical Pest Management*, 29: 33-38.
- Jones, J.D.G. & Dangl, J.L. (2006). The plant immune system. *Nature*, 444: 323-329.
- Kandan, A., Ramanathan, A., Raguchander, T., Balasubramanian, P. & Samiyappan, R. (2010). Development and evaluation of an enzyme-linked immunosorbent assay (ELISA) and dot immunobinding assay (DIBA) for the detection of *Ganoderma* infecting palms. *Archives of Phytopathology and Plant Protection*, 43(15): 1473-1484.

- Karp, N.A. & Lilley, K.S. (2009). Investigating sample pooling strategies for DIGE experiments to address biological variability. *Proteomics*, 9: 388–397.
- Karp, N.A., McCormick, P.S., Russell, M.R. & Lilley, K.S. (2007). Experimental and statistical considerations to avoid false conclusions in proteomics studies using differential in-gel electrophoresis. *Molecular & Cellular Proteomics*, 6(8): 1354–1364.
- Karthikeyan, M., Bhaskaran, R., Radhika, K., Mathiyazhagan, S., Jayakumar, V., Sandosskumar, R. & Velazhahan, R. (2008). Development and comparison of ELISA and PCR methods for the early detection of Ganoderma disease of coconut. *Archives of Phytopathology and Plant Protection*, 41(6): 396–406.
- Khairudin, H. (1990). Results of four trials on Ganoderma basal stem rot of oil palm in Golden Hope Estates. In: Ariffin, D. and Jalani, S., *Proceeding of the Ganoderma Workshop* (pp. 113–131). Selangor, Malaysia: Palm Oil Research Institute of Malaysia.
- Khan, M., Takasaki, H. & Komatsu, S. (2005). Comprehensive phosphoproteome analysis in rice and identification of phosphoproteins responsive to different hormones/stresses. *Journal of Proteome Research*, 4: 1592–1599.
- Kiskini, A., Vissers, A., Vincken, J.P., Gruppen, H. & Wierenga, P.A. (2016). Effect of plant age on the quantity and quality of proteins extracted from sugar beet (*Beta vulgaris* L.) leaves. *Journal of Agricultural and Food Chemistry*, 64(44): 8305–8314.
- König, J., Baier, M., Horling, F., Kahmann, U., Harris, G., Schurmann, P. & Dietz, K.-J. (2002). The plant-specific function of 2-Cys peroxiredoxin mediated detoxification of peroxides in the redox-hierarchy of photosynthetic electron flux. *Proceedings of the National Academy of Sciences*, 99(8): 5738–5743.
- Koroleva, O.A. & Bindschedler, L.V. (2011). Efficient strategies for analysis of low abundance proteins in plant proteomics. In: Ivanov, A.R. & Lazarev, A.V. (Eds.), *Sample preparation in biological mass spectrometry* (pp. 381–409). Netherlands: Springer.
- Kumar, A. & Bais, H. (2012). Wired to the roots. *Plant Signaling & Behavior*, 7: 1598–1604.
- Kunze, G., Zipfel, C., Robatzek, S., Niehaus, K., Boller, T. & Felix, G. (2004). The N terminus of bacterial elongation factor Tu elicits innate immunity in Arabidopsis plants. *Plant Cell*, 16: 3496–3507.

- Laurent, J., Vogel, C., Kwon, T., Craig, S.A., Boutz, D.R., Huse, H.K., Nozue, K., Walia, H., Whiteley, M., Ronald, P.C. & Marcotte, E.M. (2010). Protein abundances are more conserved than mRNA abundances across diverse taxa. *Proteomics*, 10(23): 4209–4212.
- Legrain, P., Aebersold, R., Archakov, A., Bairoch, A., Bala, K., Beretta, L., Bergeron, J., Borchers, C.H., Corthals, G.L., Costello, C.E., Deutsch, E.W., Domon, B., Hancock, W., He, F., Hochstrasser, D., Marko-Varga, G., Salekdeh, G.H., Sechi, S., Snyder, M., Srivastava, S., Uhlén, M., Wu, C.H., Yamamoto, T., Paik, Y.K. & Omenn, G.S. (2011). The human proteome project: current state and future direction. *Molecular and Cellular Proteomics*, 10(7): doi: 10.1074/mcp.M111.009993.
- Lelong, C.D.C., Roger, J.M., Brégand, S., Dubertret, F., Lanore, M., Sitorus, N.A., Raharjo, D.A. & Caliman, J-P. (2010). Evaluation of oil-palm fungal disease infestation with canopy hyperspectral reflectance data. *Sensors*, 10: 734-747.
- Li, M., Xu, J., Qiu, Z., Zhang, J., Ma, F. & Zhang, J. (2014). Screening and identification of resistance related proteins from apple leaves inoculated with *Marssonina coronaria* (EII. & J. J. Davis). *Proteome Science*, 12(7): doi:10.1186/1477-5956-12-7.
- Liaghat, S., Ehsani, R., Mansor, S., Shafri, H.Z.M., Meon, S., Sankaran, S. & Azam, S.H.M.N. (2014). Early detection of basal stem rot disease (Ganoderma) in oil palms based on hyperspectral reflectance data using pattern recognition algorithms. *International Journal of Remote Sensing*, 25(10): 3427-3439.
- Lim, H.P. & Fong, Y.K. (2005). Research on basal stem rot (BSR) of ornamental palms caused by basidiospores from *Ganoderma boninense*. *Mycopathologia*, 159: 171-179.
- Lim, T.K., Hamm, R.T. & Mohamad, R. (1990). Persistency and volatile behaviour of selected chemical in treated soil against three basidiomycetes root disease pathogens. *Tropical Pest Management*, 36: 23-26.
- Ling, K.S., Zhu, H.Y., Jiang, Z.Y. & Gonsalves, D. (2000). Effective application of DAS-ELISA for detection of grapevine leafroll associated closterovirus-3 using a polyclonal antiserum developed from recombinant coat protein. *European Journal of Plant Pathology*, 106: 301–309.
- Loei, H., Lim, J., Tan, M., Lim, T.K., Lin, Q.S., Chew, F.T., Kulaveerasingam, H. & Chung, M.C. (2013). Proteomic analysis of the oil palm fruit mesocarp reveals elevated oxidative phosphorylation activity is critical for increased storage oil production. *Journal of Proteome Research*, 12(11): 5096-109.

- Loh, C.F. (1976). Preliminary valuation of some systemic fungicides for Ganoderma control and phytotoxicity to oil palm. *Malayan Agriculture Journal*, 32: 223-230.
- Lu, C., Zainal, Z., Tucker, G.A., & Lycett, G.W. (2001). Developmental abnormalities and reduced fruit softening in tomato plants expressing an antisense Rab11 GTPase gene. *Plant Cell*, 13: 1819–1833.
- Lukasik, E. & Takken, F.L.W. (2009). STANDING strong, resistance proteins instigators of plant defence. *Current Opinion in Plant Biology*, 12(4): 427–436.
- Luna, E., Pastor, V., Robert, J., Flors, V., Mauch-Mani, B. & Ton, J. (2011). Callose Deposition: A Multifaceted Plant Defense Response. *Molecular Plant Microbe Interactions*, 24(2): 183-193.
- Mackey, D., Holt, B.F., Wiig, A. & Dangl, J. L. (2002). RIN4 interacts with *Pseudomonas syringae* type III effector molecules and is required for RPM1-mediated resistance in Arabidopsis. *Cell Press*, 108(6): 743-754.
- Maier, T., Güell, M. & Serrano, L. (2009). Correlation of mRNA and protein in complex biological samples. *FEBS Letters*, 583(24): 3966–3973.
- Malinovsky, F.G., Fangel, J.U. & Willats, W.G.T. (2014). The role of the cell wall in plant immunity. *Frontiers in Plant Science*, 9(178): doi: 10.3389/fpls.2014.00178.
- Manosalva, P.M., Bruce, M. & Leach, J.E. (2011). Rice 14-3-3 protein (GF14e) negatively affects cell death and disease resistance. *Plant Journal*, 68: 777–787.
- Markom, M.A., Md Shakaff, A.Y., Adom, A.H., Ahmad, M.N., Wahyu Hidayat, A.H.A. & Ahmad Fikri, N. (2009). Intelligent electronic nose system for basal stem rot disease detection. *Computers and Electronics in Agriculture*, 66: 140–146.
- Martin, G.B., Bogdanove, A.J. & Sessa, G. (2003). Understanding the functions of plant disease resistance proteins. *Annual Review of Plant Biology*, 54: 23-61.
- Mcdowell, J.M. & Simon, S.A. (2006). Recent insights into R gene evolution. *Molecular Plant Pathology*, 7: 437-448.
- McElver, J., Patton, D., Rumbaugh, M., Liu, C., Yang, L.J., & Meinke, D. (2000). The

TITAN5 gene of Arabidopsis encodes a protein related to the ADP ribosylation factor family of GTP binding proteins. *Plant Cell*, 12: 1379–1392.

Mercière, M., Laybats, A., Carasco-Lacombe, C., Tan, J.S., Klopp, C., Durand-Gasselín, T., Syed Alwee, S.S.R., Camus-Kulandaivelu, L. & Breton, F. (2015). Identification and development of new polymorphic microsatellite markers using genome assembly for *Ganoderma boninense*, causal agent of oil palm basal stem rot disease. *Mycological Progress*, 14:103-113.

Micali, C.O., Neumann, U., Grunewald, D., Panstruga, R. & O'Connell, R. (2011). Biogenesis of a specialized plant-fungal interface during host cell internalization of *Golovinomyces orontii* haustoria. *Cellular Microbiology*, 13: 210–22610.

Michelet, L., Zaffagnini, M., Morisse, S., Sparla, F., Pérez-Pérez, M. E., Francia, F., Danon, A., Marchand, C.H., Fermani, S., Trost, P. & Lemaire, S.D. (2013). Redox regulation of the Calvin-Benson cycle: something old, something new. *Frontiers in Plant Science*, 4: 470.

Miller, R.N.G., Holderness, M., Bridge, P.D. & Chung, C.F. (1999). Genetic diversity of *Ganoderma* in oil palm plantings. *Plant Pathology*, 48: 595-603.

Mohd As'wad, A., Sariah, M., Paterson, R., Zainal Abidin, M. & Lima, N. (2011). Ergosterol analyses of oil palm seedlings and plants infected with *Ganoderma*. *Crop Protection*, 30: 1438–1442.

Morey, K.J., Ortega, J.L. & Sengupta-Gopalan, C. (2002). Cytosolic glutamine synthetase in soybean is encoded by a multigene family, and the members are regulated in an organ-specific and developmental manner. *Plant Physiology*, 128: 182–193.

Morris, J.H., Knudsen, G.M., Verschueren, E., Johnson, J.R., Cimermanic, P., Greninger, A.L. & Pico, A.R. (2014). Affinity purification–mass spectrometry and network analysis to understand protein-protein interactions. *Nature Protocol*, 9(11): 2539–2554.

Muniroh, M.S., Sariah, M., Zainal Abidin, M.A., Lima, N. & Paterson, R.R. (2014). Rapid detection of *Ganoderma*-infected oil palms by microwave ergosterol extraction with HPLC and TLC. *Journal of Microbiological Methods*, 100: 143-147.

Murphy, D.J. (2007). Future prospects for oil palm in the 21st century: Biological and related challenges. *European Journal of Lipid Science Technology*, 109: 296-306.

- Muthuramalingam, M., Seidel, T., Laxa, M., Nunes de Miranda, S.M., Gartner, F., Stroher, E., Kandlbinder, A. & Dietz, K.-J. (2009). Multiple redox and non-redox interactions define 2-cys peroxiredoxin as a regulatory hub in the chloroplast. *Molecular Plant*, 2(6): 1273–1288.
- Najihah, N.I., Hanafi, M.M, Idris, A.S. & Hakim, M.A. (2015). Silicon treatment in oil palms confers resistance to basal stem rot disease caused by *Ganoderma boninense*. *Crop Protection*, 67: 151-159.
- Nakamura, T. & Oda, Y. (2007). Mass spectrometry-based quantitative proteomics. *Biotechnology and Genetic Engineering Reviews*, 24: 147-164.
- Navaratnam, S. J. (1964). Basal stem rot of oil palms on ex-coconut estates. *Planter*, 40: 256-259.
- Nedukha, O.M. (2015). Callose: Localization, functions, and synthesis in plant cells. *Cytology and Genetics*, 49(1): 49–57.
- Nowogórska, A. & Patykowski, J. (2015). Selected reactive oxygen species and antioxidant enzymes in common bean after *Pseudomonas syringae* pv. *phaseolicola* and *Botrytis cinerea* infection. *Acta Physiologiae Plantarum*, 37: 1725–1734
- Nozu, Y., Tsugita, A. & Kamijo, K. (2006). Proteomic analysis of rice leaf, stem and root tissues during growth course. *Proteomics*, 6: 3665–3670.
- Nurnadiah, E., Aimrun, W., Amin, M.S.M & Idris, A.S. (2014). Preliminary study on detection of basal stem rot (BSR) disease at oil palm tree using electrical resistance. *Agriculture and Agricultural Science Procedia*, 2: 90-94.
- O'Brien, J., Daudi, A., Butt, V. & Paul Bolwell, G. (2012). Reactive oxygen species and their role in plant defence and cell wall metabolism. *Planta*, 236: 765–779.
- Ohdate, T., Kita, K. & Inoue, Y. (2010). Kinetics and redox regulation of Gpx1, an atypical 2-cys peroxiredoxin, in *Saccharomyces cerevisiae*. *FEMS Yeast Research*, 10(6): 787-90.
- Oliveira, B.M., Coorsen, J.R., Martins-de-Souza, D. (2014). 2DE: the phoenix of proteomics. *Journal of Proteomics*, 104: 140-150.

- Oliveira, I.C., Brears, T., Knight, T.J., Clark, A. & Coruzzi, G.M. (2002). Overexpression of cytosolic glutamine synthetase. Relation to nitrogen, light and photorespiration. *Plant Physiology*, 129(3): 1170-80.
- Ooi, L.H. & Heriansyah, H. (2005). Palm pulverisation in sustainable oil palm replanting. *Plant Production Science*, 8(3): 345-348.
- Paterson, R.R.M. (2007). Ganoderma disease of oil palm – A white rot perspective necessary for integrated control. *Crop Protection*, 26: 1369-1376.
- Pedras, M.S.C., Yaya, E.E. & Glawischnig, E. (2011). The phytoalexins from cultivated and wild crucifers: chemistry and biology. *Natural Product Reports*, 28: 1381–1405.
- Peña, J.M., Torres-Sánchez, J., de Castro, A.I., Kelly, M. & López-Granados, F. (2013). Weed mapping in early-season maize fields using object-based analysis of unmanned aerial vehicle (UAV) images. *PLoS ONE*, 8: e77151.
- Pilon, M., Ravet, K. & Tapken, W. (2011). The biogenesis and physiological function of chloroplast superoxide dismutases. *Biochimica et Biophysica Acta*, 1807: 989–998.
- Pitteri, S.J., JeBailey, L., Faça, V.M., Thorpe, J.D., Silva, M.A., Ireton, R.C., Horton, M.B., Wang, H., Pruitt, L.C., Zhang, Q., Cheng, K.H., Urban, N., Hanash, S.M. & Dinulescu, D.M. (2009). Integrated proteomic analysis of human cancer cells and plasma from tumor bearing mice for ovarian cancer biomarker discovery. *PLoS ONE*, 4(11): e7916. doi:10.1371/journal.pone.0007916.
- Price, Z., Mayes, S., Billotte, N., Hafeez, F., Dumortier, F. & MacDonald, D. (2007). Oil Palm. In: Kole, C. (Ed.), *Genome Mapping and Molecular Breeding in Plants Vol 6 Technical Crops* (pp. 93-108). Berlin: Springer.
- Prieto, D.A., Johann, Jr. D.J., Wei, B.R., Ye, X., Chan, K.C., Nissley, D.V., Simpson, R.M., Citrin, D.E., Mackall, C.L., Linehan, W.M. & Blonder, J. (2014). Mass spectrometry in cancer biomarker research: a case for immunodepletion of abundant blood-derived proteins from clinical tissue specimens. *Biomarkers in Medicine*, 8(2): 269–286.
- Qin, J., Gu, F., Liu, D., Yin, C., Zhao, S., Chen, H., Zhang, J., Yang, C., Zhan, X. & Zhang, M. (2013). Proteomic analysis of elite soybean Jidou17 and its parents using iTRAQ-based quantitative approaches. *Proteome Science*, 11: 12

- Rao A.K. (1990). Basal stem rot (*Ganoderma*) in oil palm smallholdings. In: Ariffin D, Jalani S, editors. Proceedings of the Ganoderma Workshop, Palm Oil Research Institute of Malaysia. pp. 113–131.
- Rao, V., Lim, C.C., Chia, C.C. & Teo, K.W. (2003). Studies on *Ganoderma* spread and control. *The Planter*, 79(927):367-83.
- Rapala-Kozik, M., Wolak, N., Kujda, M. & Bana, A.K. (2012). The upregulation of thiamine (vitamin B1) biosynthesis in *Arabidopsis thaliana* seedlings under salt and osmotic stress conditions is mediated by abscisic acid at the early stages of this stress response. *BMC Plant Biology*, 12: 2.
- Rees, R.W., Flood, J., Hasan, Y., Potter, U. & Cooper, R.M. (2009). Basal stem rot of oil palm (*Elaeis guineensis*); mode of root infection and lower stem invasion by *Ganoderma boninense*. *Plant Pathology*, 58: 982–989.
- Rees, R.W., Flood, J., Hasan, Y., Wills, M.A. & Cooper, R.M. (2012). *Ganoderma boninense* basidiospores in oil palm plantations: evaluation of their possible role in stem rots of *Elaeis guineensis*. *Plant Pathology*, 61: 567–578.
- Ribeiro, D., Farias, L., de Almeida, J., Kashiwabara, P., Ribeiro, A., Silva-Filho, M., Menck, C. & Van Sluys, M.J. (2005). Functional characterization of the th1 promoter region from *Arabidopsis thaliana*. *Journal of Experimental Botany*, 56: 1797–1804.
- Robatzek, S. (2007). Vesicle trafficking in plant immune responses. *Cellular Microbiology*, 9(1): 1-8.
- Rojas, A.M., Fuentes, G., Rausell, A. & Valenia, A. (2012). The Ras protein superfamily: Evolutionary tree and role of conserved amino acids. *The Journal of Cell Biology*, 196(2): 189-201.
- Rossard, S., Roblin, G. & Atanassova, R. (2010). Ergosterol triggers characteristic elicitation steps in *Beta vulgaris* leaf tissues. *Journal of Experimental Botany*, 61 (6): 1807-1816.
- Ryan, A., Kaplan, E., Nebel, J-C., Polycarpou, E., Crescente, V., Lowe, E., Preston, G.M. & Sim, E. (2014). Identification of NAD(P)H quinone oxidoreductase activity in azoreductases from *P. aeruginosa*: Azoreductases and NAD(P)H quinone oxidoreductases belong to the same FMN-dependent superfamily of enzymes. *PLoS ONE*, 9(6): e98551. doi:10.1371/journal.pone.0098551

- Sadiq, S. & Agranoff, D. (2008). Pooling serum samples may lead to loss of potential biomarkers in SELDI-ToF MS proteomic profiling. *Proteome Science*, 6(16): doi:10.1186/1477-5956-6-16.
- Sanderson, F.R., Pilotti, C.A. & Bridge, P.D. (2000). Basidiospores: their influence on our thinking regarding a control strategy for basal stem rot of oil palm. In Flood, J., Bridge, P.D. & Holderness, M. (Eds.), *Ganoderma Diseases of Perennial Crops* (pp 89-100). United Kingdom: CABI Publishing.
- Santner, A. & Estelle, M. (2010). The ubiquitin-proteasome system regulates plant hormone signaling. *Plant Journal*, 61(6): 1029-1040.
- Santoso, H., Gunawan, T., Jatmiko, R.H., Darmosarkoro, W. & Minasny, B. (2011). Mapping and identifying basal stem rot disease in oil palms in North Sumatra with QuickBird imagery. *Precision Agriculture*, 12(2): 233-248.
- Schmidt, F. & Völker, U. (2011). Investigation of pathogen responses to the host cell environment. *Proteomics*, 11: 3203–3211.
- Senkler, M. & Braun, H.P. (2012). Functional annotation of 2D protein maps: The GelMap portal. *Frontiers in Plant Science*, 3(87): doi.org/10.3389/fpls.2012.00087.
- Shafri, H.Z.M., Izzuddin Anuar, M. & Iqbal Saripan, M. (2009). Modified vegetation indices for Ganoderma disease detection in oil palm from field spectroradiometer data. *Journal of Applied Remote Sensing*, 3(1): 033556.
- Singh, G. (1991a). Ganoderma – the scourge of oil palms in the coastal areas. *The Planter*, 67: 421-444.
- Singh, G. (1991b). Ganoderma: the scourge of oil palms in the coastal areas. Ariffin, D. & Sukaimi, J. (Eds.), *Proceedings of Ganoderma Workshop* (pp. 81-97). Selangor, Malaysia: Palm Oil Research Institute of Malaysia.
- Soepena, H., Purba, R.Y. & Pawirosukarto, S. (2000). A control strategy for basal stem rot (Ganoderma) on oil palm. In: Flood, J., Bridge, P.D. & Holderness, M. (Eds.), *Ganoderma Diseases of Perennial Crops* (pp. 83-88). United Kingdom: CABI Publication.
- Sollner, S. & Macheroux, P. (2009). New roles of flavoproteins in molecular cell biology: an unexpected role for quinone reductases as regulators of proteasomal

degradation. *Federation of European Biochemical Societies Journal*, 276(16): 4313-4324.

Song, I.K., Lee, J.J., Cho, J.H., Jeong, J., Shin, D.H. & Lee, K.J. (2016). Degradation of redox-sensitive proteins including peroxiredoxins and DJ-1 is promoted by oxidation-induced conformational changes and ubiquitination. *Scientific Reports*, 6: 34432. doi: 10.1038/srep34432.

Sparla, F., Tedeschi, G. & Trost, P. (1996). NAD(P)H:(quinone-acceptor) oxidoreductase of tobacco leaves is a flavin mononucleotide-containing flavoenzyme. *Plant Physiology*, 112(1): 249-258.

Suga, M., Akita, F., Hirata, K., Ueno, G., Murakami, H., Nakajima, Y., Shimizu, T., Yamashita, K., Yamamoto, M., Ago, H. & Shen, J-R. (2015). Native structure of photosystem II at 1.95 Å resolution viewed by femtosecond X-ray pulses. *Nature*, 517: 99–103.

Sundström, J.F., Vaculova, A., Smertenko, A.P., Savenkov, E.I., Golovko, A., Minina, E., Tiwari, B.S., Rodriguez-Nieto, S., Zamyatin, A.A. Jr, Välineva, T., Saarikettu, J., Frilander, M.J., Suarez, M.F., Zavialov, A., Ståhl, U., Hussey, P.J., Silvennoinen, O., Sundberg, E., Zhivotovsky, B. & Bozhkov, P.V. (2009). Tudor staphylococcal nuclease is an evolutionarily conserved component of the programmed cell death degradome. *Nature Cell Biology*, 11(11):1347-54.

Swiderski, M.R., Birker, D & Jones, J.D.G. (2009). The TIR domain of TIR-NB-LRR resistance proteins is a signaling domain involved in cell death induction. *Molecular Plant Microbe Interactions*, 22(2): 157-165.

Tameling, W.L.L. & Takken, F.L.W. (2008). Resistance proteins: scouts of the plant innate immune system. *European Journal of Plant Pathology*, 121(3): 243–255.

Tan, Y.C., Yeoh, K.A., Wong, M.Y. & Ho, C.L. (2013). Expression profiles of putative defence-related proteins in oil palm (*Elaeis guineensis*) colonized by *Ganoderma boninense*. *Journal of Plant Physiology*, 170(16): 1455-1460.

Tawfik, O.H., Mohd Shafri, H.Z. & Mohammed, A.A. (2013). Disease detection from field spectrometer data. *IJUM Engineering Journal*, 14(2): 133-143.

Teh, C.L., Tey, C.C. & Normahnani, M.N. (2010). Integrated Disease Management of Ganoderma in Sabah. Paper presented in EMPA Seminar on Ganoderma Disease of Oil Palm in East Malaysia at Sabah Hotel, Sandakan.

- Thakur, M. & Sohal, B.S. (2013). Role of elicitors in inducing resistance in plants against pathogen infection: A review. *ISRN Biochemistry*, Article ID 762412.
- Thelen, J.J. & Ohlrogge, J.B. (2002). Metabolic engineering of fatty acid biosynthesis in plants. *Metabolic Engineering*, 4: 12–21.
- Thompson, A. (1931). Stem-rot of the oil palm in Malaya. Bulletin Department of Agriculture, Straits Settlements and F.M.S. Science Series 6.
- Toh Choon, R.L., Sariah, M. & Siti Mariam, M.N. (2012). Ergosterol from the soilborne fungus *Ganoderma boninense*. *Journal of Basic Microbiology*, 52(5): 608–612.
- Torres, M.A. (2010). ROS in biotic interactions. *Physiologia Plantarum*, 138: 414–429.
- Tronchet, M., Balagué, C., Kroj, T., Jouanin, L. & Roby, D. (2010). Cinnamyl alcohol dehydrogenases-C and D, key enzymes in lignin biosynthesis, play an essential role in disease resistance in Arabidopsis. *Molecular Plant Pathology*, 11: 83–9210.
- Turner, P.D. (1968). Two wild palms as possible sources of basal stem rot in coastal oil palm plantings. *Planter*, 44:645-649.
- Turner, P.D. (1981). *Oil Palm Diseases and Disorders* (pp. 88-110). Oxford, United Kingdom: Oxford University Press.
- Uematsu, K., Suzuki, N., Iwamae, T., Inui, M. & Yukawa, H. (2012). Increased fructose 1,6-bisphosphate aldolase in plastids enhances growth and photosynthesis of tobacco plants. *Journal of Experimental Botany*, 63(8): 3001–3009.
- Underwood, W. (2012). The plant cell wall: A dynamic barrier against pathogen invasion. *Frontiers in Plant Science*, 3: 85. doi: 10.3389/fpls.2012.00085.
- Utomo, C. & Niepold, F.J. (2000). Development of diagnostic methods for detecting *Ganoderma*-infected oil palms. *Journal of Phytopathology*, 148: 507–514.
- Utomo, C., Werner, S., Niepold, F. & Deising, H.B. (2005). Identification of *Ganoderma*, the causal agent of basal stem rot disease in oil palm using a molecular method. *Mycopathologia*, 159: 159-170.

- Valcu, C.M., Junqueira, M., Shevchenko, A. & Schlink, K. (2009). Comparative proteomic analysis of responses to pathogen infection and wounding in *Fagus sylvatica*. *Journal of Proteome Research*, 8(8): 4077-91.
- Vanholme, R., Demedts, B., Morreel, K., Ralph, J., & Boerjan, W. (2010). Lignin biosynthesis and structure. *Plant Physiology*, 153: 895–905.
- van Geem, M., Gols, R., van Dam, N., van der Putten, W., Fortuna, T. & Harvey, J. (2013). The importance of aboveground–belowground interactions on the evolution and maintenance of variation in plant defense traits. *Frontiers in Plant Science*, 4: 431.
- Vasiliou, V., Ross, D. & Nebert, D.W. (2006). Update of the NAD(P)H:quinone oxidoreductase (NQO) gene family. *Human Genomics*, 2(5): 329–335.
- Vincent, D., Balesdent, M-H., Gibon, J., Claverol, S., Lapailierie, D., Lomenech, A-M., Blaise, F., Rouxel, T., Martin, F., Bonneau, M., Amselem, J., Dominguez, V., Howlett, B.J., Wincker, P., Joets, J., Lebrun, M-H. & Plomion, C. (2009). Hunting down fungal secretomes using liquid-phase IEF prior to high resolution 2-DE. *Electrophoresis*, 30: 4118–4136.
- Voelker, T.A., Worrell, A.C., Anderson, L., Bleibaum, J., Fan, C., Hawkins, D.J., Radke, S.E. & Davies, H.M. (1992). Fatty acid biosynthesis redirected to medium chains in transgenic oilseed plants. *Science*, 257: 72–74.
- Vogel, C. & Marcotte, E.M. (2012). Insights into the regulation of protein abundance from proteomic and transcriptomic analyses. *Nature Reviews Genetics*, 13(4): 227-232.
- von Ballmoos, C., Cook, G.M. & Dimroth, P. (2008). Unique rotary ATP synthase and its biological diversity. *Annual Review of Biophysics*, 37: 43–64.
- von Ballmoos, C., Wiedenmann, A. & Dimroth, P. (2009). Essentials for ATP synthesis by F1FO ATP synthases. *Annual Review of Biochemistry*, 78: 649–672.
- Vorwerk, S., Somerville, S. & Somerville, C. (2004). The role of plant cell wall polysaccharides composition in disease resistance. *Trends in Plant Science*, 9: 203-209.
- Wagner, E., Luche, S., Penna, L., Chevallet, M., Van Dorsselaer, A., Leize-Wagner, E. & Rabilloud, T. (2002). A method for detection of overoxidation of cysteines:

peroxiredoxins are oxidized in vivo at the active-site cysteine during oxidative stress. *Biochemical Journal*, 366: 777–785.

Wakefield, E.M. (1920). Diseases of the oil palm in West Africa. *Kew Bulletin*, 1920: 306-308.

Walther, T.C & Mann, M. (2010). Mass spectrometry–based proteomics in cell biology. *Journal of Cell Biology*, 190(4): 491-500.

Wang, W., Scali, M., Vignani, R., Spadafora, A., Sensi, E., Mazzuca, S. & Cresti, M. (2003). Protein extraction for two-dimensional electrophoresis from olive leaf, a plant tissue containing high levels of interfering compounds. *Electrophoresis*, 24(14): 2369-2375.

Wang, Y., Chantreau, M., Sibout, R. & Hawkins, S. (2013). Plant cell wall lignification and monolignol metabolism. *Frontiers in Plant Science*, 4: 220.doi: 10.3389/fpls.2013.00220.

Westermeier, R. (2006). Sensitive, quantitative, and fast modifications for coomassie blue staining of polyacrylamide gels. *Proteomics*, 6: 61–64.

Whitelegge, J. 2013. Intact protein mass spectrometry and top-down proteomics. *Expert Review of Proteomics*, 10(2): 127–129.

Wiwart, M., Perkowski, J., Budzyński, W., Suchowilska, E., Buśko, M. & Matysiak, A., (2011). Concentrations of ergosterol and trichothecenes in the grains of three *Triticum* species. *Czech Journal of Food Sciences*, 29(4): 430–440.

Wong, P.F. & Sazaly, A. (2005). Post-germination changes in *Hevea brasiliensis* seeds proteome. *Plant Science*, 169: 303–311.

Wood, Z. A., Schroder, E., Robin Harris, J. & Poole, L.B. (2003). Structure, mechanism and regulation of peroxiredoxins. *Trends in Biochemical Sciences*, 28(1): 32-40.

Xing, S.P., Wallmeroth, N., Berendzen, K.W. & Grefen, C. (2016). Techniques for the analysis of protein-protein interactions in vivo. *Plant Physiology*, 171(2): 727-758.

Yang, B., Srivastava, S., Deyholos, M.K. & Kav, N.N.V. (2007). Transcriptional profiling of canola (*Brassica napus* L.) responses to the fungal pathogen *Sclerotinia sclerotiorum*. *Plant Science*, 173: 156–171.

- Yates, J.R.III. (2004). Mass spectral analysis in proteomics. *Annual Review of Biophysics and Biomolecular Structure*, 33: 297–316.
- Yuskianti, V., Glen, M., Puspitasari, D., Francis, A., Rimbawanto, A., Gafur, A., Indrayadi, H. & Mohammed, C.L. (2014). Species-specific PCR for rapid identification of *Ganoderma philippii* and *Ganoderma mastoporum* from *Acacia mangium* and *Eucalyptus pellita* plantations in Indonesia. *Forest Pathology*, 44(6): 477–485.
- Zerial, M. & McBride, H. (2001). Rab proteins as membrane organizers. *Nature Reviews Molecular Cell Biology*, 2: 107–117.
- Zeyen, R.J., Carver, T.L.W. & Lyngkjaer, M.F. 2002. Epidermal cell papillae. In: Belanger R.R. & Bushnell W.R. (Eds), *The powdery mildews: a comprehensive treatise* (pp. 107-125). Minnesota, USA: APS Press.
- Zhang, Q., Linnemann, T.V., Schreiber, L. & Bartels, D. (2016). The role of transketolase and octulose in the resurrection plant *Craterostigma plantagineum*. *Journal of Experimental Botany*, 67(11): 3551–3559.
- Zhang, Y., Fonslow, B.R., Shan, B., Baek, M.-C. & Yates, J.R. III. (2013). Protein analysis by shotgun/bottom-up proteomics. *Chemical Reviews*, 113(4): 2343–2394.
- Zhao, J., Buchwaldt, L., Rimmer, S.R., Sharpe, A., McGregor, L., Bekkaoui, D. & Hegedus, D. (2009). Patterns of differential gene expression in *Brassica napus* cultivars infected with *Sclerotinia sclerotiorum*. *Molecular Plant Pathology*, 10: 635–649.
- Zhao, J., Wang, J., An, L., Doerge, R. W., Chen, Z.J., Grau, C.R., Meng, J. & Osborn, T.C. (2007). Analysis of gene expression profiles in response to *Sclerotinia sclerotiorum* in *Brassica napus*. *Planta*, 227: 13–24.
- Zheng, L., Jia, D., Fei, X., Luo, X. & Yang, Z. (2009). An assessment of the genetic diversity within *Ganoderma* strains with AFLP and ITS PCR-RFLP. *Microbiological Research*, 164: 312–321.
- Zimaro, T., Gottig, N., Garavaglia, B.S., Gehring, C. & Ottado, J. (2011). Unraveling plant responses to bacterial pathogens through proteomics. *Journal of Biomedicine and Biotechnology*, 2011: Article ID 354801.

Zipfel, C. & Felix, G. (2005). Plants and animals: a different taste for microbes? *Current Opinion in Plant Biology*, 8: 353–360.

Zipfel, C., Kunze, G., Chinchilla, D., Caniard, A., Jones, J., Boller, T. & Felix, G. (2006). Perception of the bacterial PAMP EF-Tu by the receptor EFR restricts *Agrobacterium*-mediated transformation. *Cell*, 125(4): 749–760.

Zurbriggen, M.D., Carrillo, N. & Hajirezaei, M.R. (2010). ROS signaling in the hypersensitive response: when, where and what for? *Plant Signaling and Behavior*, 5(4): 393-396.

University of Malaya

## LIST OF PUBLICATIONS AND PAPERS PRESENTED

### Publications

1. Daim, L. D. J., Ooi, T. E. K, Nalisha, I., Hirzun, M.Y., Harikrishna, K., Nazia, A. M. and Karsani, S. A. (2015). Comparative proteomic analysis of oil palm leaves infected with *Ganoderma boninense* revealed changes in proteins involved in photosynthesis, carbohydrate metabolism, and immunity and defence. *Electrophoresis*, 36: 1699–1710.
2. Daim, L. D. J, Ooi, T. E. K, Hirzun, M.Y., Nazia, A. M. and Karsani, S. A. (2015). Optimization of protein extraction and two-dimensional electrophoresis protocols for oil palm leaf. *Protein Journal*, 34: 304–312.

### Poster

1. International Conference on Crop Improvement: Issues and prospects for biotechnology intervention. 2013.  
Plant-microbe interaction category: best poster prize  
Title: Early defence responses to basal stem rot disease in oil palm.  
Leona Daniela Jeffery Daim, Saiful Anuar Karsani, Nazia Abdul Majid and Hirzun Mohd Yusof.

### Oral Presentations

1. International Postgraduate Research Awards Seminar 2014 (InPRAS 2014), Universiti Malaya.  
Title: Comparative proteomics studies of basal stem rot disease in oil palm.
2. International Postgraduate Research Awards Seminar 2016 (InPRAS 2016), Universiti Malaya.  
Title: Comparative proteomics studies of basal stem rot disease in oil palm.